Chapter 5
Fractional-Order Chaotic Systems

5.1 Introduction to Chaotic Dynamics

In general, a nonlinear system is a system which is not linear, that is, a system which does not satisfy the superposition principle. In mathematics, a nonlinear system is any problem, where the variables to be solved cannot be written as a linear combination of independent components. If the equation contains a nonlinear function (power or cross product), the system is nonlinear as well. The system is nonlinear also if it has a nonlinear transfer characteristic as, for example, current-voltage characteristic of a diode. Last but not least, we should mention typical nonlinearity. The system is nonlinear if there is some typical nonlinearity as, for instance, saturation, hysteresis, etc. These characteristics are basic properties of the nonlinear systems.

Nonlinear systems are very interesting to engineers, physicists and mathematicians because most real physical systems are inherently nonlinear in nature. Nonlinear equations are difficult to be solved by analytical methods and give rise to interesting phenomena such as bifurcation and chaos. Even simple nonlinear (or piecewise linear) dynamical systems can exhibit completely a unpredictable behavior, the so-called deterministic chaos. Chaos theory has been so surprising because chaos can also be found within trivial systems. At this point we have to say that the word "chaos" is not uniquely defined. In the most used sense, chaotic dynamics are dynamics originated by regular dynamical equations with no stochastic coefficients, but at the same time, with trajectories that are similar or indistinguishable from some stoachastic processes (Zaslavsky, 2005).

There are a few definitions of the chaotic dynamics, e.g.: (i) a system with at least one positive Lyapunov exponent is chaotic; (ii) a system with positive entropy is chaotic; (iii) a system equivalent to hyperbolic or Anosov system is chaotic, etc. The common part of all definitions is the existence of local instability and divergence of initially close trajectories. At the same time, all definitions are not exactly equivalent.

In the next sections we focus on the well-known nonlinear systems, which exhibit chaos and hyperchaos (e.g., (Petráš, 2009b; Petráš et al., 2009), etc.).

I. Petráš, *Fractional-Order Nonlinear Systems*

5.2 Concept of Chua's Circuit

5.2.1 Classical Chua's Oscillator

Classical Chua's circuit, which is shown in Fig. 5.1, is a simple electronic circuit that exhibits nonlinear dynamical phenomena such as bifurcation and chaos. In fact, in order to exhibit chaos, an autonomous electronic circuit must satisfy some essential criteria which are necessary (not sufficient) conditions for the appearance of chaos (Kennedy, 1993a): the circuit must contain at least three energy-storage elements, at least one nonlinear element and at least one locally active resistor. The Chua's diode, being a nonlinear locally active resistor, allows Chua's circuit to satisfy the last two conditions. Chua's circuit satisfies all the above-mentioned criteria. The active resistor supplies energy to separate trajectories, the nonlinearity provides folding, and the three-dimensional state space permits persistent stretching and folding in a bounded region of the state space.

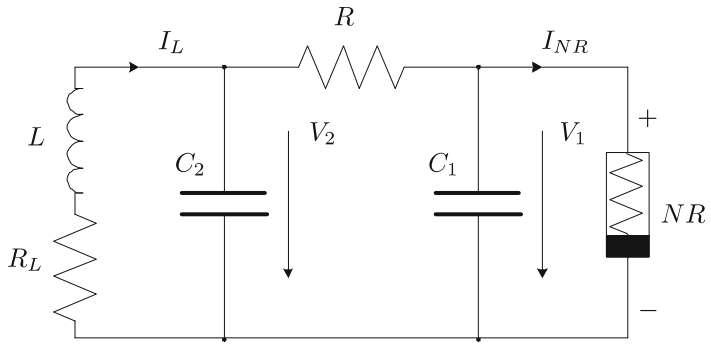

Fig. 5.1 Chua's circuit.

The simplest and most widely studied nonlinear Chua's circuit consists of five elements: two capacitors C_1 and C_2, an inductor L, a resistor R and a nonlinear resistor (NR), known as Chua's diode.

By applying Kirchhoff's circuit laws, such circuit, generally known as Chua's oscillator, can be described by the following equations (Matsumoto, 1984):

$$\begin{aligned}
\frac{dV_1(t)}{dt} &= \frac{1}{C_1}\left[G(V_2(t)-V_1(t))-f(V_1(t))\right],\\
\frac{dV_2(t)}{dt} &= \frac{1}{C_2}\left[G(V_1(t)-V_2(t))+I_L(t)\right],\\
\frac{dI_L(t)}{dt} &= \frac{1}{L}\left[-V_2(t)-R_L I_L(t)\right],
\end{aligned} \tag{5.1}$$

where conductance $G = 1/R$, $I_L(t)$ is the current through the inductance L, $V_1(t)$ and $V_2(t)$ are the voltages over the capacitors C_1 and C_2, respectively, and $f(V_1(t))$ is the piecewise-linear $v-i$ characteristic of NR - Chua's diode, depicted in Fig. 5.2, which can be described by the following state equations:

$$I_{NR}(t) = f(V_1(t)) = G_b V_1(t) + \frac{1}{2}(G_a - G_b)(|V_1(t) + B_p| - |V_1(t) - B_p|), \quad (5.2)$$

with B_p being the breakpoint voltage of a diode, and $G_a < 0$ and $G_b < 0$ being some appropriate constants (slope of the piecewise-linear resistance).

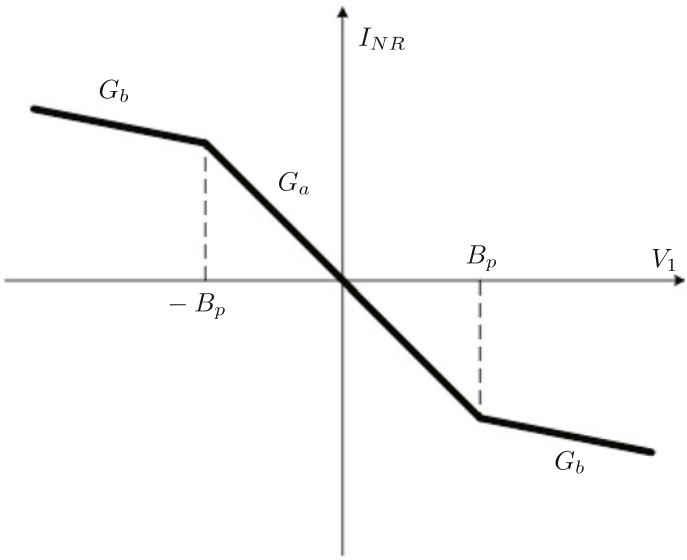

Fig. 5.2 Typical three-segment piecewise-linear $v-i$ characteristic of the nonlinear resistor.

By defining the rescaling

$$\begin{aligned} x &= V_1/B_p, \;\; y = V_2/B_p, \qquad z = I_L/B_p G, \\ \alpha &= C_2/C_1, \;\; \beta = C_2/(LG^2), \; \gamma = C_2 R/(LG), \\ m_1 &= G_b/G, \; m_0 = G_a/G, \qquad \tau = t|G/C_2|, \end{aligned} \quad (5.3)$$

we can transform (5.1) into the following corresponding dimensionless form of Chua's circuit (Chua et al., 1993; Deregel, 1993):

$$\begin{aligned} \frac{dx(t)}{dt} &= \alpha\,(y(t) - x(t) - f(x))\,, \\ \frac{dy(t)}{dt} &= x(t) - y(t) + z(t), \end{aligned} \quad (5.4)$$

$$\frac{dz(t)}{dt} = -\beta y(t) - \gamma z(t),$$

where

$$f(x) = m_1 x(t) + \frac{1}{2}(m_0 - m_1) \times (|x(t)+1| - |x(t)-1|) \tag{5.5}$$

and τ in transformation equations (5.3) is the dimensionless time.

Because of the piecewise-linear nature of *NR*, the vector field of Chua's circuit can be decomposed into three distinct affine regions. It depends on the values of $\pm B_p$. We call these regions the outer D_{-1}, $(V_1 < -B_p)$, the inner (middle) region $D_0, (|V_1| < B_p)$ and the outer $D_1, (V_1 > B_p)$, respectively. The global dynamics of Chua's circuit may be determined by piecing together the three-dimensional vector fields of the regions D_{-1}, D_0, and D_1, then we obtain a qualitative description of the whole circuit.

The equilibrium points of Chua's oscillator (5.1) are defined by

$$\begin{aligned} 0 &= \frac{1}{C_1}\left[G(V_2(t) - V_1(t)) - I_{NR}(t))\right], \\ 0 &= \frac{1}{C_2}\left[G(V_1(t) - V_2(t)) + I_L(t)\right], \\ 0 &= \frac{1}{L}\left[-V_2(t) - R_L I_L(t)\right], \end{aligned} \tag{5.6}$$

where $I_{NR}(t)$ is given by relation (5.2). The origin is obviously an equilibrium point.

In D_0 (inner) region, where $|V_1| \leq B_p$, the state equations of Chua's oscillator are linear. The Jacobian matrix has the following form:

$$\mathbf{J}_{G_a} = \begin{bmatrix} \dfrac{-(G+G_a)}{C_1} & \dfrac{G}{C_1} & 0 \\ \dfrac{G}{C_2} & \dfrac{-G}{C_2} & \dfrac{1}{C_2} \\ 0 & -\dfrac{1}{L} & -\dfrac{R_L}{L} \end{bmatrix}. \tag{5.7}$$

The characteristic equation of Chua's system in the inner region is

$$\begin{aligned} \det|\lambda \mathbf{I} - \mathbf{J}_{G_a}| = \lambda^3 &+ \left(\frac{G+G_a}{C_1} + \frac{G}{C_2} + \frac{R_L}{L}\right)\lambda^2 \\ &+ \left(\frac{GG_a}{C_1C_2} + \frac{G+G_a}{C_1L}R_L + \frac{GR_L}{C_2L} + \frac{1}{C_2L}\right)\lambda \\ &+ \frac{R_L G G_a + (G+G_a)}{C_1C_2L} = 0. \end{aligned} \tag{5.8}$$

In D_{-1} and D_1 (outer) regions, where $|V_1| > B_p$, the state equations of Chua's oscillator are linear. The Jacobian matrix has the following form:

$$\mathbf{J}_{G_b} = \begin{bmatrix} \dfrac{-(G+G_b)}{C_1} & \dfrac{G}{C_1} & 0 \\ \dfrac{G}{C_2} & \dfrac{-G}{C_2} & \dfrac{1}{C_2} \\ 0 & -\dfrac{1}{L} & -\dfrac{R_L}{L} \end{bmatrix}. \tag{5.9}$$

The characteristic equation of Chua's system in the outer region is

$$\begin{aligned} \det|\lambda\mathbf{I}-\mathbf{J}_{G_b}| = \lambda^3 &+ \left(\frac{G+G_b}{C_1}+\frac{G}{C_2}+\frac{R_L}{L}\right)\lambda^2 \\ &+ \left(\frac{GG_b}{C_1C_2}+\frac{G+G_b}{C_1L}R_L+\frac{GR_L}{C_2L}+\frac{1}{C_2L}\right)\lambda \\ &+ \frac{R_LGG_b+(G+G_b)}{C_1C_2L} = 0. \end{aligned} \tag{5.10}$$

The dynamic behavior of any type of Chua's circuit is determined by the six eigenvalues (Chua et al., 1986). They can be obtained by solving the characteristic equations (5.8) and (5.10) and depend on the value of electrical components.

When $G > |G_a|$ or $G < |G_b|$, the circuit has a unique equilibrium point at the origin and two virtual equilibria E_- and E_+ (lie outside regions D_{-1} and D_1). Otherwise it has three equilibrium points ar E_-, 0, and E_+. The equilibrium point E_- in the D_{-1} region has three eigenvalues. It usually consists of a real (λ_1) and a pair of complex conjugate values ($\lambda_{2,3}$). We assume that eigenvalue λ_1 is stable and eigenvalues $\lambda_{2,3}$ are unstable. With symmetry, it is the same to equilibrium point E_+.

For more detailed description of stability analysis of equilibrium points, the dynamics of the outer and inner regions, we refer the reader to (Kennedy, 1993b; Pivka et al., 1994).

Given the techniques of fractional calculus, there are a number of ways in which the order of system could be amended. In the next parts we will show several of them.

5.2.2 Fractional-Order Chua's Oscillator

As we already mentioned in Chapter 2, there are many electric and magnetic phenomena where the fractional calculus can be used. In this section we consider two of them — models of real capacitor and real inductor.

The circuit behavior can be described by three fractional differential equations with various orders. Applying Kirchhoff's laws for two current nodes and one voltage loop and relation (2.75), and (2.78) into circuit depicted in Fig. 5.1, we obtain the following mathematical model of the circuit for state variables $V_1(t)$, $V_2(t)$ and $I(t)$:

$$C_1\,{}_0D_t^{q_1}V_1(t) + I_{NR}(t) = \frac{V_2(t) - V_1(t)}{R_2},$$
$$C_2\,{}_0D_t^{q_2}V_2(t) - I(t) = \frac{V_1(t) - V_2(t)}{R_2}, \tag{5.11}$$
$$L_1\,{}_0D_t^{q_3}I(t) + V_2(t) + R_L I(t) = 0.$$

Equations (5.11) can be rewritten into the following form (Petráš, 2008):

$${}_0D_t^{q_1}V_1(t) = \frac{1}{C_1R_2}[V_2(t) - V_1(t)] - \frac{f(V_1(t))}{C_1},$$
$${}_0D_t^{q_2}V_2(t) = \frac{1}{C_2R_2}[V_1(t) - V_2(t)] + \frac{I(t)}{C_2}, \tag{5.12}$$
$${}_0D_t^{q_3}I(t) = \frac{1}{L_1}[-V_2(t) - R_L I(t)],$$

where V_1 is the voltage across the capacitor C_1, V_2 is the voltage across the capacitor C_2, I is the current through the inductance L_1, q_1 is the real order of the capacitor C_1, q_2 is the real order of the capacitor C_2, q_3 is the real order of the inductor L_1, $f(V_1)$ is the piecewise-linear $v - i$ characteristic of nonlinear Chua's diode, which can be described by (5.2).

By using the transformation (5.3), we can rewrite Eqs. (5.12) into the following dimensionless form (Petráš, 2008):

$${}_0D_t^{q_1}x(t) = \alpha\,(y(t) - x(t) - f(x)),$$
$${}_0D_t^{q_2}y(t) = x(t) - y(t) + z(t), \tag{5.13}$$
$${}_0D_t^{q_3}z(t) = -\beta y(t) - \gamma z(t),$$

where $f(x)$ is the piecewise-linear nonlinearity (5.5).

5.2.2.1 Experimental Measurements

Classical Chua's oscillator can also be realized by electrical elements according to the scheme shown in Fig. 5.3, which is a very simple electronic circuit that exhibits nonlinear dynamical phenomena such as bifurcation and chaos (Kennedy, 1992). Chua's diode (5.2) – nonlinear resistor – was realized by operating amplifier LM 358 and resistors R_1, R_7, and R_8 ($R_7 = R_8$) as negative impedance converter (Bartissol and Chua, 1988).

For experimental verification of Chua's system depicted in Fig. 5.3 and described by Eqs. (5.12) and (5.2), the following values of electrical elements were chosen (Caponetto et al., 2010; Petráš, 2008):

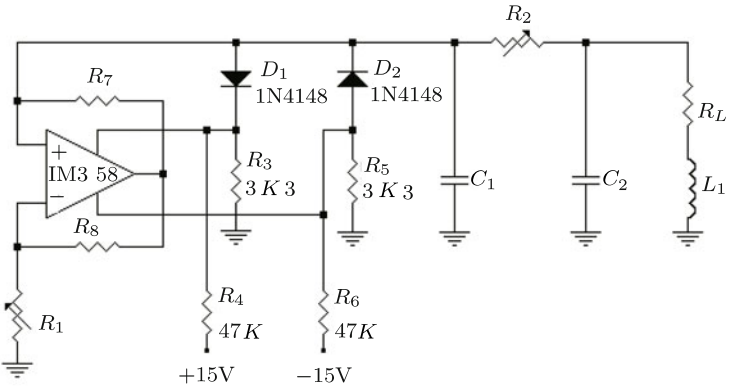

Fig. 5.3 Practical realization of Chua's circuit.

$$C_1 = 4.71\,nF,\ C_2 = 48\,nF,\ L_1 = 4.64\,mH, \tag{5.14}$$
$$R_L = 15.8\,\Omega,\ R_1 = 897\,\Omega,\ R_2 = 998\,\Omega,\ R_7 = R_8 = 393\,\Omega.$$

We use the metalized paper capacitors C_1 and C_2 with the real order $q_1 = q_2 = 0.98$ and we assume the real order of inductor $q_3 = 0.94$ (see e.g. (Schafer and Kruger, 2008; Westerlund and Ekstam, 1994; Westerlund, 2002)). The total order of the system is $\bar{q} = 2.90$.

The measured breakpoints of the non-linear characteristic (5.2) are:

$$-B_p = (-8.79V,\ 7.7\,mA),\ \ B_p = (9.12V,\ -7.9\,mA).$$

Assuming the three-segment piecewise-linear voltage-current transfer characteristic of negative impedance converter (5.2), we have the slope $G_a = -1/R_1 = -1.1148\,mA/V$ for $R_7 = R_8$ and the slope G_b was calculated using the breakpoints B_p and it has the value $G_b = -0.8710\,mA/V$.

The resistors R_3, R_4, R_5, R_6, and the diodes D_1 and D_2 generate the positive and negative halves of the nonlinearity.

In Fig. 5.4 is depicted the photo of the digital oscilloscope screen (Tektronix TDS1002, 60 Mhz). It is a real measurement of voltages $V_1 - V_2$ for circuit presented in Fig. 5.3 with the parameters of electrical components (5.14). The result shown in Fig. 5.4 is the double-scroll attractor of fractional-order Chua's system described by Eqs. (5.12) and (5.2). We can observe an amplification of the system.

An alternative scheme of the practical implementation of the Chua's oscillator with two operating amplifiers for a different kind of nonlinearity with saturation can be found, for instance, in (Chua et al., 1993; Kennedy, 1993b) or for an IC chip implementation we refer to (Cruz, 1993).

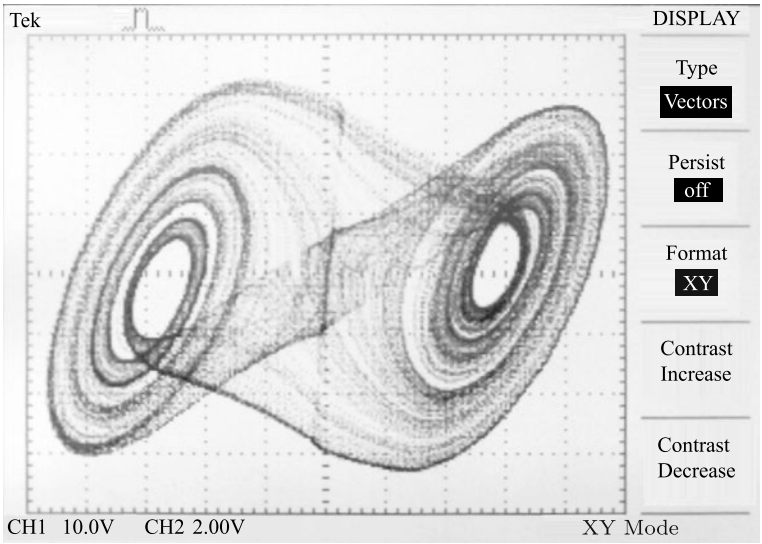

Fig. 5.4 Photo of oscilloscope screen: Strange attractor of the Chua's system (5.12).

5.2.2.2 Simulation Results

For simulation purposes we will use a numerical solution of Chua's equations (5.13) obtained by using the relationship (2.53) derived from the Grünwald-Letnikov definition (2.15), which leads to equations in the form:

$$\begin{aligned} x(t_k) &= (\alpha(y(t_{k-1}) - x(t_{k-1}) - f(x(t_{k-1})))) h^{q_1} - \sum_{j=v}^{k} c_j^{(q_1)} x(t_{k-j}), \\ y(t_k) &= (x(t_k) - y(t_{k-1}) + z(t_{k-1})) h^{q_2} - \sum_{j=v}^{k} c_j^{(q_2)} y(t_{k-j}), \\ z(t_k) &= (-\beta y(t_k) - \gamma z(t_{k-1})) h^{q_3} - \sum_{j=v}^{k} c_j^{(q_3)} z(t_{k-j}), \end{aligned} \tag{5.15}$$

where

$$f(x(t_{k-1})) = m_1 x(t_{k-1}) + \frac{1}{2}(m_0 - m_1) \times (|x(t_{k-1}) + 1| - |x(t_{k-1}) - 1|) \tag{5.16}$$

and where T_{sim} is the simulation time, $k = 1, 2, 3, \ldots, N$, for $N = [T_{sim}/h]$, and $(x(0), y(0), z(0))$ is the start point (initial conditions). The binomial coefficients $c_j^{(q_i)}, \forall i$, are calculated according to relation (2.54).

Similar and comparable results we have measured can be obtained by simulation using Eqs. (5.15) for time step $h = 0.001$ and the short memory principle with length $L_m = 10$ (10000 values and coefficients from history). Figure 5.5 shows the double-

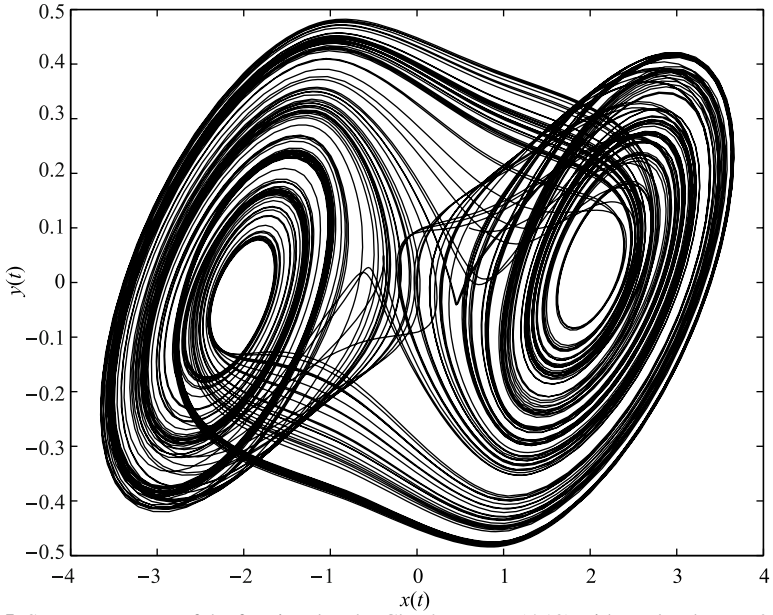

Fig. 5.5 Strange attractor of the fractional-order Chua's system (5.13) with total order $\bar{q} = 2.90$ for the parameters: $\alpha = 10.1911$, $\beta = 10.3035$, $\gamma = 0.1631$, $q_1 = q_2 = 0.98$, $q_3 = 0.94$, $m_0 = -1.1126$, $m_1 = -0.8692$, and simulation time $T_{sim} = 100\,s$.

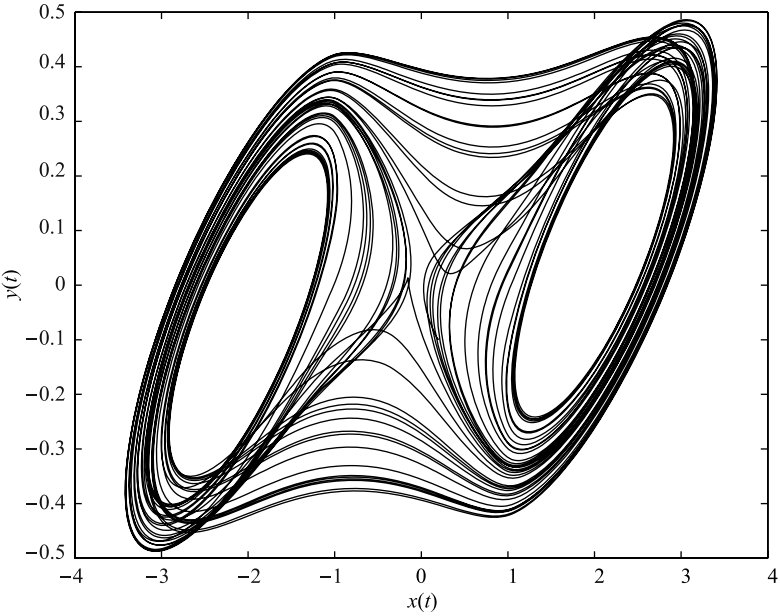

Fig. 5.6 Strange attractor from the fractional-order Chua's system (5.13) with total order $\bar{q} = 2.84$ for the parameters: $\alpha = 10.725$, $\beta = 10.593$, $\gamma = 0.268$, $q_1 = 0.93$, $q_2 = 0.99$, $q_3 = 0.92$, $m_0 = -1.1726$, $m_1 = -0.7872$ and simulation time $T_{sim} = 100\,s$.

scroll attractor of Chua's circuit (5.13) computed numerically for initial conditions $(x(0), y(0), z(0)) = (0.6, 0.1, -0.6)$ and for the value of electrical parts (5.14) by using a short memory principle ($L_m = 10$).

In Fig. 5.6 is depicted the result from (Zhu et al., 2009), where simulation was performed without using the short memory principle ($v = 1$) for time step $h = 0.001$ and also for a different set of parameters and initial conditions $(x(0), y(0), z(0)) = (0.2, -0.1, 0.1)$.

For simulation we are able to use the Matlab/Simulink approach as well. The state-space expression of the fractional-order Chua's equations (5.13) with parameters α, β, and γ is given by using the integration operation and the properties (2.50) and (2.51), and has the following form:

$$\begin{aligned} x(t) &= {}_0D_t^{1-q_1}\left(\int_0^t [\alpha(y(t) - x(t) - f(x))]\,dt\right), \\ y(t) &= {}_0D_t^{1-q_2}\left(\int_0^t [x(t) - y(t) + z(t)]\,dt\right), \\ z(t) &= {}_0D_t^{1-q_3}\left(\int_0^t [-\beta y(t) - \gamma z(t)]\,dt\right). \end{aligned} \tag{5.17}$$

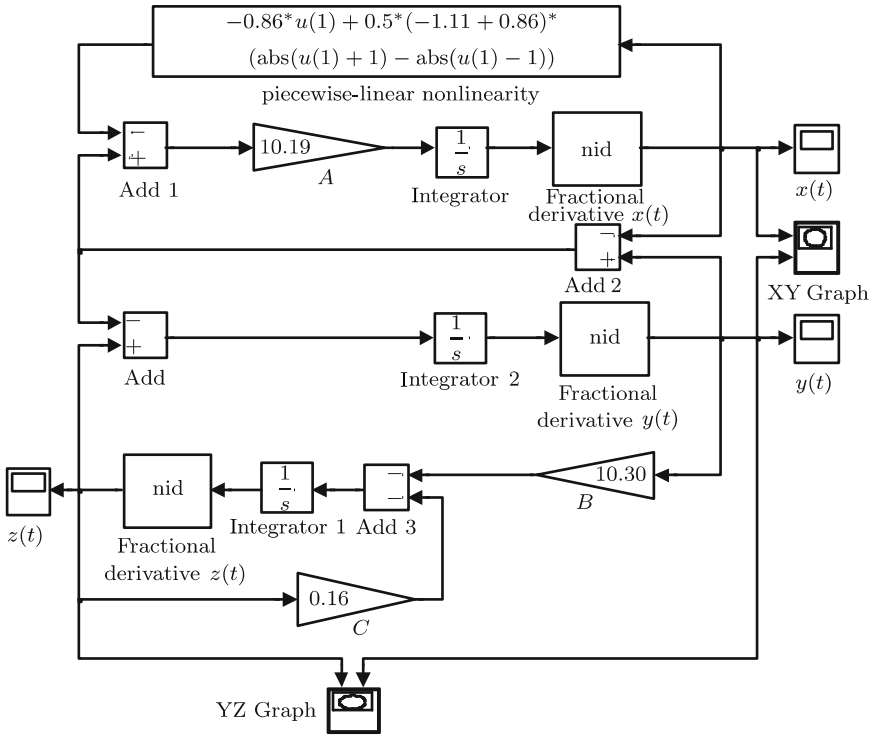

Fig. 5.7 Matlab/Simulink block diagram (model) for Chua's system (5.13).

The system model developed from the state equations (5.17) for system parameters α, β, and γ by using the Matlab/Simulink environment is depicted in Fig. 5.7. For simulation of the fractional derivative (integral) we used a Simulink block *nid* created by Duarte Valerio (Valerio, 2005) with the combination of the classical integrator by using the property of commutation of two operators.

In Fig. 5.8 is depicted the simulation results obtained by numerical simulation in the Matlab/Simulink for the following values of the parameters: $A \equiv \alpha = 10.19$, $B \equiv \beta = 10.30$, $C \equiv \gamma = 0.16$, $q_1 = q_2 = 0.98$, and $q_3 = 0.94$, for the initial conditions: $(x(0), y(0), z(0)) = (0.6, 0.1, -0.6)$ and for the slopes of Chua's diode (5.5) characteristic: $m_0 = -1.11$ and $m_1 = -0.86$.

As we can observe in Fig. 5.8, the obtained simulation results are comparable to the results depicted in Fig. 5.5.

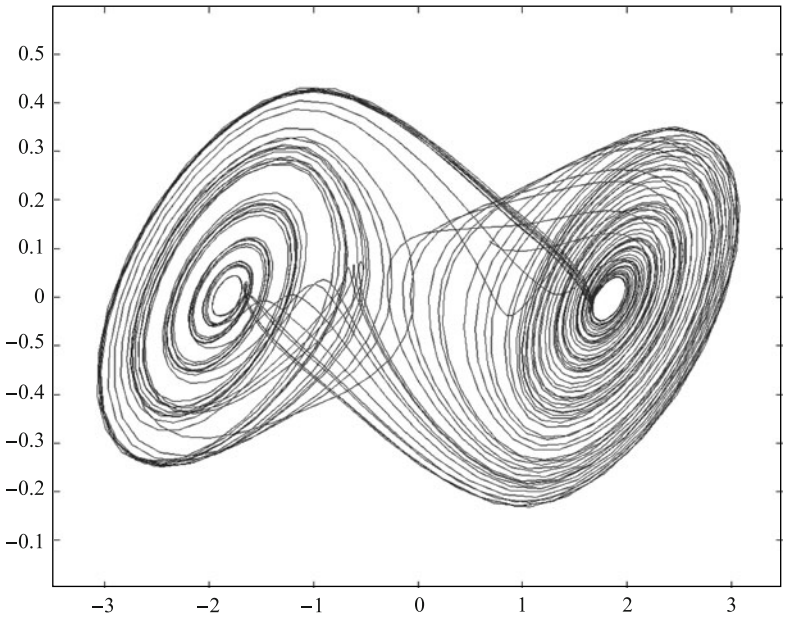

Fig. 5.8 Simulation result (x vs. y) of Chua's system (5.13).

5.2.3 Fractional-Order Chua-Podlubny's Oscillator

This system uses an approach where the order of any of three constitutive equations (5.4) can be changed so that the total order gives the desired value. In Chua-Podlubny's case, in equation one the first differentiation is replaced by a fractional one. The final dimensionless equations of the system are (Podlubny, 1999):

$$
\begin{aligned}
{}_0D_t^q x(t) &= \alpha\, {}_0D_t^{q-1}\left(y(t)-x(t)\right) - \frac{2\alpha}{7}\left(4x(t)-x^3(t)\right),\\
\frac{dy(t)}{dt} &= x(t)-y(t)+z(t),\\
\frac{dz(t)}{dt} &= -\frac{100}{7}y(t) = -\beta y(t),
\end{aligned}
\tag{5.18}
$$

where $\alpha = C_2/C_1$ and $\beta = C_2R_2^2/L_1$, and fractional order $q < 1$, $q \in \mathrm{R}$.

5.2.4 Fractional-Order Chua-Hartley's Oscillator

The Chua-Hartley's system is different from the usual Chua's system (5.4) in that the piecewise-linear nonlinearity is replaced by an appropriate cubic nonlinearity which yields very similar behavior. Derivatives on the left side of the differential equations are replaced by the fractional derivatives as follows (Hartley et al., 1995):

$$
\begin{aligned}
{}_0D_t^q x(t) &= \alpha\left(y(t) + \frac{x(t)-2x^3(t)}{7}\right),\\
{}_0D_t^q y(t) &= x(t)-y(t)+z(t),\\
{}_0D_t^q z(t) &= -\beta y(t) = -\frac{100}{7}y(t),
\end{aligned}
\tag{5.19}
$$

where $q \leq 1$, $q \in \mathrm{R}$ is the fractional order of derivatives.

5.2.5 Fractional-Order Memristor-Based Chua's Oscillator

Since the memristor was postulated by L. O. Chua in 1971 and discovered by R. Williams et al. (HP laboratory) in 2008 (realized as a $Pt - TiO_2 - Pt$ device), it becomes the fourth circuit element. This fact allows us to use the memristor as a nonlinear element in circuits which exhibit chaos. In the case of Chua's circuit, the nonlinear resistor NR is replaced by an active memristor M as shown in Fig. 5.9.

The memristor in Fig. 5.9 is a flux-controlled memristor whose characteristic is given by literature (Chua, 1971):

$$
I_M(t) = W(\phi(t))V_1(t), \tag{5.20}
$$

where $W(\phi(t))$ is the incremental memductance defined as (Chua, 1971)

$$
W(\phi) = \frac{dq(\phi)}{d\phi}. \tag{5.21}
$$

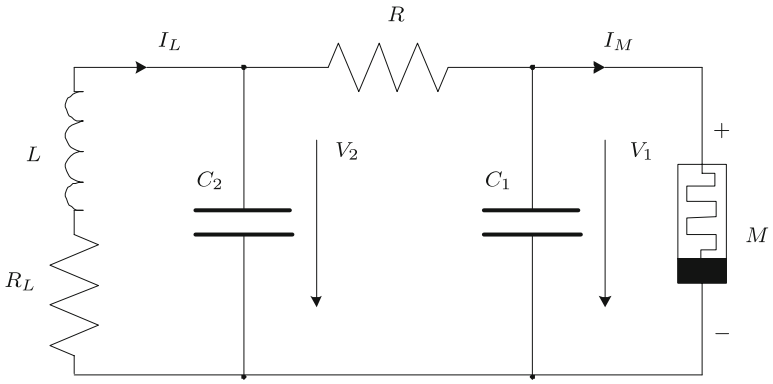

Fig. 5.9 Chua's circuit with active memristor.

Taking this into account we can write the equations for the memristor-based chaotic circuit depicted in Fig. 5.9 as follows:

$$\begin{aligned}
\frac{dV_1(t)}{dt} &= \frac{1}{C_1}\left[G(V_2(t)-V_1(t))-I_M(t))\right],\\
\frac{dV_2(t)}{dt} &= \frac{1}{C_2}\left[G(V_1(t)-V_2(t))+I_L(t)\right],\\
\frac{dI_L(t)}{dt} &= \frac{1}{L}\left[-V_2(t)-R_L I_L(t)\right],\\
\frac{d\phi(t)}{dt} &= V_1(t),
\end{aligned} \tag{5.22}$$

where $G = 1/R$, and $I_M(t)$ is defined by Eq. (5.20).

For the flux-controlled memristor a monotone-increasing piecewise-linear characteristic (Itoh and Chua, 2008, 2009) was assumed. The memristor constitutive relation is shown in Fig. 5.10 and can be expressed as

$$q(\phi) = b\phi + 0.5(a-b)\times(|\phi+1|-|\phi-1|), \tag{5.23}$$

where $a, b > 0$. The memductance function obtained from the $q(\phi)$ function is:

$$W(\phi) = \frac{dq(\phi)}{d\phi}\begin{cases} a, & |\phi|<1,\\ b, & |\phi|>1. \end{cases} \tag{5.24}$$

Several modifications of the memristor-based Chua's circuit, where chaos was observed, were described and analyzed in (Itoh and Chua, 2008). For a practical implementation of the memristor it is possible to use operating amplifiers (Zhong, 1994) and then a smooth cubic nonlinearity could be used for replacing a $q-\phi$ function depicted in Fig. 5.10.

The dynamics of the Chua's circuit with a passive memristor (flux-controlled memristor and negative conductance) depicted in Fig. 5.11 are given by the following set of differential equations:

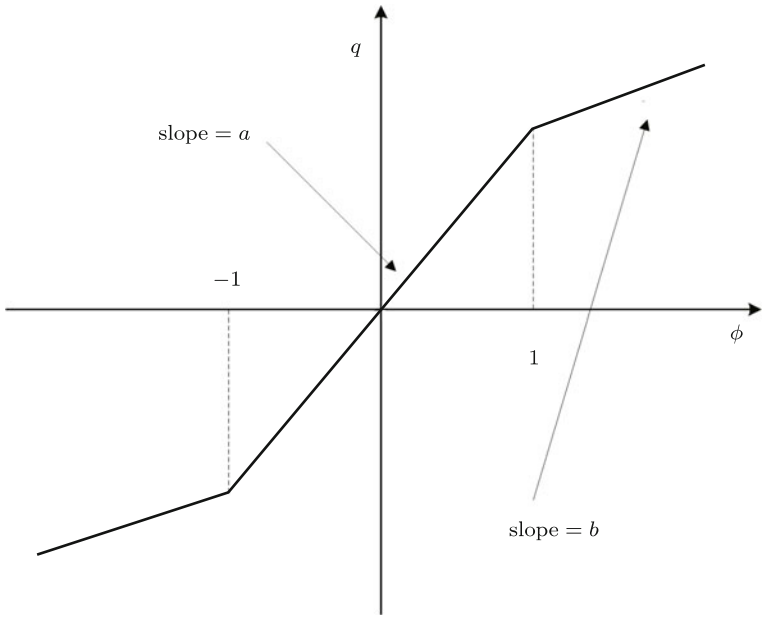

Fig. 5.10 The constitutive relation of a piecewise-linear flux-controlled memristor.

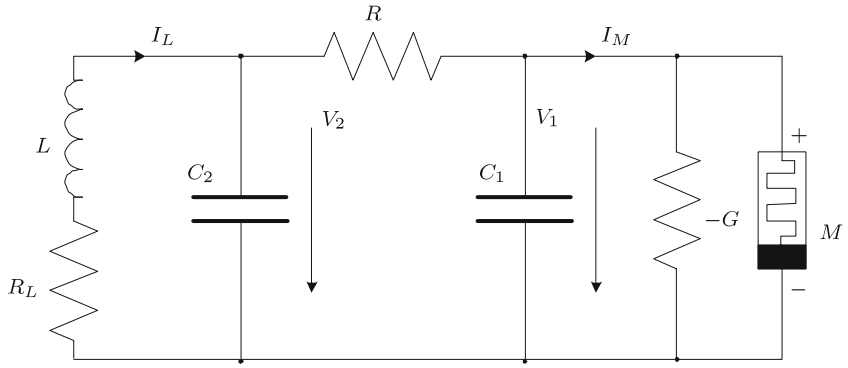

Fig. 5.11 Chua's circuit with flux-controlled memristor and negative conductance.

$$\begin{aligned}
\frac{dV_1(t)}{dt} &= \frac{1}{C_1}\left[\frac{(V_2(t)-V_1(t))}{R} + GV_1(t) - W(\phi)V_1(t))\right],\\
\frac{dV_2(t)}{dt} &= \frac{1}{C_2}\left[\frac{(V_1(t)-V_2(t))}{R} + I_L(t)\right],\\
\frac{dI_L(t)}{dt} &= \frac{1}{L}\left[-V_2(t) - R_L I_L(t)\right],\\
\frac{d\phi(t)}{dt} &= V_1(t),
\end{aligned} \tag{5.25}$$

where functions $q(\phi)$ and $W(\phi)$ are given in (5.23) and (5.24), respectively.

If we set

$$\begin{array}{l} x = V_1, \quad y = V_2, \quad z = I_L, \quad w = \phi, \quad C_2 = 1, \quad R = 1, \\ \alpha = 1/C_1, \quad \beta = 1/L, \quad \gamma = R_L/L, \quad \zeta = G, \end{array} \tag{5.26}$$

then Eqs. (5.25) can be transformed into the dimensionless form (Itoh and Chua, 2008):

$$\begin{aligned} \frac{dx(t)}{dt} &= \alpha\left(y(t) - x(t) + \zeta x(t) - W(w)x(t)\right), \\ \frac{dy(t)}{dt} &= x(t) - y(t) + z(t), \\ \frac{dz(t)}{dt} &= -\beta y(t) - \gamma z(t), \\ \frac{dw(t)}{dt} &= x(t), \end{aligned} \tag{5.27}$$

where piecewise-linear function $W(w)$ is given below:

$$W(w) = \begin{cases} a: & |w| < 1, \\ b: & |w| > 1. \end{cases} \tag{5.28}$$

The equilibrium points of the system (5.27) are given by setting the left side of equations to 0 except the last one. We set w as constant, which corresponds to the w –axis (Itoh and Chua, 2008). The Jacobian matrix at this equilibrium state is (Itoh and Chua, 2008):

$$\mathbf{J}_W = \begin{bmatrix} \alpha(-1 + \zeta - W(w)) & \alpha & 0 & 0 \\ 1 & -1 & 1 & 0 \\ 0 & -\beta & -\gamma & 0 \\ 1 & 0 & 0 & 0 \end{bmatrix}. \tag{5.29}$$

For the following parameter set (Itoh and Chua, 2008): $\alpha = 10$, $\beta = 13$, $\gamma = 0.35$, $\zeta = 1.5$, $a = 0.3$, and $b = 0.8$, four eigenvalues λ_i $(i = 1,2,3,4)$ for $|w| < 1$ can be written as

$$\lambda_{1,2} \approx -1.31103 \pm 2.74058j,\ \lambda_3 \approx 3.27207,\ \lambda_4 = 0$$

and four eigenvalues for $|w| > 1$ can be written as

$$\lambda_{1,2} \approx 0.07865 \pm 2.84655j,\ \lambda_3 \approx -4.50731,\ \lambda_4 = 0.$$

They are characterized by an unstable saddle-focus point and numerical simulations for the above paremeters show that the system (5.27) has chaotic behavior. In Fig. 5.12 and Fig. 5.13 are depicted chaotic attractors in 3D state space for $T_{sim} = 200\,s$.

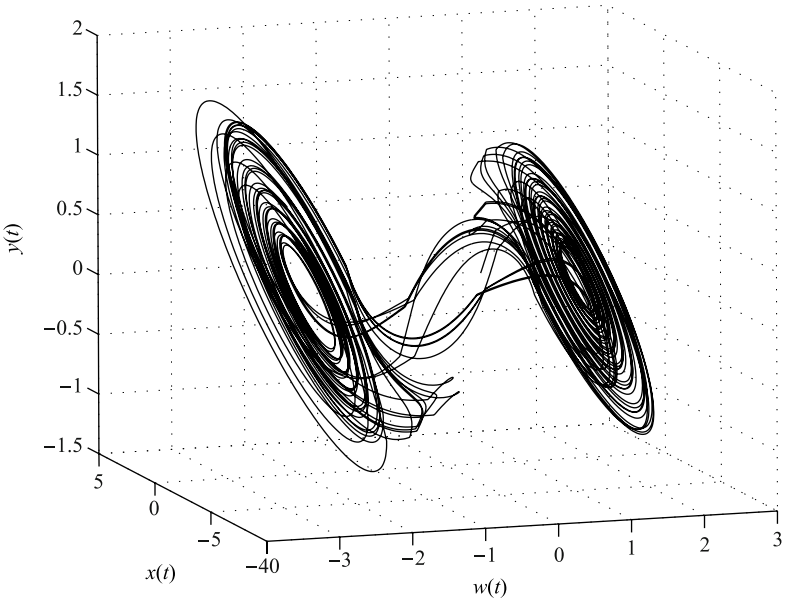

Fig. 5.12 Strange attractor of the memristor-based Chua's system (5.27) in $w-x-y$ state space, for parameters $\alpha = 10,\ \beta = 13,\ \gamma = 0.35,\ \zeta = 1.5,\ a = 0.3$, and $b = 0.8$, initial conditions: $x(0) = 0.8, y(0) = 0.05, z(0) = 0.007, w(0) = 0.6$ and simulation time $T_{sim} = 200\,s$.

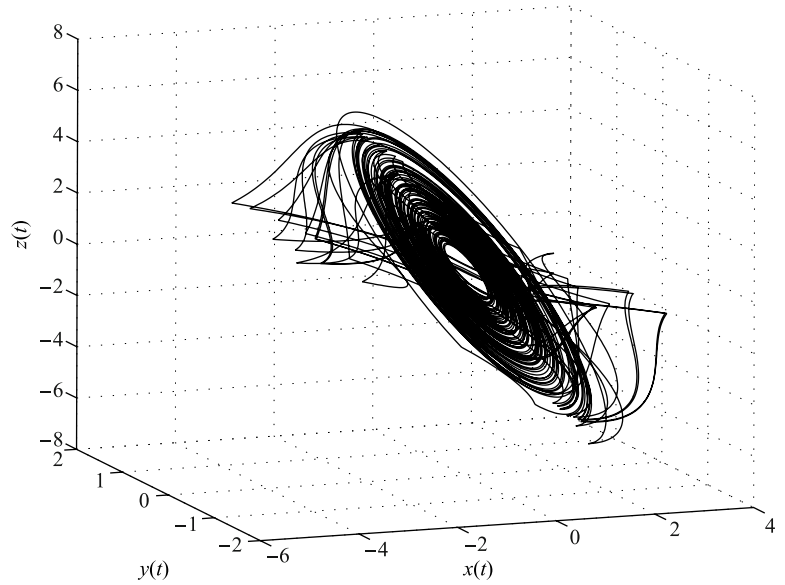

Fig. 5.13 Strange attractor of the memristor-based Chua's system (5.27) in $x-y-z$ state space, for parameters $\alpha = 10,\ \beta = 13,\ \gamma = 0.35,\ \zeta = 1.5,\ a = 0.3$, and $b = 0.8$, initial conditions: $x(0) = 0.8, y(0) = 0.05, z(0) = 0.007, w(0) = 0.6$ and simulation time $T_{sim} = 200\,s$.

In Fig.5.14 and Fig. 5.15 are depicted the attractors of the memristor-based Chua's system (5.27) for parameters $\alpha = 10,\ \beta = 13,\ \gamma = 0.35,\ \zeta = 1.5,\ a = 0.3,$ $b = 0.8$, initial conditions: $x(0) = 0.8, y(0) = 0.05, z(0) = 0.007, w(0) = 0.6$ and simulation time $T_{sim} = 200\,s$, projected onto $y-w$, and $z-w$ planes, respectively.

If we consider a fractional-order model for each electrical element in the circuit depicted in Fig. 5.11, we can write a more general mathematical model for this circuit. As already mentioned, real capacitor and real inductor are "fractional" and for real memristor we postulated a fractional-order model as well $(d^{\alpha}\phi(t)/dt^{\alpha} = V(t))$. By using a technique of fractional calculus we obtain the following equations:

$$\begin{aligned} {}_0D_t^{q_1}x(t) &= \alpha\left(y(t) - x(t) + \zeta x(t) - W(w)x(t)\right), \\ {}_0D_t^{q_2}y(t) &= x(t) - y(t) + z(t), \\ {}_0D_t^{q_3}z(t) &= -\beta y(t) - \gamma z(t), \\ {}_0D_t^{q_4}w(t) &= x(t), \end{aligned} \tag{5.30}$$

where function $W(w)$ is given in (5.28) and where q_1, q_2, q_3, and q_4 are fractional orders of real electrical elements (memristive systems): capacitor C_1, capacitor C_2, inductor L, and memristor M, respectively.

The stability of the new fractional-order memristor-based Chua's system can be investigated by using Theorem 4.6. For the fractional incommensurate-order system (5.30), we can rewrite real order as $q_i = v_i/u_i$, $v_i, u_i \in Z^+$ for $i = 1,2,3,4$ and if we set $\gamma = 1/m$, where m is the LCM of the denominators, the characteristic equation of the system (5.30) for the Jacobian matrix $\mathbf{J}_W$ is:

$$\det(\mathrm{diag}([\lambda^{mq_1}\ \lambda^{mq_2}\ \lambda^{mq_3}\ \lambda^{mq_4}]) - \mathbf{J}_W) = 0$$

and then the stability condition is defined as follows:

$$|\arg(\lambda_i)| > \gamma\frac{\pi}{2}$$

for all eigenvalues λ_i.

In the case of piecewise-nonlinearity depicted in Fig. 5.10, we should investigate the characteristic equation for the linear part with slope a and for the linear part with slope b. If $|w| < 1$ then we are dealing with slope a and the Jacobian matrix is

$$\mathbf{J}_{Wa} = \begin{bmatrix} \alpha(-1+\zeta-a) & \alpha & 0 & 0 \\ 1 & -1 & 1 & 0 \\ 0 & -\beta & -\gamma & 0 \\ 1 & 0 & 0 & 0 \end{bmatrix} \tag{5.31}$$

and if $|w| > 1$ then we are dealing with slope b and the Jacobian matrix is

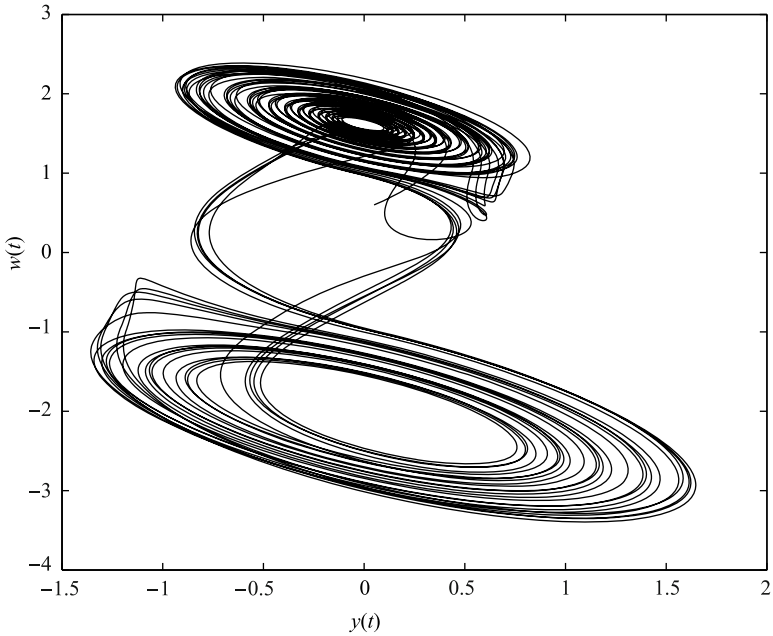

Fig. 5.14 Strange attractor of the memristor-based Chua's system projected onto $y - w$ plane.

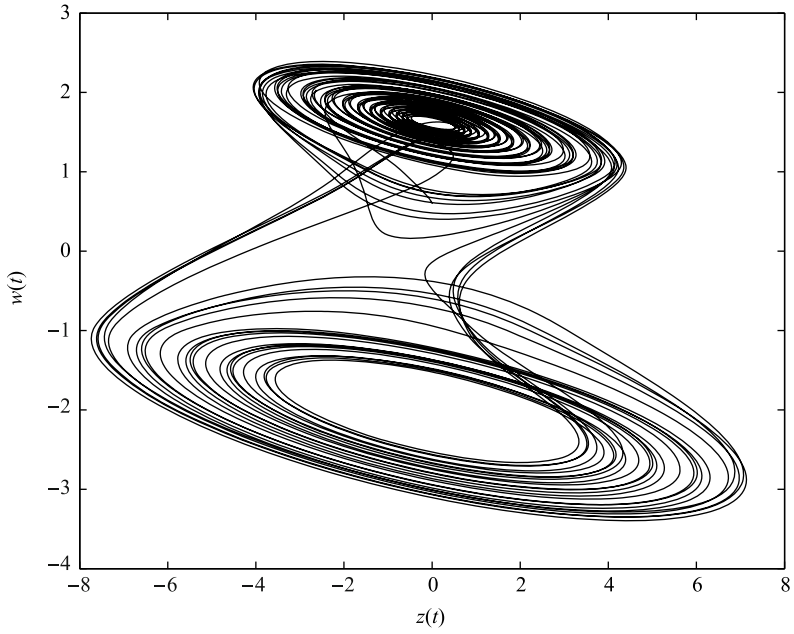

Fig. 5.15 Strange attractor of the memristor-based Chua's system projected onto $z - w$ plane.

$$\mathbf{J}_{Wb} = \begin{bmatrix} \alpha(-1+\zeta-b) & \alpha & 0 & 0 \\ 1 & -1 & 1 & 0 \\ 0 & -\beta & -\gamma & 0 \\ 1 & 0 & 0 & 0 \end{bmatrix}. \tag{5.32}$$

The characteristic equation for the linear part with the slope a with matrix (5.31) is

$$\det(\mathrm{diag}([\lambda^{mq_1}\,\lambda^{mq_2}\,\lambda^{mq_3}\,\lambda^{mq_4}]) - \mathbf{J}_{Wa}) = 0$$

and for linear part with the slope b and matrix (5.32) it has the form

$$\det(\mathrm{diag}([\lambda^{mq_1}\,\lambda^{mq_2}\,\lambda^{mq_3}\,\lambda^{mq_4}]) - \mathbf{J}_{Wb}) = 0.$$

When we consider a simple case where the fractional-order memristor-based Chua's system has commensurate order, which means $q_1 = q_2 = q_3 = q_4 \equiv q$, the stability can be investigated according to Theorem 4.5, where the condition is:

$$|\arg(\mathrm{eig}(\mathbf{J}_W))| = |\arg(\lambda_i)| > q\frac{\pi}{2}$$

for all eigenvalues λ_i.

As in the previous case, stability should be investigated for both piecewise-linear parts of memristor characteristic shown in Fig. 5.10. In this case it means that we should find the angle of all eigenvalues for both Jacobian matrices $\mathbf{J}_{Wa}$ and $\mathbf{J}_{Wb}$ respectively. A necessary stability condition for fractional-order systems (5.30) to remain chaotic is keeping at least one eigenvalue λ in the unstable region.

Because the frequency approximation techniques (Carlson and Halijak, 1963; Oustaloup et al., 2000) are unreliable in recognising chaos in fractional-order nonlinear systems (Tavazoei and Haeri, 2007a), for simulation purposes we use a numerical solution of the memristor-based Chua's equations (5.30) obtained by the method descibed in (Petráš, 2009a, 2010). It is a time domain method derived by using the relationship (2.53), which leads to equations in the following form:

$$\begin{aligned} x(t_k) &= \left(\alpha(y(t_{k-1}) - x(t_{k-1}) + \zeta x(t_{k-1}) - W(w(t_{k-1}))x(t_{k-1}))\right)h^{q_1} - \\ &\quad - \sum_{j=v}^{k} c_j^{(q_1)} x(t_{k-j}), \\ y(t_k) &= \left(x(t_k) - y(t_{k-1}) + z(t_{k-1})\right)h^{q_2} - \sum_{j=v}^{k} c_j^{(q_2)} y(t_{k-j}), \\ z(t_k) &= \left(-\beta y(t_k) - \gamma z(t_{k-1})\right)h^{q_3} - \sum_{j=v}^{k} c_j^{(q_3)} z(t_{k-j}), \\ w(t_k) &= x(t_k)h^{q_4} - \sum_{j=v}^{k} c_j^{(q_4)} w(t_{k-j}), \end{aligned} \tag{5.33}$$

where

$$\begin{aligned} W(w(t_{k-1})) &= a \quad \text{for} \quad |w(t_{k-1})| < 1, \\ W(w(t_{k-1})) &= b \quad \text{for} \quad |w(t_{k-1})| > 1, \end{aligned} \tag{5.34}$$

and where T_{sim} is the simulation time, $k = 1,2,3,\ldots,N$, for $N = [T_{sim}/h]$, and $(x(0), y(0), z(0), w(0))$ is the start point (initial conditions).

The binomial coefficients $c_j^{(q_i)}, \forall i$ are calculated according to relation (2.54).

If we consider the parameter set $\alpha = 10,\ \beta = 13,\ \gamma = 0.35,\ \zeta = 1.5,\ a = 0.3,$ and $b = 0.8$, according to Definition 4.5, for these parameters we are able to calculate a minimal commensurate order for which the system (5.30) remains chaotic. In this case it is $q > 0.98$.

Let us consider the paremeter set $\alpha = 10,\ \beta = 13,\ \gamma = 0.1,\ \zeta = 1.5,\ a = 0.3,$ and $b = 0.8$. For these parameters a minimal commensurate order is $q > 0.95$. We performed a simulation for the above parameters and commensurate order $q = 0.97$ $(q_1 = q_2 = q_3 = q_4 = 0.97)$. The total order of the system is 3.88.

In Fig. 5.16 and Fig. 5.17 are depicted chaotic attractors in 3D state space for $T_{sim} = 200\,s$. Both simulations were performed without using the short memory principle $(v = 1)$ for time step $h = 0.005$ with the initial conditions: $x(0) = 0.8, y(0) = 0.05, z(0) = 0.007, w(0) = 0.6$.

In Fig.5.18 and Fig. 5.19 are depicted the attractors of the memristor-based Chua's system (5.30) for parameters (5.35), $a = 0.3, b = 0.8$, orders $q_1 = q_2 = q_3 = q_4 = 0.97$, initial conditions: $x(0) = 0.8, y(0) = 0.05, z(0) = 0.007, w(0) = 0.6$ and simulation time $T_{sim} = 100\,s$, projected onto $y-w$, and $z-w$ planes, respectively.

When we consider real orders of capacitors models (Westerlund and Ekstam, 1994): $q_1 = q_2 = 0.98$, real order of inductor model (Schafer and Kruger, 2008): $q_3 = 0.99$, and we assume a real order of memristor model: $q_4 = 0.97$, for the parameters:

$$\alpha = 10, \quad \beta = 13, \quad \gamma = 0.1, \quad \zeta = 1.5, \tag{5.35}$$

$a = 0.3,\ b = 0.8$, the initial conditions: $x(0) = 0.8, y(0) = 0.05, z(0) = 0.007, w(0) = 0.6$, simulation time $T_{sim} = 100\,s$, and time step $h = 0.005$, we get the chaotic double-scroll attractor as well for the total system order 3.92.

In Fig. 5.20 and Fig. 5.21 are depicted chaotic attractors in 3D state space for $T_{sim} = 100\,s$. The simulations were performed without using the short memory principle $(v = 1)$ for time step $h = 0.005$ with the initial conditions: $x(0) = 0.8, y(0) = 0.05, z(0) = 0.007, w(0) = 0.6$. In this case, we just estimated the real order of the memristor. Simulations show double-scroll atractors and we can observe a chaotic behavior.

The characteristic equation of the system (5.30) with parameters (5.35), orders $q_1 = q_2 = 0.98 = 98/100,\ q_3 = 0.99 = 99/100,\ q_4 = 0.97 = 97/100$, for Jacobian (5.31) is

$$\lambda^{392} - \lambda^{294} + \frac{\lambda^{293}}{10} - 12\lambda^{196} + \frac{129\lambda^{195}}{10} - \frac{136\lambda^{97}}{5} = 0$$

and for Jacobian (5.32) it has form

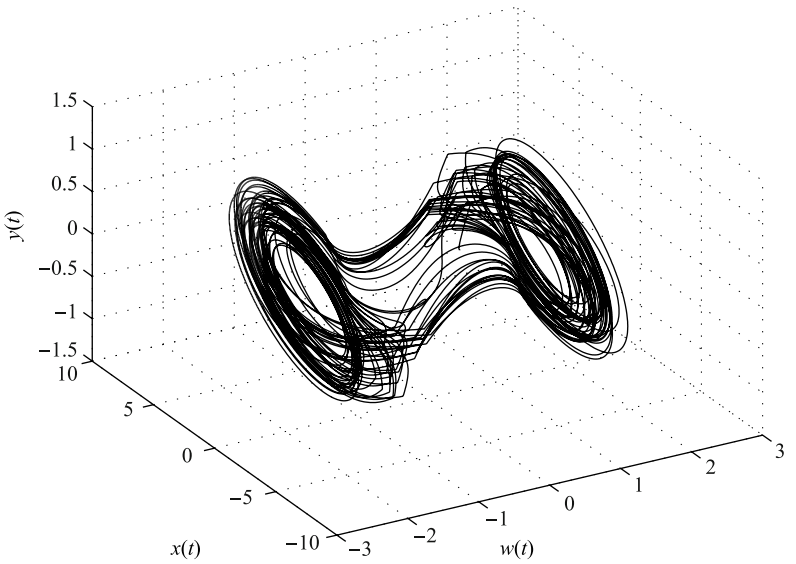

Fig. 5.16 Strange attractor of the memristor-based Chua's system (5.30) in $w-x-y$ state space, for parameters $\alpha = 10,\ \ \beta = 13,\ \ \gamma = 0.1,\ \ \zeta = 1.5,\ \ a = 0.3, b = 0.8$, orders $q_1 = q_2 = q_3 = q_4 = 0.97$, initial conditions: $x(0) = 0.8, y(0) = 0.05, z(0) = 0.007, w(0) = 0.6$ and simulation time $T_{sim} = 200\,s$.

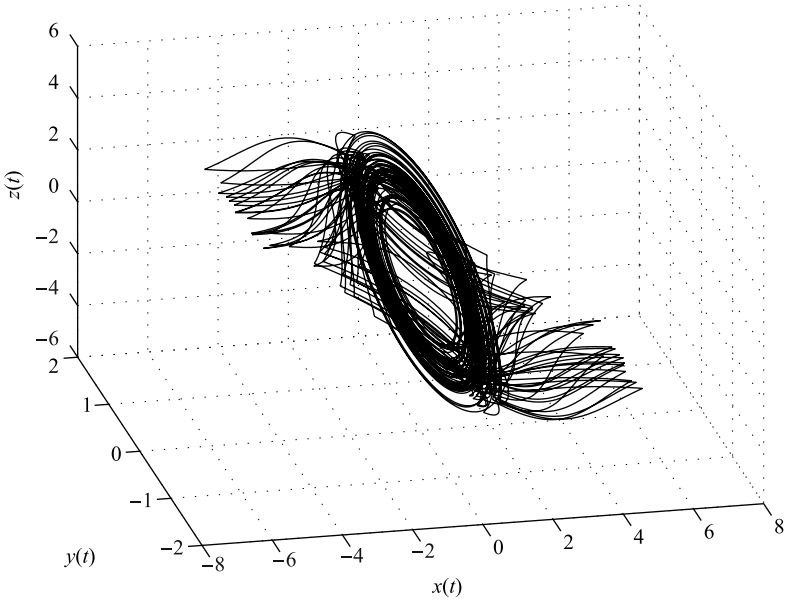

Fig. 5.17 Strange attractor of the memristor-based Chua's system (5.30) in $x-y-z$ state space, for parameters $\alpha = 10,\ \ \beta = 13,\ \ \gamma = 0.1,\ \ \zeta = 1.5,\ \ a = 0.3, b = 0.8$, orders $q_1 = q_2 = q_3 = q_4 = 0.97$, initial conditions: $x(0) = 0.8, y(0) = 0.05, z(0) = 0.007, w(0) = 0.6$ and simulation time $T_{sim} = 200\,s$.

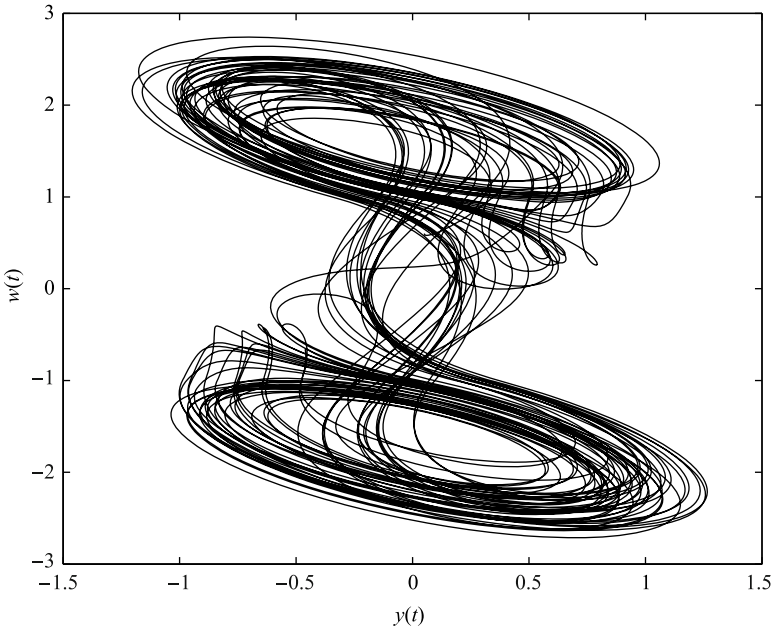

Fig. 5.18 Strange attractor of the memristor-based Chua's system projected onto $y - w$ plane.

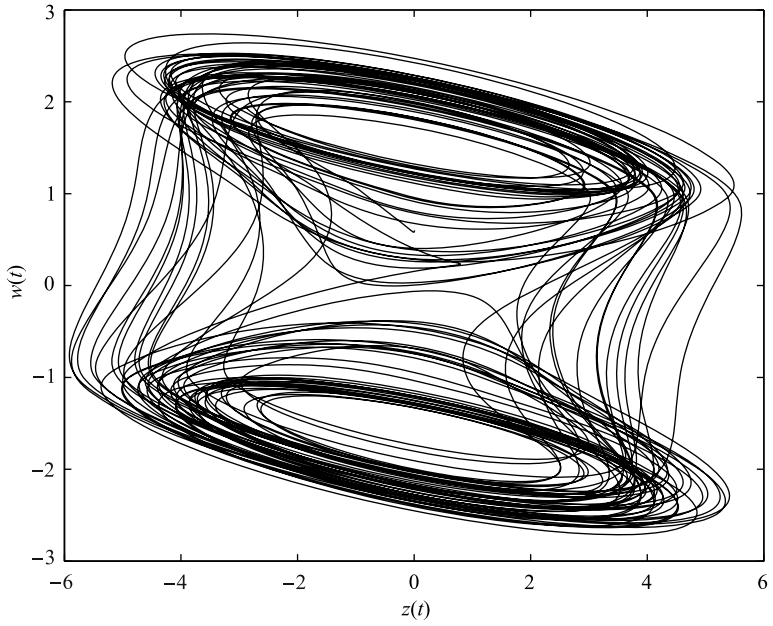

Fig. 5.19 Strange attractor of the memristor-based Chua's system projected onto $z - w$ plane.

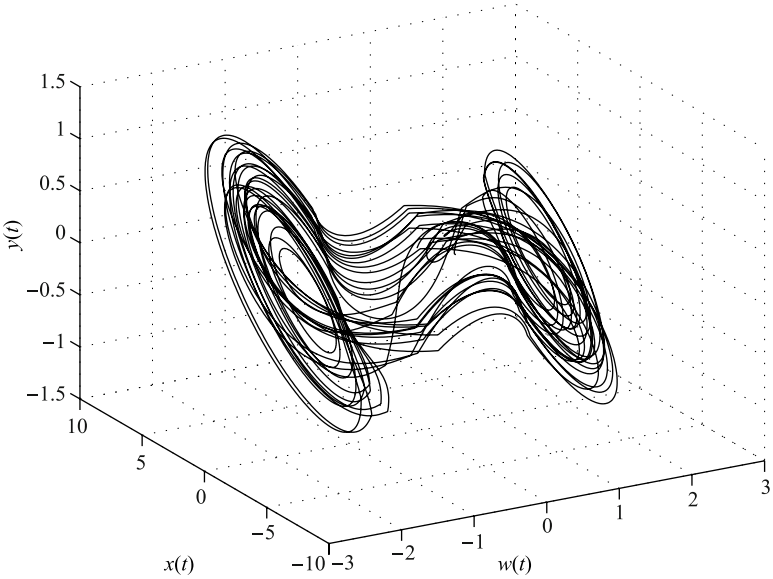

Fig. 5.20 Strange attractor of the memristor-based Chua's system (5.30) in $w-x-y$ state space, for parameters $\alpha = 10,\ \ \beta = 13,\ \ \gamma = 0.1,\ \ \zeta = 1.5,\ \ a = 0.3, b = 0.8$, orders $q_1 = q_2 = 0.98$, $q_3 = 0.99,\ q_4 = 0.97$, initial conditions: $x(0) = 0.8, y(0) = 0.05, z(0) = 0.007, w(0) = 0.6$ and simulation time $T_{sim} = 100\,s$.

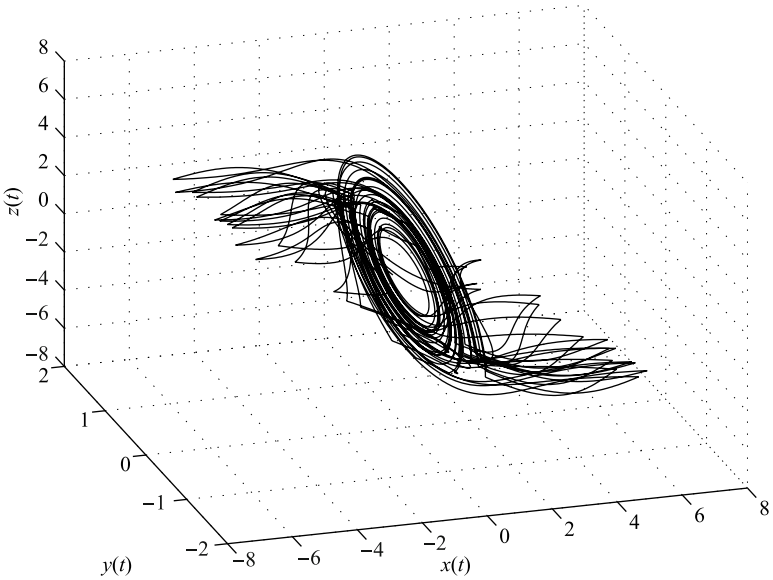

Fig. 5.21 Strange attractor of the memristor-based Chua's system (5.30) in $x-y-z$ state space, for parameters $\alpha = 10,\ \ \beta = 13,\ \ \gamma = 0.1,\ \ \zeta = 1.5,\ \ a = 0.3, b = 0.8$, orders $q_1 = q_2 = 0.98$, $q_3 = 0.99,\ q_4 = 0.97$, initial conditions: $x(0) = 0.8, y(0) = 0.05, z(0) = 0.007, w(0) = 0.6$ and simulation time $T_{sim} = 100\,s$.

$$\lambda^{392} + 4\lambda^{294} + \frac{\lambda^{293}}{10} - 7\lambda^{196} + \frac{67\lambda^{195}}{5} + \frac{383\lambda^{97}}{10} = 0.$$

Both above characteristic equations are polynomials of very high order and it is difficult to find the roots of such polynomials. For the system to remain chaotic, there should be at least one root λ in the unstable region, which means that $|\arg(\lambda)| < \pi/200$.

Because of roots calculation problem, we can predict one unstable eigevalue and assume that the stability condition for chaos is satisfied. It can be indirectly proved via the double-scroll attractor, which can be observed in Fig. 5.20.

In Fig. 5.22 and Fig. 5.23 are depicted the attractors of the memristor-based Chua's system (5.30) for parameters (5.35), $a = 0.3$, $b = 0.8$, orders $q_1 = q_2 = 0.98$, $q_3 = 0.99$, $q_4 = 0.97$, initial conditions: $x(0) = 0.8, y(0) = 0.05, z(0) = 0.007, w(0) = 0.6$ and simulation time $T_{sim} = 100\,s$, projected onto $y-w$, and $z-w$ planes, respectively. These strange attractors also indirectly confirm that the system is chaotic.

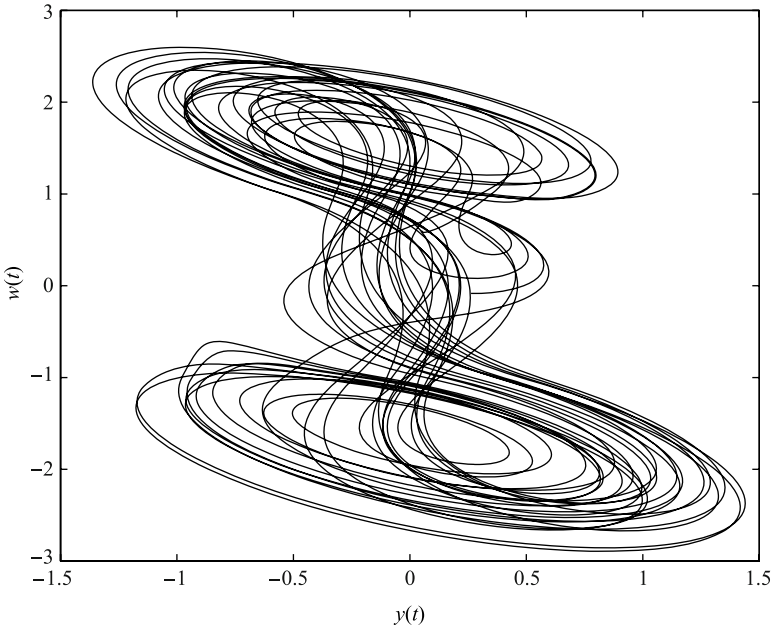

Fig. 5.22 Strange attractor of the memristor-based Chua's system projected onto $y-w$ plane.

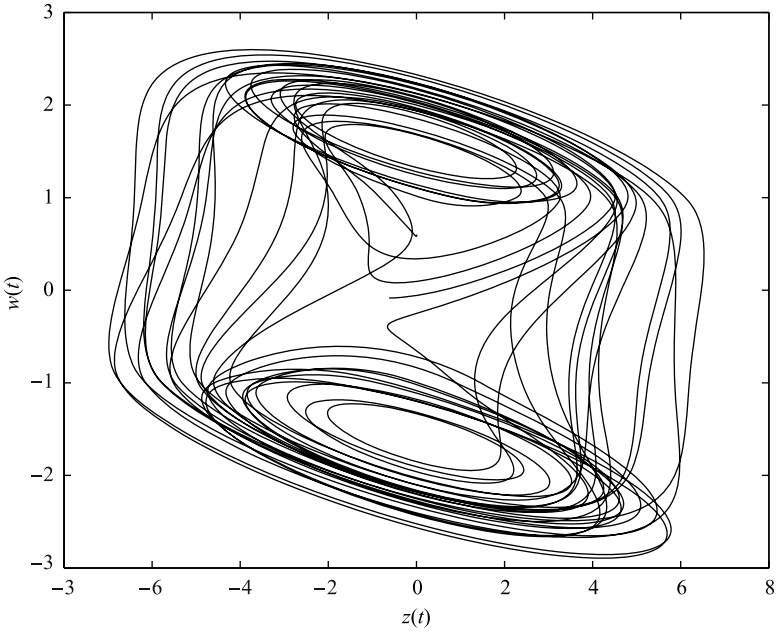

Fig. 5.23 Strange attractor of the memristor-based Chua's system projected onto $z-w$ plane.

5.3 Fractional-Order Van der Pol Oscillator

The Van der Pol oscillator (VPO) represents a nonlinear system with an interesting behavior that exhibits naturally in several applications. It has been used for study and design of many models including biological phenomena, such as the heartbeat, neurons, acoustic models, radiation of mobile phones, and as a model of electrical oscillators (implemented with a tunnel diode, memristor or operating amplifier).

The VPO model was used by Van der Pol in 1920 to study oscillations in vacuum tube circuits. In the standard form, it is given by a nonlinear differential equation of type:

$$y''(t)+\varepsilon(y(t)^2-1)y'(t)+y(t)=0, \tag{5.36}$$

where ε is the control parameter. Equation (5.36) can be rewritten into its state-space representation as follows:

$$\begin{aligned}\frac{dy_1}{dt} &= y_2(t),\\ \frac{dy_2}{dt} &= -y_1(t)-\varepsilon(y_1^2(t)-1)y_2(t),\end{aligned} \tag{5.37}$$

with an equilibrium point in origin. The Jacobian matrix of the system (5.37) is

$$\mathbf{J} = \begin{bmatrix} 0 & 1 \\ -1 - 2\varepsilon y_1^* y_2^* & -\varepsilon(y_1^{*2} - 1) \end{bmatrix} \tag{5.38}$$

for the equilibrium point $E^* = (y_1^*, y_2^*)$.

A modified version of the classical VPO was proposed by fractional derivative of order q in a state space formulation of Eq. (5.37). It has the following form (Chen and Chen, 2008; Barbosa et al., 2007):

$$\begin{aligned} {}_0D_t^q y_1(t) &= y_2(t), \\ \frac{dy_2}{dt} &= -y_1(t) - \varepsilon(y_1^2(t) - 1)y_2(t), \end{aligned} \tag{5.39}$$

where the order is $0 < q < 1$ and $\varepsilon > 0$. The resulting fractional-order Van der Pol oscillator (FrVPO) reduces to the classical VPO when $q = 1$. The total system order is changed from the integer value 2 to the fractional value $1 + q < 2$. If we consider $q = 0.9 = 9/10$ and $\varepsilon = 1$ then the characteristic equation of the system (5.39) for $\gamma = 1/10$ is $\det(\lambda^\gamma \mathbf{I} - \mathbf{J}) = 0$, that is,

$$\lambda^{19} + \lambda^9 + 1 = 0.$$

All equation roots λ_i satisfy the condition $|\arg(\lambda_i)| > \pi/20$ for $(i = 1, 2, \ldots, 19)$ and therefore the system is stable. Detailed analysis of the fractional-order Van der Pol system for various system orders has been made in (Barbosa et al., 2007; Ge and Hsu, 2007). This analysis may be useful for a better understanding and control of such system.

In Fig. 5.24 is depicted the limit cycle in the phase plane of the fractional-order Van der Pol oscillator (5.39) for simulation time $T_{sim} = 30\,s$ and time step $h = 0.005$.

Let us consider the modified version of the FrVPO in the following form:

$$\begin{aligned} {}_0D_t^{q_1} y_1(t) &= y_2(t), \\ {}_0D_t^{q_2} y_2(t) &= -y_1(t) - \varepsilon(y_1^2(t) - 1)y_2(t), \end{aligned} \tag{5.40}$$

where q_1 and q_2 are orders $(0 < q_{1,2} < 2)$ and $\varepsilon > 0$. If we consider $q_1 = q_2 \equiv q$ in (5.40), we obtain a commensurate-order system. The characteristic equation of the commensurate-order system (5.40) is $\det(\lambda^q \mathbf{I} - \mathbf{J}) = 0$ and the stability condition is $|\arg(\mathrm{eig}(\mathbf{J}))| > q\pi/2$.

For simulation purpose, we derived a numerical solution of the FrVPO, obtained by using the relations (2.53) and (2.54), which has the following form:

$$\begin{aligned} y_1(t_k) &= y_2(t_{k-1})h^{q_1} - \sum_{j=v}^{k} c_j^{(q_1)} y_1(t_{k-j}), \\ y_2(t_k) &= \left(-y_1(t_k) - \varepsilon(y_1^2(t_k) - 1)y_2(t_{k-1})\right) h^{q_2} - \sum_{j=v}^{k} c_j^{(q_2)} y_2(t_{k-j}), \end{aligned} \tag{5.41}$$

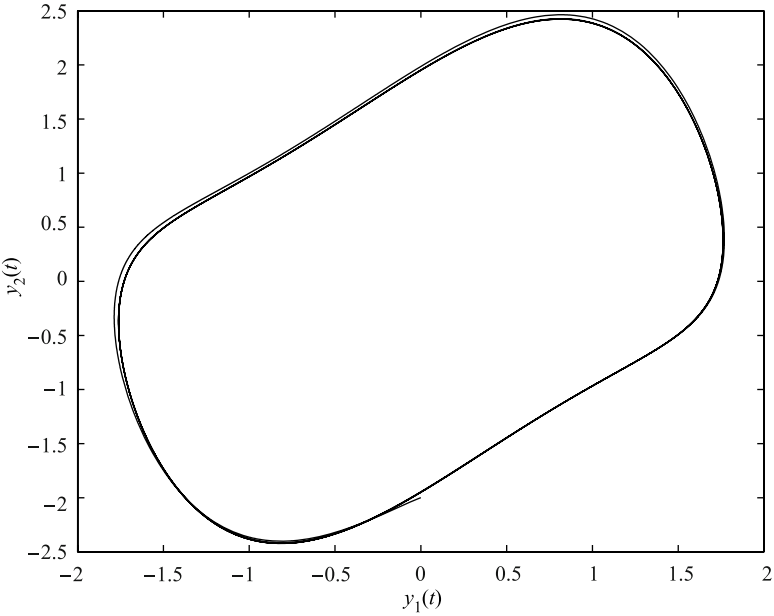

Fig. 5.24 Limit cycle in phase plane $y_1 - y_2$ for FrVPO with fractional order $q = 0.9$, parameter $\varepsilon = 1$, and initial conditions $(y_1(0), y_2(0)) = (0, -2)$.

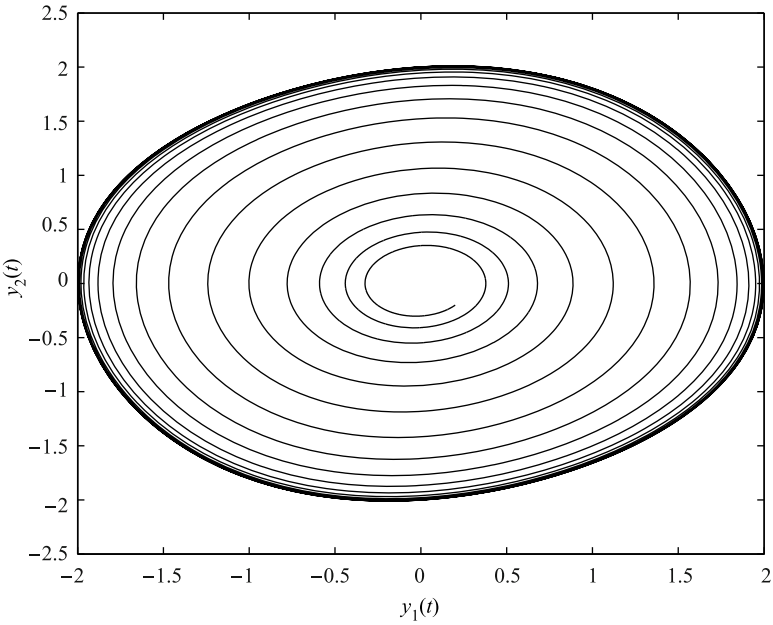

Fig. 5.25 Oscillation in phase plane $y_1 - y_2$ for FrVPO with integer-orders $q_1 = q_2 = 1.0$, parameter $\varepsilon = 0.1$, and initial conditions $(y_1(0), y_2(0)) = (0.2, -0.2)$.

where T_{sim} is the simulation time, $k = 1,2,3,\ldots,N$, for $N = [T_{sim}/h]$, and $(y_1(0), y_2(0))$ is the start point (initial conditions). The binomial coefficients $c_j^{(q_i)}, \forall i$ are calculated according to relation (2.54).

In Fig. 5.25 and Fig. 5.26 are depicted the oscillations in the phase plane of the fractional-order Van der Pol oscillator (5.39) for various orders q_1 and q_2, parameter ε, simulation time $T_{sim} = 60\,s$ and time step $h = 0.005$.

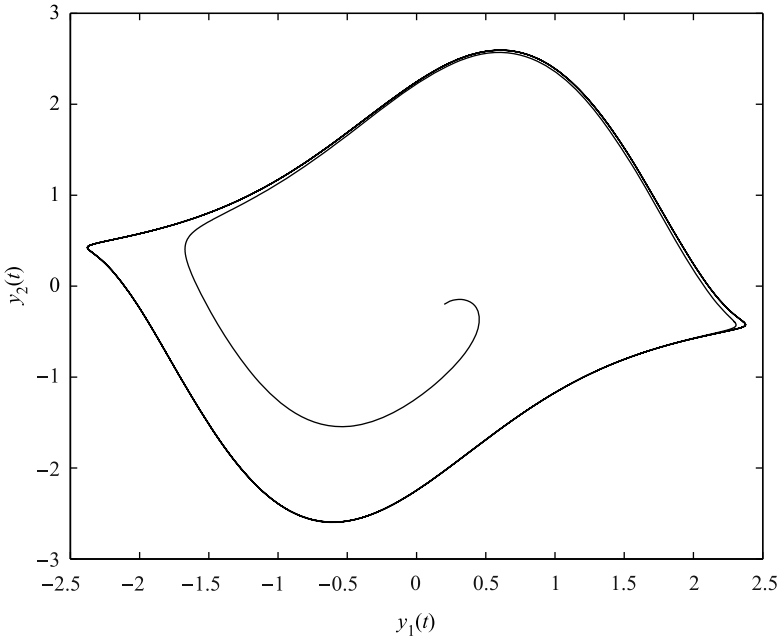

Fig. 5.26 Limit cycle in phase plane $y_1 - y_2$ for FrVPO with fractional-orders $q_1 = 1.2,\ q_2 = 0.8$, parameter $\varepsilon = 1$, and initial conditions $(y_1(0), y_2(0)) = (0.2, -0.2)$.

5.4 Fractional-Order Duffing's Oscillator

Duffing's oscillator, introduced in 1918 by G. Duffing, with negative linear stiffness, damping and periodic excitation is often written in the form

$$x''(t) - x(t) + \alpha x'(t) + x^3(t) = \delta \cos(\omega t). \tag{5.42}$$

Equation (5.42) can be extended to the complex domain in order to study strange attractors and chaotic bahavior of forced vibrations of industrial machinery. The periodically forced complex Duffing's oscillators have the form

$$z''(t) - z(t) + \alpha z'(t) + \varepsilon z|z^2(t)| = \gamma' \cos(\omega t), \tag{5.43}$$

where $\gamma' = \sqrt{2\gamma}e^{j\pi/4}$, γ, α, ω are positive parameters, $z = x + jy$ is a complex function. Equation (5.43) can be reduced to the famous Duffing's oscillator (5.42) when $z = x, (y = 0)$ and $\varepsilon = 1$. When we substitute $z = x + jy$ into Eq. (5.43), we get a system of two coupled nonlinear second-order differential equations (Gao and Yu, 2005):

$$\begin{aligned} x''(t) - x(t) + \alpha x'(t) + \varepsilon x(t)(x^2(t) + y^2(t)) &= \gamma \cos(\omega t), \\ y''(t) - y(t) + \alpha y'(t) + \varepsilon y(t)(x^2(t) + y^2(t)) &= \gamma \cos(\omega t). \end{aligned} \tag{5.44}$$

To get the fractional-order Duffing's system, Equation (5.42) can be rewritten as a system of the first-order autonomous differential equations in the form:

$$\begin{aligned} \frac{x(t)}{dt} &= y(t), \\ \frac{y(t)}{dt} &= x(t) - x^3(t) - \alpha y(t) + \delta \cos(\omega t). \end{aligned} \tag{5.45}$$

Here, the conventional derivatives in Eqs. (5.45) are replaced by the fractional derivatives as follows:

$$\begin{aligned} {}_0D_t^{q_1} x(t) &= y(t), \\ {}_0D_t^{q_2} y(t) &= x(t) - x^3(t) - \alpha y(t) + \delta \cos(\omega t), \end{aligned} \tag{5.46}$$

where q_1, q_2 are two fractional orders and α, δ, ω are the system parameters.

The Jacobian matrix of the Duffing's system is

$$\mathbf{J} = \begin{bmatrix} 0 & 1 \\ 1 - 3x^* & -\alpha \end{bmatrix} \tag{5.47}$$

for the equilibrium point $E^* = (x^*, y^*)$. The characteristic equation of the linearized incommensurate-order system (5.46) for $\gamma = 1/m$ is $\det(\lambda^{\gamma}\mathbf{I} - \mathbf{J}) = 0$, where m is the LCM of the denominators u_i, if we set $q_i = v_i/u_i$, $v_i, u_i \in Z^+$ for $i = 1, 2$. The stability condition is $|\arg(\lambda_i)| > \gamma\pi/2$ for all roots λ_i of the characteristic equation.

A numerical solution of the fractional-order Duffing's system (5.46), obtained by using the relations (2.53) and (2.54), has the following form:

$$\begin{aligned} x(t_k) &= y(t_{k-1})h^{q_1} - \sum_{j=v}^{k} c_j^{(q_1)} x(t_{k-j}), \\ y(t_k) &= \left(x(t_k) - x^3(t_k) - \alpha y(t_{k-1}) + \delta \cos(\omega t_k)\right) h^{q_2} - \sum_{j=v}^{k} c_j^{(q_2)} y(t_{k-j}), \end{aligned} \tag{5.48}$$

where T_{sim} is the simulation time, $k = 1, 2, 3, \ldots, N$, for $N = [T_{sim}/h]$, and $(x(0), y(0))$ is the start point (initial conditions).

Let us investigate the integer-order Duffing's system (5.45) with parameters $\alpha = 0.15$, $\delta = 0.3$, $\omega = 1$. This system has three fixed points (equilibria): $E_1 = (1.07288371;0)$, $E_2 = (-0.90615851;0)$, and $E_3 = (-0.16672520;0)$ and their stability can be studied by computing the corresponding eigenvalues. For equilibrium E_1 we obtain the eigenvalues $\lambda_{1,2} = -0.0750 \pm 1.487624\,j$, for E_2 we get $\lambda_1 \approx 1.8547928$, $\lambda_2 \approx -2.004792873$ and for E_3 we have $\lambda_1 \approx 1.1521106$, $\lambda_2 \approx -1.3021106$. The eigenvalues λ_1 and λ_2 of the equilibrium points E_2 and E_3 are saddle points which satisfy the stability condition for chaotic behavior.

In Fig. 5.27 is depicted chaotic attractor of the integer-order Duffing's system (5.45) for the following parameters $\alpha = 0.15$, $\delta = 0.3$, $\omega = 1$ with initial conditions $(x(0), y(0)) = (0.21, 0.13)$ for simulation time $T_{sim} = 200\,s$ and time step $h = 0.005$.

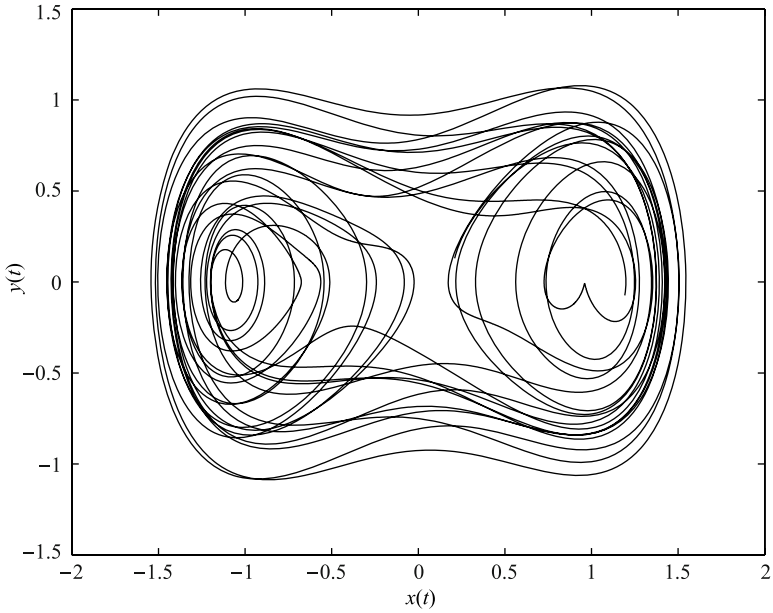

Fig. 5.27 Phase trajectory (attractor) in plane $x - y$ for the integer-order Duffing's system (5.45) with parameters $\alpha = 0.15$, $\delta = 0.3$, $\omega = 1$, and initial conditions $(x(0), y(0)) = (0.21, 0.13)$.

When we assume commensurate orders $q_1 = q_2 = 0.95$ and parameters $\alpha = 0.5$, $\delta = 1.3$, $\omega = 1$ in system (5.46), we obtain a stable limit cycle. All roots of the characteristic equation satisfy the stability condition.

In Fig. 5.28 is depicted the limit cycle of the fractional-order Duffing's system (5.46) for the following parameters $\alpha = 0.5$, $\delta = 1.3$, $\omega = 1$, derivative orders $q_1 = q_2 = 0.95$ with initial conditions $(x(0), y(0)) = (1.0, 1.0)$ for simulation time $T_{sim} = 100\,s$ and time step $h = 0.005$.

In addition, we consider an incommensurate-order system (5.46) with parameters $\alpha = 0.15$, $\delta = 0.3$, $\omega = 1$ and orders $q_1 = 0.9 = 9/10$, and $q_2 = 1.0 = 10/10$. The system has three equilibria and we should investigate the stability of all equilibrium

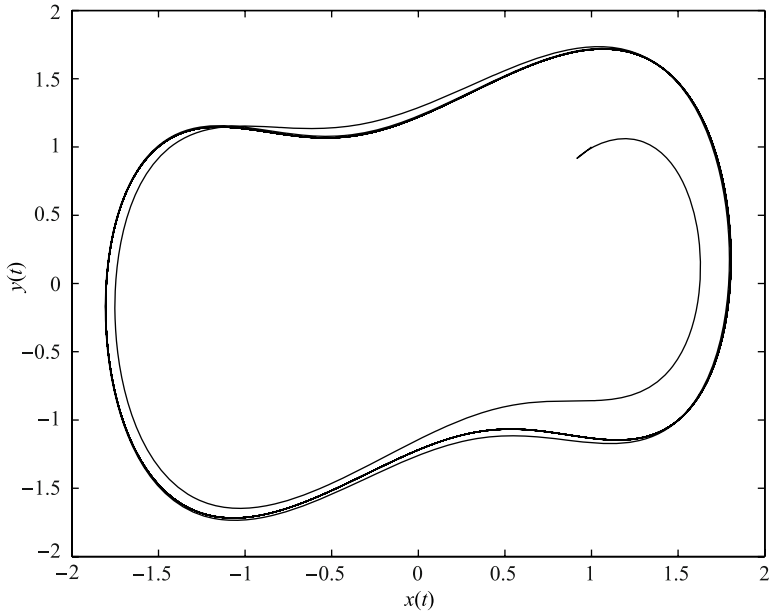

Fig. 5.28 Phase trajectory (limit cycle) in plane $x-y$ for the fractional-order Duffing's system (5.46) with parameters $\alpha = 0.5$, $\delta = 1.3$, $\omega = 1$, derivative orders $q_1 = q_2 = 0.95$, and initial conditions $(x(0), y(0)) = (1.0, 1.0)$.

points. Because of the system parameters, the equilibrium points are the same as in the case of integer-order system. For the equilibrium E_1 the characteristic equation of linearized system is

$$\lambda^{19} + 3/20\lambda^{9} - 3.7184755 = 0,$$

and it has one unstable root $\lambda \approx 1.0673$ because $|\arg(\lambda)| < \pi/20$. For the equilibrium E_2 the characteristic equation of the linearized system is

$$\lambda^{19} + 3/20\lambda^{9} - 1.5001756 = 0,$$

and it has one unstable root $\lambda \approx 1.0151$ because $|\arg(\lambda)| < \pi/20$. Both equilibrium points are unstable nodes. The equilibrium E_3 is a stable focus. The condition to have at least one root in the unstable region in order for the system to be chaotic is satisfied.

In Fig. 5.29 is depicted double scroll attractor of the fractional-order Duffing's system (5.46) for the following parameters $\alpha = 0.15$, $\delta = 0.3$, $\omega = 1$, derivative orders $q_1 = 0.9, q_2 = 1.0$ with initial conditions $(x(0), y(0)) = (0.21, 0.13)$ for simulation time $T_{sim} = 200\,s$ and time step $h = 0.005$.

An alternative and a bit modified version of the fractional-order Duffing's system and its phase portraits, Poincaré maps, bifurcation diagram and chaotic behavior was

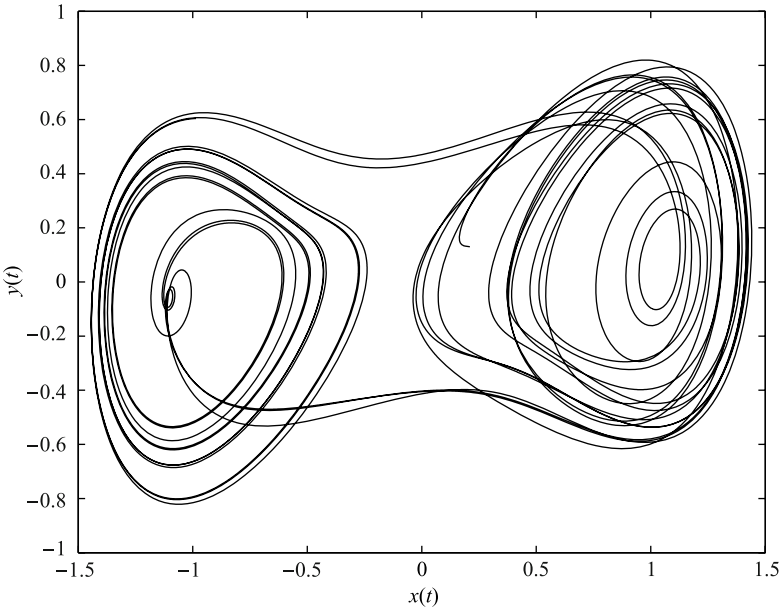

Fig. 5.29 Phase trajectory (attractor) in plane $x-y$ for the fractional-order Duffing's system (5.46) with parameters $\alpha = 0.15$, $\delta = 0.3$, $\omega = 1$, derivative orders $q_1 = 0.9, q_2 = 1.0$, and initial conditions $(x(0), y(0)) = (0.21, 0.13)$.

studied in (Ge and Ou, 2007). The chaotic system reported in the above-mentioned paper considered the Duffing's chaotic system to be an autonomous system with four state variables $x(t)$, $y(t)$, $z(t)$, and $w(t)$ and has the following form:

$$\begin{aligned} {}_0D_t^{q_1} x(t) &= y(t), \\ {}_0D_t^{q_2} y(t) &= -x(t) - x^3(t) - ay(t) + bz(t), \\ {}_0D_t^{q_3} z(t) &= w(t), \\ {}_0D_t^{q_4} w(t) &= -cz(t) - dz^3(t), \end{aligned} \tag{5.49}$$

where a, b, c are constant parameters of the system and q_1, q_2, q_3 and q_4 are fractional-order numbers. Usually, the system parameter b is allowed to be variable.

Chaos was found in system (5.49) for the lowest total order of the system 3.8 (Ge and Ou, 2007).

5.5 Fractional-Order Lorenz's System

The Lorenz oscillator is a three-dimensional dynamical system that exhibits chaotic flow. The Lorenz attractor was named after Edward N. Lorenz, who derived it from

the simplified equations of convection rolls arising in the equations of the atmosphere in 1963. He for the first time used the term "butterfly effect", which in chaos theory means sensitive dependence on initial conditions. Lorenz wrote a paper in 1979 entitled "Predictability: Does the Flap of a Butterfly's Wings in Brazil Set Off a Tornado in Texas?" Small variations of the initial condition of a dynamical system may produce large variations in the long-term behavior of the system. The phrase refers to the idea that a butterfly's wings might create tiny changes in the atmosphere that may ultimately alter the path of a tornado or delay, accelerate or even prevent the occurrence of a tornado in a certain location. The flapping wing represents a small change in the initial condition of the system, which causes a chain of events leading to large-scale alterations of events.

Lorenz's chaotic system is desribed by

$$\begin{aligned} \frac{dx(t)}{dt} &= \sigma(y(t)-x(t)), \\ \frac{dy(t)}{dt} &= x(t)(\rho - z(t)) - y(t), \\ \frac{dz(t)}{dt} &= x(t)y(t) - \beta z(t), \end{aligned} \tag{5.50}$$

where σ is called the Prandtl number and ρ is called the Rayleigh number. All $\sigma, \rho, \beta > 0$, but usually $\sigma = 10$, $\beta = 8/3$ and ρ is varied. The system exhibits chaotic behavior for $\rho = 28$ and displays orbits for other values.

Lorenz's system has three equilibria, where one is obviously in origin $E_1 = (0;0;0)$ and the other two are: $E_2 = (\sqrt{(\beta\rho - \beta)};\ \sqrt{(\beta\rho - \beta)};\ \rho - 1)$, $E_3 = (-\sqrt{(\beta\rho - \beta)};\ -\sqrt{(\beta\rho - \beta)};\ \rho - 1)$. The Jacobian matrix of Lorenz's system (5.50) at the equilibrium point $E^* = (x^*, y^*, z^*)$ is given by

$$\mathbf{J} = \begin{bmatrix} -\sigma & \sigma & 0 \\ \rho - z^* & -1 & -x^* \\ y^* & x^* & -\beta \end{bmatrix}. \tag{5.51}$$

The equilibrium points of the system with the above parameters are: $E_1 = (0;0;0)$, $E_2 = (8.4853;8.4853;27)$, and $E_3 = (-8.4853;-8.4853;27)$.

The fractional-order Lorenz's system is described as (e.g. (Li and Yan, 2007)):

$$\begin{aligned} {}_0D_t^{q_1} x(t) &= \sigma(y(t)-x(t)), \\ {}_0D_t^{q_2} y(t) &= x(t)(\rho - z(t)) - y(t), \\ {}_0D_t^{q_3} z(t) &= x(t)y(t) - \beta z(t), \end{aligned} \tag{5.52}$$

where q_1, q_2, and q_3 are derivative orders.

The numerical solution of the fractional-order Lorenz's system has the following form:

$$x(t_k) = (\sigma(y(t_{k-1}) - x(t_{k-1})))h^{q_1} - \sum_{j=v}^{k} c_j^{(q_1)} x(t_{k-j}),$$

$$y(t_k) = (x(t_k)(\rho - z(t_{k-1})) - y(t_{k-1}))h^{q_2} - \sum_{j=v}^{k} c_j^{(q_2)} y(t_{k-j}), \tag{5.53}$$

$$z(t_k) = (x(t_k)y(t_k) - \beta z(t_{k-1}))h^{q_3} - \sum_{j=v}^{k} c_j^{(q_3)} z(t_{k-j}),$$

where T_{sim} is the simulation time, $k = 1,2,3,\ldots,N$, for $N = [T_{sim}/h]$, and $(x(0), y(0), z(0))$ is the start point (initial conditions). The binomial coefficients $c_j^{(q_i)}, \forall i$ are calculated according to the relation (2.54).

To determine a minimal order for which the Lorenz system is chaotic with the parameters $(\sigma,\rho,\beta) = (10,28,8/3)$, we can use the relation (4.42). In this case the minimal commensurate order is $q > 0.9941$, if we consider $q_1 = q_2 = q_3 \equiv q$.

Let us set $q_1 = q_2 = q_3 = 0.995$, the fractional-order Lorenz's system (5.52) has a chaotic attractor as depicted in Fig. 5.30 – Fig. 5.32.

In Fig. 5.30 – Fig. 5.32 are depicted the simulation results of the Lorenz system (5.52) for the following parameters: $\sigma = 10, \rho = 28, \beta = 8/3$, orders $q_1 = q_2 = q_3 = 0.995$ and computational time $100\,s$ for time step $h = 0.005$.

In case of the incommensurate orders (q_1, q_2, q_3) of the system (5.52), the stability at the equilibrium can be investigated via characteristic equation $\det(\lambda^{\gamma}\mathbf{I} - \mathbf{J}) = 0$, for $\gamma = 1/m$, where m is the LCM of the denominators u_i, if we set $q_i = v_i/u_i$, $v_i, u_i \in Z^+$ for $i = 1,2,3$, and the stability condition $|\arg(\lambda)| > \gamma\pi/2$.

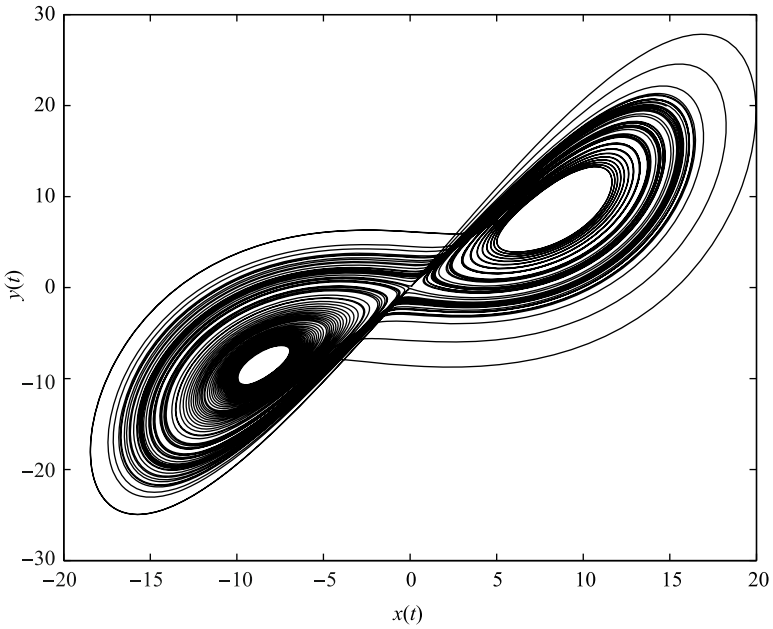

Fig. 5.30 Simulation result of the Lorenz system (5.52) in $x-y$ plane for parameters: $\sigma = 10, \rho = 28, \beta = 8/3$, orders $q_1 = q_2 = q_3 = 0.995$, and initial conditions $(x(0), y(0), z(0)) = (0.1, 0.1, 0.1)$.

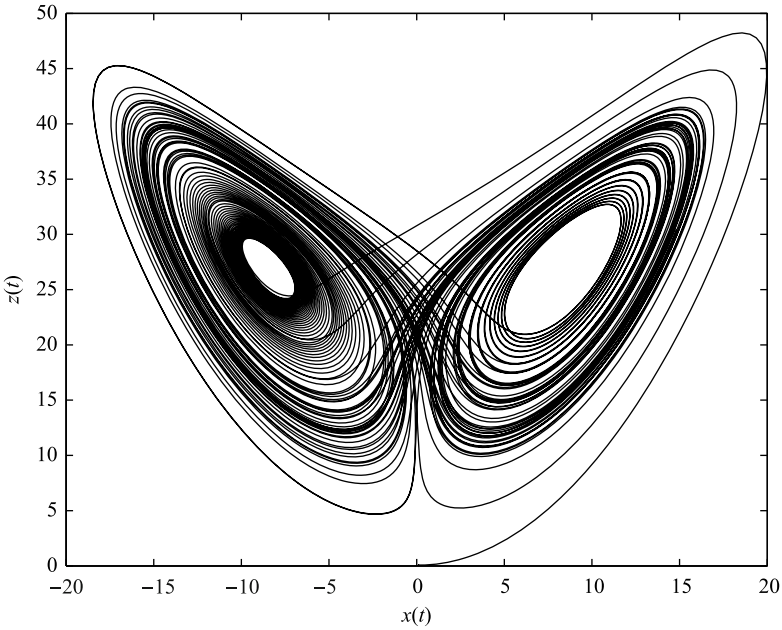

Fig. 5.31 Simulation result of the Lorenz system (5.52) in $x-z$ plane for parameters: $\sigma = 10, \rho = 28, \beta = 8/3$, orders $q_1 = q_2 = q_3 = 0.995$, and initial conditions $(x(0), y(0), z(0)) = (0.1, 0.1, 0.1)$.

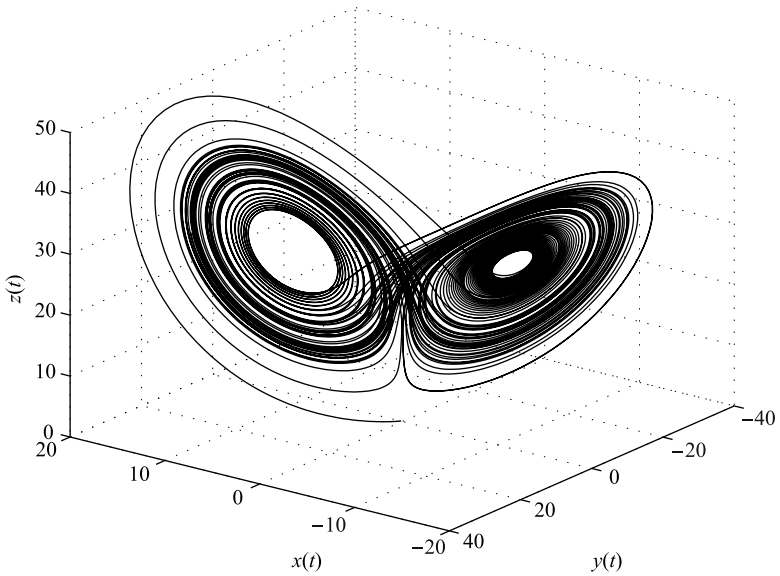

Fig. 5.32 Simulation result of the Lorenz system (5.52) in state space for parameters: $\sigma = 10, \rho = 28, \beta = 8/3$, orders $q_1 = q_2 = q_3 = 0.995$, and initial conditions $(x(0), y(0), z(0)) = (0.1, 0.1, 0.1)$.

5.6 Fractional-Order Chen's System

In 1999, Chen found another a simple three-dimensional autonomous system, which is not topologically equivalent to Lorenz's system and which has a chaotic attractor as well. Chen's system is described by the following equations (Lu and Chen, 2002; Zhou et al., 2004):

$$\begin{aligned}\frac{dx(t)}{dt} &= a(y(t)-x(t)),\\ \frac{dy(t)}{dt} &= (c-a)x(t)-x(t)z(t)+cy(t),\\ \frac{dz(t)}{dt} &= x(t)y(t)-bz(t),\end{aligned} \tag{5.54}$$

where $(a,b,c)\in R^3$. When $(a,b,c)=(35,3,28)$ the chaotic attractor exists.

The equilibrium points of the system with the above parameters are: $E_1 = (0;0;0)$, $E_2 = (7.9373;7.9373;21)$, and $E_3 = (-7.9373;-7.9373;21)$.

The Jacobian matrix of Chen's system (5.54) at the equilibrium point $E^* = (x^*,y^*,z^*)$ is given by

$$\mathbf{J} = \begin{bmatrix} -a & a & 0\\ c-a-z^* & c & -x^*\\ y^* & x^* & -\beta \end{bmatrix}. \tag{5.55}$$

For the equilibrium E_1 we obtain the eigenvalues $\lambda_1 = -3$, $\lambda_2 \approx 23.8359$, and $\lambda_3 \approx -30.8359$, for E_2 we get $\lambda_1 \approx -18.4280$, and $\lambda_{2,3} \approx 4.2140 \pm 14.8846j$, and for E_3 we have $\lambda_1 \approx -18.4280$, $\lambda_{2,3} \approx 4.2140 \pm 14.8846j$. The eigenvalues λ_1, λ_2 and λ_3 show that the equilibrium E_1 is a saddle point, the equilibria E_2 and E_3 are saddle-focus points. All of them satisfy the stability condition to keep chaotic behavior.

The fractional-order Chen's system is described as (Lu and Chen, 2006):

$$\begin{aligned}{}_0D_t^{q_1}x(t) &= a(y(t)-x(t)),\\ {}_0D_t^{q_2}y(t) &= (c-a)x(t)-x(t)z(t)+cy(t),\\ {}_0D_t^{q_3}z(t) &= x(t)y(t)-bz(t),\end{aligned} \tag{5.56}$$

where $0 < q_1,q_2,q_3 \le 1$, its total order is denoted by $\bar{q} = (q_1,q_2,q_3)$.

Numerical solution of the fractional-order Chen's system has the following form:

$$\begin{aligned}x(t_k) &= \left(a(y(t_{k-1})-x(t_{k-1}))\right)h^{q_1} - \sum_{j=v}^{k} c_j^{(q_1)}x(t_{k-j}),\\ y(t_k) &= \left(dx(t_k)-x(t_k)z(t_{k-1})+cy(t_{k-1})\right)h^{q_2} - \sum_{j=v}^{k} c_j^{(q_2)}y(t_{k-j}),\\ z(t_k) &= \left(x(t_k)y(t_k)-bz(t_{k-1})\right)h^{q_3} - \sum_{j=v}^{k} c_j^{(q_3)}z(t_{k-j}),\end{aligned} \tag{5.57}$$

where $d = (c-a)$, T_{sim} is the simulation time, $k = 1,2,3,\ldots,N$, for $N = [T_{sim}/h]$, and $(x(0), y(0), z(0))$ is the start point (initial conditions). The binomial coefficients $c_j^{(q_i)}$, $\forall i$ are calculated according to the relation (2.54).

To determine a minimal order for which the Chen system is chaotic with the parameters $(a,b,c) = (35,3,28)$, we can use the relation (4.42). In this case the minimal commensurate order is $q > 0.8244$, if we consider $q_1 = q_2 = q_3 \equiv q$.

Let us consider the parameters $(a,b,c,d) = (35,3,28,-7)$ and the commensurate orders $q_1 = q_2 = q_3 = 0.9$ in the numerical solution (5.57).

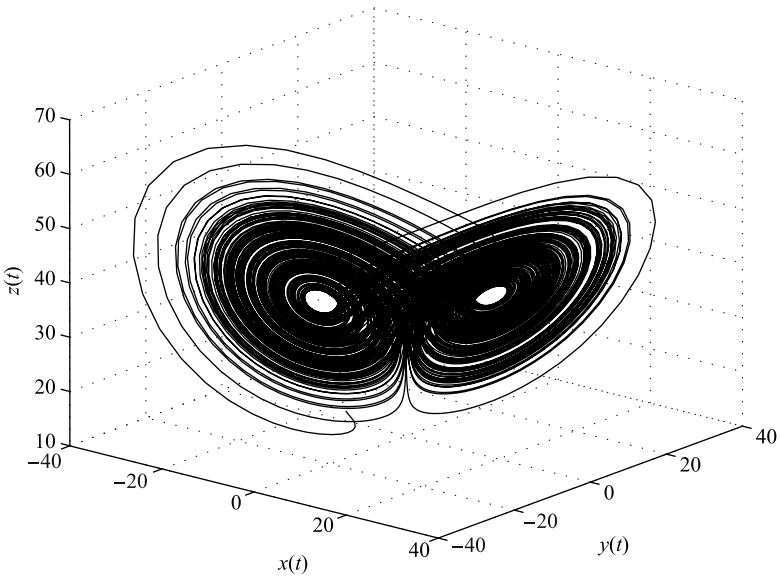

Fig. 5.33 Simulation result of Chen's system (5.56) in state space for parameters: $a = 35, b = 3, c = 28, d = -7$, orders $q_1 = q_2 = q_3 = 0.9$, and initial conditions $(x(0), y(0), z(0)) = (-9, -5, 14)$.

In Fig. 5.33 is depicted the simulation result (double scroll-attractor) of the fractional commensurate-order Chen's system (5.56) computed for simulation time $T_{sim} = 100\,s$ and time step $h = 0.005$. For these parameter sets the characteristic equation of the equilibrium points E_2 and E_3 is

$$\lambda^{27} + 10\lambda^{18} + 84\lambda^{9} + 4410 = 0$$

and unstable roots are $\lambda_{1,2} = 1.3417 \pm 0.1944\,j$, because $|\arg(\lambda_{1,2})| \approx 0.1439 < \pi/2m$, where $m = 10$. These equilibrium points are unstable foci. The equilibrium E_1 is a saddle point connecting two scrolls.

Simulation results of the fractional incommensurate-order Chen's system (5.56) are described in Section 4.3 and depicted in Fig. 4.13, where in Eqs. (5.56) we

used the parameters $a = 35$, $b = 3$, $c = 28$, $d = -7$, and orders $q_1 = 0.8,\ q_2 = 1.0$, $q_3 = 0.9$. The stability of such system was investigated as well.

5.7 Fractional-Order Lü's System

The so-called Lü's system is known as a bridge between the Lorenz system and Chen's system. Its fractional version is described as follows (Deng and Li, 2005):

$$\begin{aligned} {}_0D_t^{q_1}x(t) &= a(y(t)-x(t)),\\ {}_0D_t^{q_2}y(t) &= -x(t)z(t)+cy(t),\\ {}_0D_t^{q_3}z(t) &= x(t)y(t)-bz(t), \end{aligned} \tag{5.58}$$

where $0 < q_1, q_2, q_3 \leq 1$, are derivatives orders, and a, b, c are system parameters.

The system (5.58) has three equilibrium points $E_1 = (0;0;0)$, $E_2 = (\sqrt{bc};\sqrt{bc};c)$ and $E_3 = (-\sqrt{bc};-\sqrt{bc};c)$.

The Jacobian matrix for equilibria $E^* = (x^*, y^*, z^*)$ is defined as

$$\mathbf{J} = \begin{bmatrix} -a & a & 0 \\ -z^* & c & -x^* \\ y^* & x^* & -b \end{bmatrix}. \tag{5.59}$$

Numerical solution of the fractional-order Lü's system (5.58) is given as follows:

$$\begin{aligned} x(t_k) &= \left(a(y(t_{k-1}) - x(t_{k-1}))\right)h^{q_1} - \sum_{j=v}^{k} c_j^{(q_1)} x(t_{k-j}),\\ y(t_k) &= \left(-x(t_k)z(t_{k-1}) + cy(t_{k-1})\right)h^{q_2} - \sum_{j=v}^{k} c_j^{(q_2)} y(t_{k-j}),\\ z(t_k) &= \left(x(t_k)y(t_k) - bz(t_{k-1})\right)h^{q_3} - \sum_{j=v}^{k} c_j^{(q_3)} z(t_{k-j}), \end{aligned} \tag{5.60}$$

where T_{sim} is the simulation time, $k = 1, 2, 3, \ldots, N$, for $N = [T_{sim}/h]$, and $(x(0), y(0), z(0))$ is the start point (initial conditions). The binomial coefficients $c_j^{(q_i)}, \forall i$ are calculated according to the relation (2.54).

Let us consider the following parameters $a = 36, b = 3, c = 20$ of the system (5.58). For equilibrium points E_1 we obtain the following eigenvalus of the Jacobian matrix (5.59): $\lambda_1 = -3$, $\lambda_2 = 20$ and $\lambda_3 = -36$. It is a saddle point. For the equilibrium $E_2 = (7.7460; 7.7460; 20)$ we get the eigenvalues $\lambda_1 \approx -22.6516$ and $\lambda_{2,3} \approx 1.8258 \pm 13.6887\,j$. It is a saddle-focus point. The equilibrium point $E_3 = (-7.7460; -7.7460; 20)$ has the same eigenvalues as the equilibrium E_2. From the above eigenvalues we can determine a minimal commensurate order to keep the system chaotic and it is $q > 0.9156$.

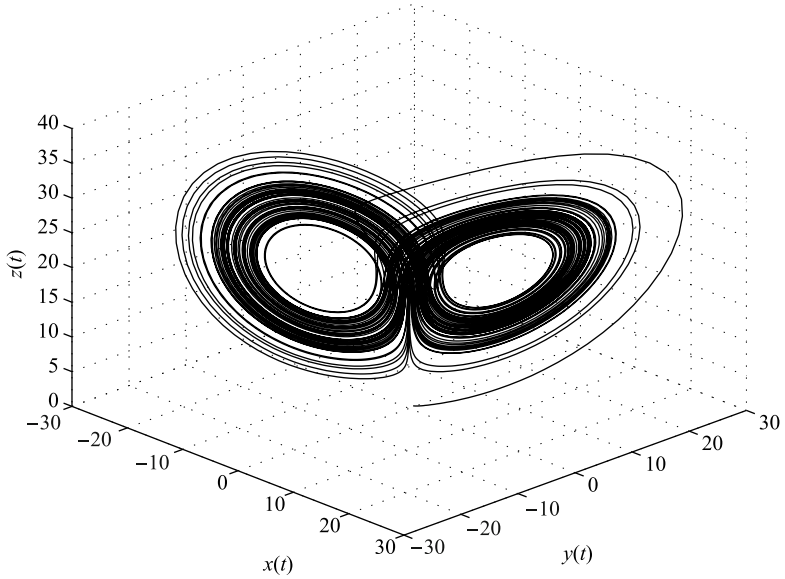

Fig. 5.34 Simulation result of the fractional-order Lü's system (5.58) in state space for parameters $a = 36, b = 3, c = 20$ and orders $q_1 = 0.95, q_2 = 0.95, q_3 = 0.95$.

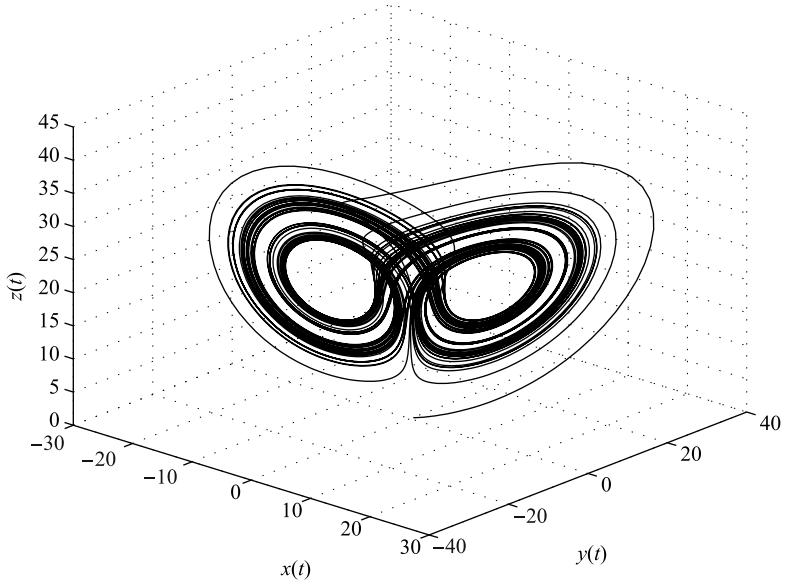

Fig. 5.35 Simulation result of the fractional-order Lü's system (5.58) in state space for parameters $a = 36, b = 3, c = 20$ and orders $q_1 = 0.985, q_2 = 0.99, q_3 = 0.98$.

In Fig. 5.34 is depicted phase trajectory for commensurate derivative orders $q_1 = 0.95, q_2 = 0.95, q_3 = 0.95$ and parameters $a = 36, b = 3, c = 20$ with the initial conditions: $(x(0), y(0), z(0)) = (0.2, 0.5, 0.3)$, for simulation time $90\,s$, and time step $h = 0.005$.

In Fig. 5.35 is depicted phase trajectory for incommensurate derivative orders $q_1 = 0.985, q_2 = 0.99, q_3 = 0.98$ and parameters $a = 36, b = 3, c = 20$ with the initial conditions: $(x(0), y(0), z(0)) = (0.2, 0.5, 0.3)$, for simulation time $90\,s$ and time step $h = 0.005$.

5.8 Fractional-Order Liu's System

A novel three-dimensional autonomous chaotic dynamical system was introduced by C. Liu, L. Liu and T. Liu and reported in literature (Liu et al., 2009). The differential equations that described the system are

$$\begin{aligned} \frac{dx(t)}{dt} &= -ax(t) - ey^2(t), \\ \frac{dy(t)}{dt} &= by(t) - kx(t)z(t), \\ \frac{dz(t)}{dt} &= -cz(t) + mx(t)y(t), \end{aligned} \tag{5.61}$$

where $a = e = 1$, $b = 2.5$, $k = m = 4$, $c = 5$ and initial conditions $(0.2, 0, 0.5)$ yield chaotic trajectory.

The system (5.61) has five equilibrium points. Two of them are complex and three are real equilibrium points $E_1 = (0; 0; 0)$, $E_2 = (-0.88388; -0.940150; 0.664786)$, and $E_3 = (-0.88388; 0.940150; -0.664786)$. In the paper (Liu et al., 2009) were calculated different equilibrium points because in spite of the following parameters declaration $a = e = 1$, $b = 2.5$, $k = m = 4$, $c = 5$ for calculations they probably used different parameters.

The corresponding Jacobian matrix for equilibria $E^* = (x^*, y^*, z^*)$ is

$$\mathbf{J} = \begin{bmatrix} -a & -2ey^* & 0 \\ -kz^* & b & -kx^* \\ my^* & mx^* & -c \end{bmatrix}. \tag{5.62}$$

The roots of the characteristic equation evaluated at equilibrium E_1 are $\lambda_1 = -1$, $\lambda_2 = -5$, and $\lambda_3 = 2.5$. It is a saddle point. The eigenvalues of the Jacobian matrix evaluated at equilibrium points E_2 and E_3 are $\lambda_1 \approx -4.387767$, and $\lambda_{2,3} \approx 0.4438837 \pm 3.346383\,j$. It is a saddle-focus point. Because all eigenvalues are unstable, the condition for chaos is satisfied and chaotic system (5.61) with the above parameters can exhibit chaotic behavior.

Its fractional-order version was described (Gejji and Bhalekar, 2010) and has the form:

$$\begin{aligned} {}_0D_t^{q_1}x(t) &= -ax(t) - ey^2(t), \\ {}_0D_t^{q_2}y(t) &= by(t) - kx(t)z(t), \\ {}_0D_t^{q_3}z(t) &= -cz(t) + mx(t)y(t), \end{aligned} \tag{5.63}$$

where q_1, q_2, q_3 are derivative orders, the total order is denoted by $\bar{q} = (q_1, q_2, q_3)$.

In case we consider a commensurate order system (5.63) with $q_1 = q_2 = q_3 \equiv q$, a minimal order q for chaotic behavior can be determinned according the condition (4.42) and it is $q > 0.916$. Thus the system deos not show chaotic behavior for $q < 0.916$.

Numerical solution of the fractional-order Liu's system (5.63) is given as follows:

$$\begin{aligned} x(t_k) &= \left(-ax(t_{k-1}) - ey^2(t_{k-1})\right)h^{q_1} - \sum_{j=v}^{k} c_j^{(q_1)} x(t_{k-j}), \\ y(t_k) &= \left(by(t_{k-1}) - kx(t_k)z(t_{k-1})\right)h^{q_2} - \sum_{j=v}^{k} c_j^{(q_2)} y(t_{k-j}), \\ z(t_k) &= \left(-cz(t_{k-1}) + mx(t_k)y(t_k)\right)h^{q_3} - \sum_{j=v}^{k} c_j^{(q_3)} z(t_{k-j}), \end{aligned} \tag{5.64}$$

where T_{sim} is the simulation time, $k = 1, 2, 3, \ldots, N$, for $N = [T_{sim}/h]$, and $(x(0), y(0), z(0))$ is the start point (initial conditions). The binomial coefficients $c_j^{(q_i)}, \forall i$ are calculated according to the relation (2.54).

In Fig. 5.36 are depicted the simulation results of the (integer-order) Liu's system (5.61) for the following parameters: $a = e = 1$, $b = 2.5$, $k = m = 4$, $c = 5$, and computational time $100\,s$, for time step $h = 0.005$.

Consider the commensurate order of the fractional-order Liu's system (5.63) with $q = 0.95$ and parameters $a = e = 1$, $b = 2.5$, $k = m = 4$. The characteristic equation of the linearized system is

$$\lambda^{285} + 3.5\lambda^{190} + 7.5\lambda^{95} + 50 = 0$$

and unstable roots are $\lambda_{1,2} \approx 1.0128 \pm 0.0153\,j$, because $|\arg(\lambda_{1,2})| = 0.0151 < \pi/2m$, where $m = 100$ (LCM of orders denominator).

In Fig. 5.37 is depicted the simulation result of the (integer-order) Liu's system (5.63) for the following parameters: $a = e = 1$, $b = 2.5$, $k = m = 4$, $c = 5$, orders $q_1 = q_2 = q_3 = 0.95$ and computational time $100\,s$ for time step $h = 0.005$.

Let us consider the incommensurate order of the fractional-order Liu's system (5.63) with $q_1 = 1.0$, $q_2 = 0.9$, and $q_3 = 0.8$ and parameters $a = e = 1$, $b = 2.5$, $k = m = 4$. The characteristic equation of the linearized system is

$$\lambda^{27} + 5\lambda^{19} - 2.5\lambda^{18} + \lambda^{17} + 5\lambda^{9} + 2.5\lambda^{8} + 50 = 0$$

and unstable roots are $\lambda_{1,2} \approx 1.1224 \pm 0.1770\,j$, because $|\arg(\lambda_{1,2})| = 0.1565 < \pi/2m$, where $m = 10$.

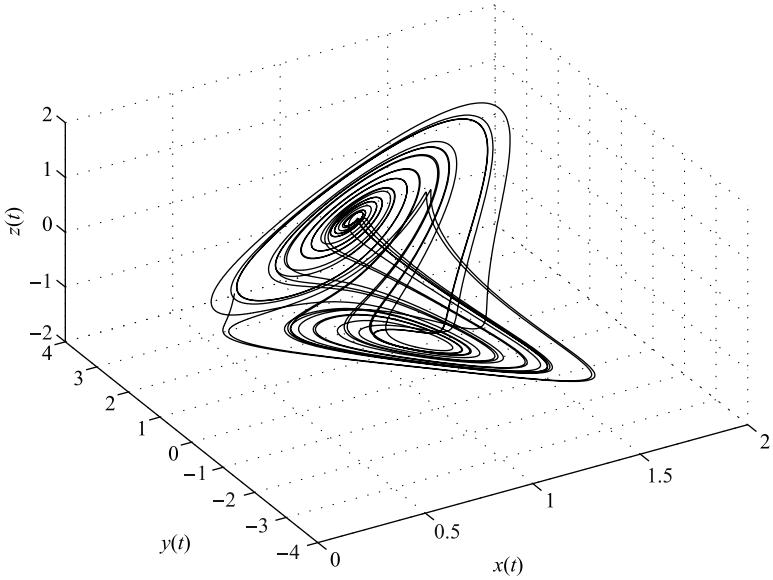

Fig. 5.36 Simulation result of the Liu's system (5.61) in state space for parameters: $a = e = 1$, $b = 2.5$, $k = m = 4$, $c = 5$, and initial conditions $(x(0), y(0), z(0)) = (0.2, 0, 0.5)$.

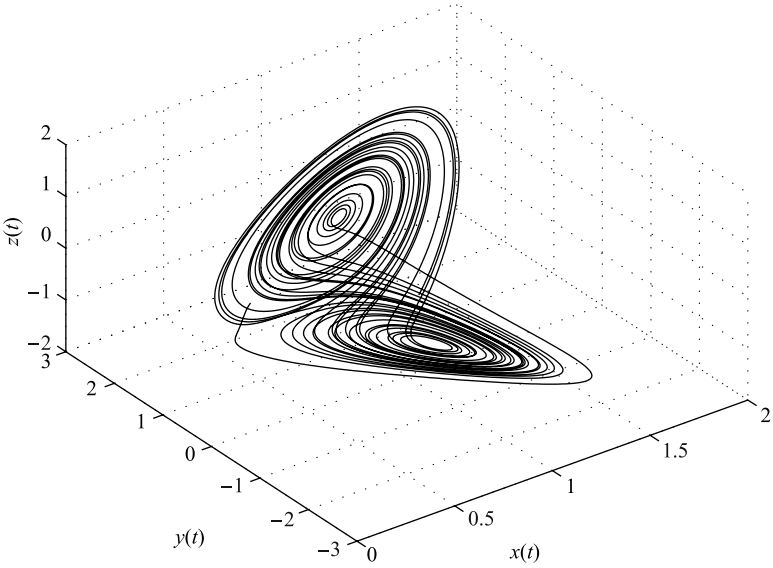

Fig. 5.37 Simulation result of the Liu's system (5.63) in state space for parameters: $a = e = 1$, $b = 2.5$, $k = m = 4$, $c = 5$, orders $q_1 = q_2 = q_3 = 0.95$, and initial conditions $(x(0), y(0), z(0)) = (0.2, 0, 0.5)$.

In Fig. 5.38 is depicted the simulation result of the (fractional-order) Liu's system (5.63) for the following parameters: $a = e = 1$, $b = 2.5$, $k = m = 4$, $c = 5$, orders $q_1 = 1.0$, $q_2 = 0.9$, and $q_3 = 0.8$, and computational time $100\,s$, for time step $h = 0.005$.

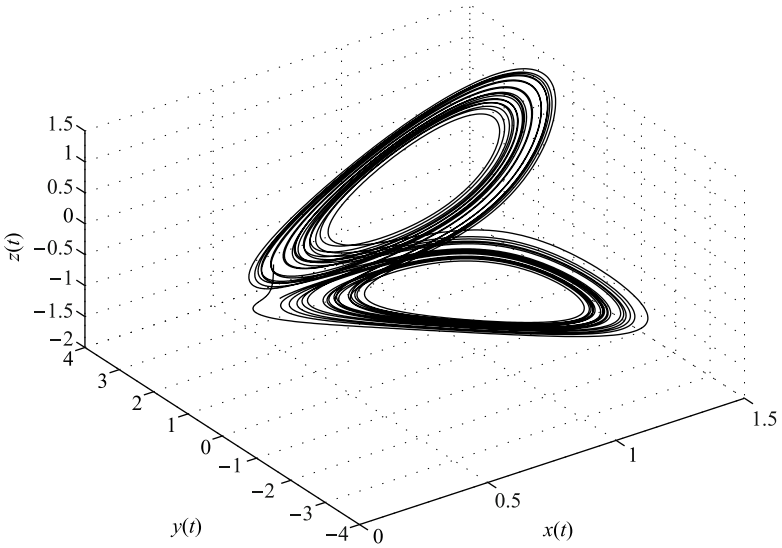

Fig. 5.38 Simulation result of the Liu's system (5.63) in state space for parameters: $a = e = 1$, $b = 2.5$, $k = m = 4$, $c = 5$, orders $q_1 = 1.0$, $q_2 = 0.9$, and $q_3 = 0.8$, and initial conditions $(x(0), y(0), z(0)) = (0.2, 0, 0.5)$.

Note that this fractional-order system has been investigated and described for various orders, where condition for chaotic behavior was cross-validated with the Lyapunov exponent together with the instability measure for each equilibrium point (Gejji and Bhalekar, 2010). Numerical experiments performed in the mentioned paper showed the existence of chaos for a minimum total order of the commensurate-order system 2.76 and in the case of incommensurate-order system it was 2.60. The total order of the system is sometimes also called a minimum effective dimension.

5.9 Fractional-Order Genesio-Tesi's System

The Genesio-Tesi's system is described by the system of equations (Genesio and Tesi, 1992):

$$\begin{aligned}\frac{dx(t)}{dt} &= y(t),\\ \frac{dy(t)}{dt} &= z(t),\\ \frac{dz(t)}{dt} &= -\beta_1 x(t) - \beta_2 y(t) - \beta_3 z(t) + \beta_4 x^2(t),\end{aligned} \tag{5.65}$$

where $\beta_1, \beta_2, \beta_3$ and β_4 are system parameters.

Genesio-Tesi's system (5.65) has two equilibrium points $E_1 = (0;0;0)$ and $E_2 = (\beta_1/\beta_4;0;0)$. The Jacobian matrix for equilibria $E^* = (x^*, y^*, z^*)$ is defined as

$$\mathbf{J} = \begin{bmatrix} 0 & 1 & 0 \\ 0 & 0 & 1 \\ -\beta_1 + 2\beta_4 x^* & -\beta_2 & -\beta_3 \end{bmatrix}. \tag{5.66}$$

The corresponding eigenvalues of the equilibrium E_1 for the parameters $\beta_1 = 1, \beta_2 = 1.1, \beta_3 = 0.44, \beta_4 = 1.0$ are $\lambda_1 \approx -0.750293$ and $\lambda_{2,3} \approx 0.155146 \pm 1.144002j$. For the equilibrium E_2 they are $\lambda_1 \approx 0.587161$ and $\lambda_{2,3} \approx -0.5135806 \pm 1.199726j$. Both of them are unstable saddle-focus points and therefore the condition for chaotic behavior is satisfied.

In Fig. 5.39 is depicted the simulation result of the (integer-order) Genesio-Tesi's system (5.65) for the following parameters: $\beta_1 = 1, \beta_2 = 1.1, \beta_3 = 0.44, \beta_4 = 1.0$, and computational time $200\,s$, for time step $h = 0.005$.

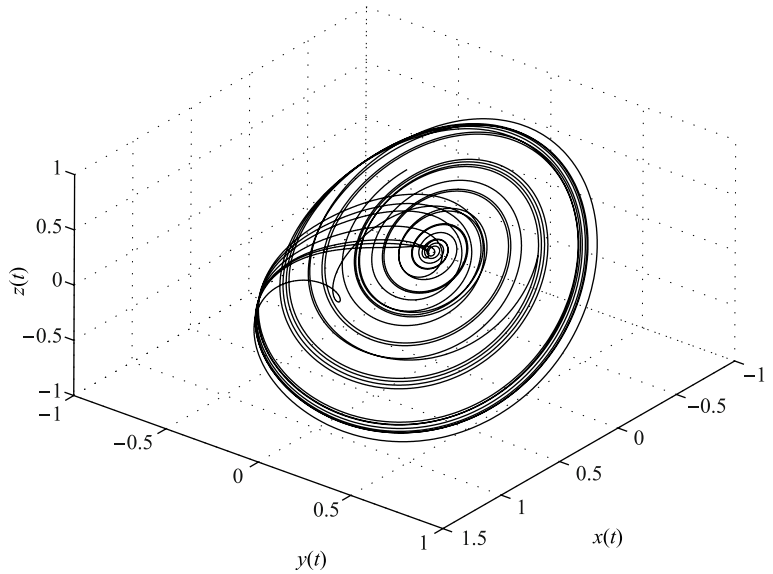

Fig. 5.39 Simulation result of the Genesio-Tesi's system (5.65) in state space for parameters: $\beta_1 = 1, \beta_2 = 1.1, \beta_3 = 0.44, \beta_4 = 1.0$, and initial conditions $(x(0), y(0), z(0)) = (-0.1, 0.5, 0.2)$.

The fractional-order Genesio-Tesi's system is defined as follows (Guo, 2005):

$$\begin{aligned} {}_0D_t^{q_1}x(t) &= y(t), \\ {}_0D_t^{q_2}y(t) &= z(t), \\ {}_0D_t^{q_3}z(t) &= -\beta_1 x(t) - \beta_2 y(t) - \beta_3 z(t) + \beta_4 x^2(t), \end{aligned} \tag{5.67}$$

where $q \in [q_1, q_2, q_3]$ and $0 < q \leq 1$.

Numerical solution of the fractional-order Genesio-Tesi's system (5.67) is given as follows:

$$\begin{aligned} x(t_k) &= (y(t_{k-1}))\, h^{q_1} - \sum_{j=v}^{k} c_j^{(q_1)} x(t_{k-j}), \\ y(t_k) &= (z(t_{k-1}))\, h^{q_2} - \sum_{j=v}^{k} c_j^{(q_2)} y(t_{k-j}), \\ z(t_k) &= \left(-\beta_1 x(t_k) - \beta_2 y(t_k) - \beta_3 z(t_{k-1}) + \beta_4 x(t_k)^2\right) h^{q_3} - \sum_{j=v}^{k} c_j^{(q_3)} z(t_{k-j}), \end{aligned} \tag{5.68}$$

where T_{sim} is the simulation time, $k = 1, 2, 3, \ldots, N$, for $N = [T_{sim}/h]$, and $(x(0), y(0), z(0))$ is the start point (initial conditions). The binomial coefficients $c_j^{(q_i)}, \forall i$ are calculated according to the relation (2.54).

Let us consider the commensurate order $q_1 = q_2 = q_3 \equiv q = 0.9$ and system parameters: $\beta_1 = 1$, $\beta_2 = 1.1$, $\beta_3 = 0.15$, $\beta_4 = 1.0$. The characteristic equation of the system (5.67) evaluated at the equilibria E_1 and E_2, respectively, is

$$\lambda^{27} + 3/20\lambda^{18} + 11/10\lambda^{9} \pm 1 = 0$$

and unstable roots for the equilibrium E_1 are $\lambda_{1,2} \approx 1.0100 \pm 0.1525j$, because $|\arg(\lambda_{1,2})| = 0.1499 < \pi/2m$, where $m = 10$ (LCM of orders denominator) and unstable root for the equilibrium E_2 is $\lambda_1 \approx 0.9498$. As shown in (Guo, 2005), the system exhibits chaotic behavior.

Now, consider the incommensurate-order system, where $q_1 = 1.0$, $q_2 = 1.0$, and $q_3 = 0.95$ and system parameters are $\beta_1 = 1.1$, $\beta_2 = 1.1$, $\beta_3 = 0.45$, $\beta_4 = 1.0$. The characteristic equation of the system (5.67) evaluated at the equilibria E_1 and E_2, respectively, is

$$\lambda^{295} + 9/20\lambda^{200} + 11/10\lambda^{100} \pm 1.1 = 0$$

and unstable roots for the equilibrium E_1 are $\lambda_{1,2} \approx 1.0014 \pm 0.0145j$, because $|\arg(\lambda_{1,2})| = 0.0145 < \pi/2m$, where $m = 100$ (LCM of orders denominator) and unstable root for the equilibrium E_2 is $\lambda_1 \approx 0.9952$.

In Fig. 5.40 is depicted the simulation result of the Genesio-Tesi's system (5.67) for the following parameters: $\beta_1 = 1.1$, $\beta_2 = 1.1$, $\beta_3 = 0.45$, $\beta_4 = 1.0$, orders $q_1 = 1.0$, $q_2 = 1.0$, $q_3 = 0.95$ and computational time $200\,s$, for time step $h = 0.005$. As we can see in the figure, the fractional-order Genesio-Tesi's system is chaotic with one scroll attractor.

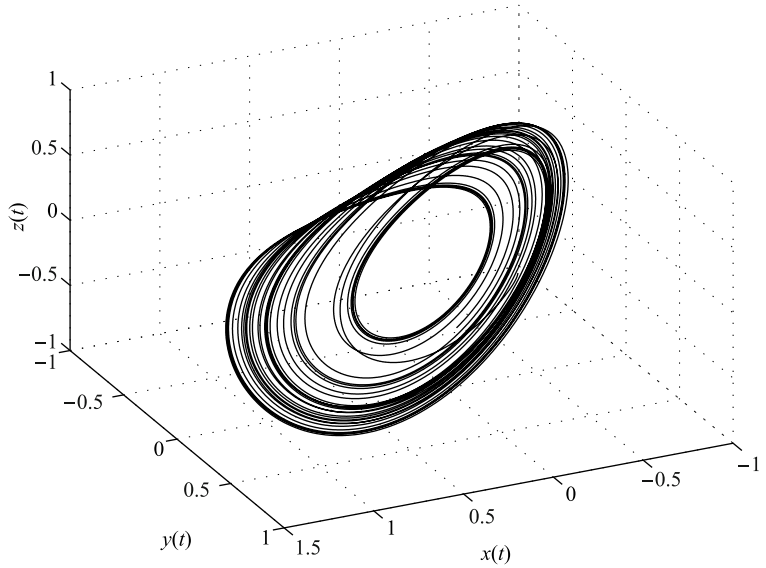

Fig. 5.40 Simulation result of the Genesio-Tesi's system (5.67) in state space for initial conditions $(x(0), y(0), z(0)) = (-0.1, 0.5, 0.2)$.

5.10 Fractional-Order Arneodo's System

Arneodo's system is described by

$$\begin{aligned} \frac{dx(t)}{dt} &= y(t), \\ \frac{dy(t)}{dt} &= z(t), \\ \frac{dz(t)}{dt} &= -\beta_1 x(t) - \beta_2 y(t) - \beta_3 z(t) + \beta_4 x^3(t), \end{aligned} \tag{5.69}$$

where $\beta_1, \beta_2, \beta_3$ and β_4 are constant parameters. This system has three equilibrium points $E_1 = (0;0;0;)$, $E_2 = (\sqrt{(\beta_4\beta_1)}/\beta_4; 0; 0)$, and $E_3 = (-\sqrt{(\beta_4\beta_1)}/\beta_4; 0; 0)$.

The Jacobian matrix for equilibria $E^* = (x^*, y^*, z^*)$ is defined as

$$\mathbf{J} = \begin{bmatrix} 0 & 1 & 0 \\ 0 & 0 & 1 \\ -\beta_1 + 3\beta_4 x^{*2} & -\beta_2 & -\beta_3 \end{bmatrix}. \tag{5.70}$$

When $\beta_1 = -5.5$, $\beta_2 = 3.5$, $\beta_3 = 1$ and $\beta_4 = -1$, the system (5.69) equilibrium points are $E_1 = (0;0;0)$, $E_2 = (2.345207;0;0)$, and $E_3 = (-2.345207;0;0)$. Corresponding eigenvalues for equilibrium E_1 are $\lambda_1 = 1$, $\lambda_{2,3} \approx -1 \pm 2.12132\,j$, and for equilibria E_2 and E_3 the eigenvalues are $\lambda_1 = -2$, $\lambda_{2,3} = 0.5 \pm 2.2912878\,j$. All equi-

libria are saddle-focus points. The condition for chaos is satisfied and the system has chaotic attractor shown in Fig. 5.41.

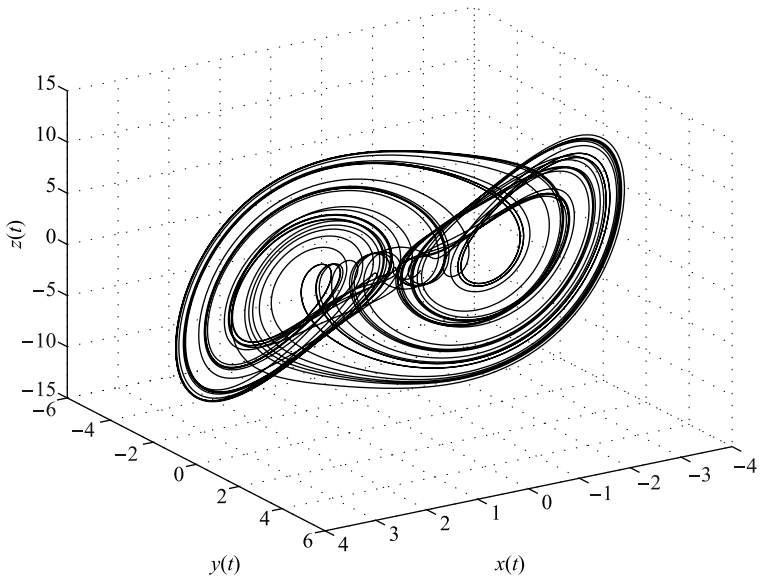

Fig. 5.41 Simulation result of the Arneodo's system (5.69) in state space for initial conditions $(x(0), y(0), z(0)) = (-0.2, 0.5, 0.2)$.

In Fig. 5.41 is depicted the chaotic attractor of Arneodo's system (5.69) for the following parameters: $\beta_1 = -5.5$, $\beta_2 = 3.5$, $\beta_3 = 1$, $\beta_4 = -1.0$, and computational time $200\,s$, for time step $h = 0.005$.

The fractional-order Arneodo's system is defined as follows (Lu, 2005):

$$\begin{aligned} {}_0D_t^{q_1} x(t) &= y(t), \\ {}_0D_t^{q_2} y(t) &= z(t), \\ {}_0D_t^{q_3} z(t) &= -\beta_1 x(t) - \beta_2 y(t) - \beta_3 z(t) + \beta_4 x^3(t), \end{aligned} \tag{5.71}$$

where $q \in [q_1, q_2, q_3]$ and $0 < q \leq 1$. This system is very similar to the Genesio-Tesi's system (5.67) but with the different kind of nonlinearity.

Numerical solution of the fractional-order Arneodo's system (5.71) is given as follows:

$$\begin{aligned} x(t_k) &= (y(t_{k-1}))\, h^{q_1} - \sum_{j=v}^{k} c_j^{(q_1)} x(t_{k-j}), \\ y(t_k) &= (z(t_{k-1}))\, h^{q_2} - \sum_{j=v}^{k} c_j^{(q_2)} y(t_{k-j}), \\ z(t_k) &= \left(-\beta_1 x(t_k) - \beta_2 y(t_k) - \beta_3 z(t_{k-1}) + \beta_4 x(t_k)^3\right) h^{q_3} - \sum_{j=v}^{k} c_j^{(q_3)} z(t_{k-j}), \end{aligned} \tag{5.72}$$

where T_{sim} is the simulation time, $k = 1,2,3,\ldots,N$, for $N = [T_{sim}/h]$, and $(x(0), y(0), z(0))$ is the start point (initial conditions). The binomial coefficients $c_j^{(q_i)}, \forall i$ are calculated according to the relation (2.54).

For the above paremeters we are able to determine a minimal commensurate order of the system (5.71), which is $q > 0.86$ in case $q_1 = q_2 = q_3 \equiv q$.

Let us consider the incommensuraty fractional-order Arneodo's system (5.71) with the following paremeters $\beta_1 = -5.5, \beta_2 = 3.5, \beta_3 = 0.8, \beta_4 = -1.0$ and orders $q_1 = q_2 = 0.97$, and $q_3 = 0.96$. Thus the total order of the system is 2.9. The characteristic equation of the system (5.71) evaluated at the equilibrium E_1 is

$$\lambda^{290} + 4/5\lambda^{194} + 7/2\lambda^{97} - 5.5 = 0$$

with unstable root $\lambda_1 \approx 1.0002$. The characteristic equation of the system (5.71) evaluated at the equilibria E_2 and E_3, respectively, is

$$\lambda^{290} + 4/5\lambda^{194} + 7/2\lambda^{97} + 11 = 0$$

and unstable roots are $\lambda_{1,2} \approx 1.0089 \pm 0.0139j$, because $|\arg(\lambda_{1,2})| = 0.0138 < \pi/2m$, where $m = 100$ (LCM of orders denominator).

In Fig. 5.42 and Fig. 5.43 are depicted the simulation results of Arneodo's system (5.71) for the following parameters: $\beta_1 = -5.5, \beta_2 = 3.5, \beta_3 = 0.8, \beta_4 = -1.0$, orders $q_1 = 0.97, q_2 = 0.97, q_3 = 0.96$, and computational time $200s$, for time step $h = 0.005$.

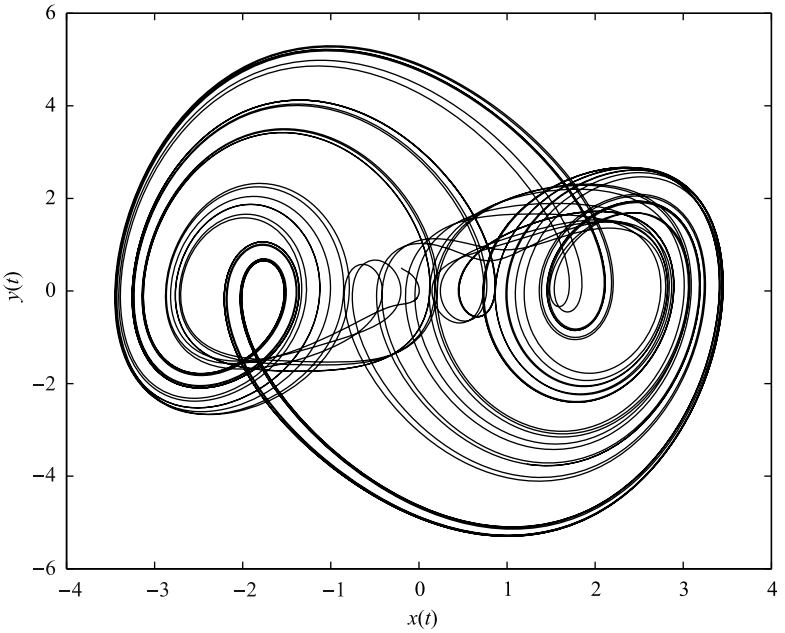

Fig. 5.42 Simulation result of the fractional-order Arneodo's system (5.71) projected onto $x-y$ plane for the initial conditions $(x(0), y(0), z(0)) = (-0.2, 0.5, 0.2)$.

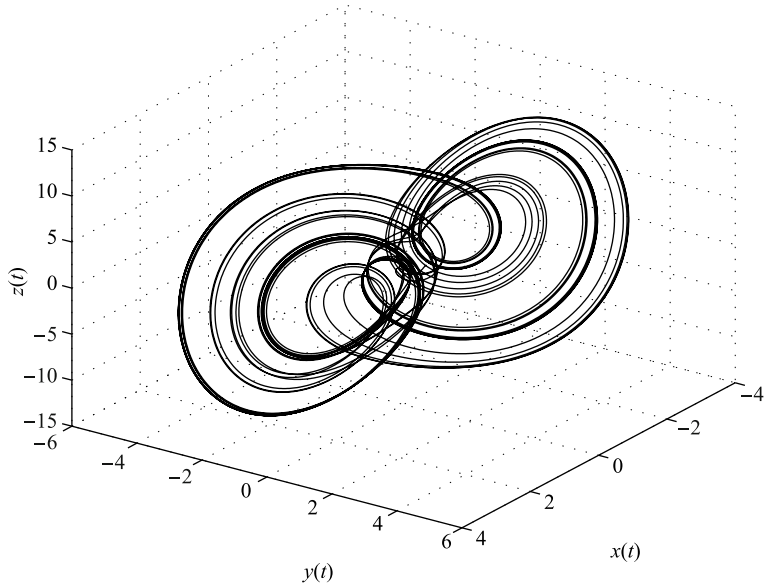

Fig. 5.43 Simulation result of the fractional-order Arneodo's system (5.71) in state space for the initial conditions $(x(0), y(0), z(0)) = (-0.2, 0.5, 0.2)$.

In the paper (Lu, 2005) were performed simulations for various commensurate order q of the fractional-order Arneodo's system (5.71). Those simulations were cross-validated with the Lyapunov exponent. The results showed that the lowest total order of the fractional-order Arneodo's system to yield chaos was 2.1.

5.11 Fractional-Order Rössler's System

Otto Rössler proposed Rössler's system with strange attractor in 1976, but the originally theoretical equations were later found to be useful in modeling equilibrium in chemical reactions. This attractor has only one manifold and can be obtained as a solution of the following equations:

$$\begin{aligned} \frac{dx(t)}{dt} &= -(y(t)+z(t)), \\ \frac{dy(t)}{dt} &= x(t)+ay(t), \\ \frac{dz(t)}{dt} &= b+z(t)\,(x(t)-c)\,, \end{aligned} \tag{5.73}$$

where for the parameters $a = 0.2$, $b = 0.2$, $c = 5.7$ this system yields chaotic behavior. This system has two equilibrium points E_1 and E_2 located at

$$E_{1,2} = \left(\frac{c \pm \sqrt{c^2 - 4ab}}{2}; -\frac{c \pm \sqrt{c^2 - 4ab}}{2a}; \frac{c \pm \sqrt{c^2 - 4ab}}{2a} \right).$$

The Jacobian matrix for the equilibria $E^* = (x^*, y^*, z^*)$ is defined as

$$\mathbf{J} = \begin{bmatrix} 0 & -1 & -1 \\ 1 & a & 0 \\ z^* & 0 & x^* - c \end{bmatrix}. \tag{5.74}$$

Consider a fractional-order generalization of the Rössler's system (5.73) as follows (Li and Chen, 2004):

$$\begin{aligned} {}_0D_t^{q_1} x(t) &= -(y(t) + z(t)), \\ {}_0D_t^{q_2} y(t) &= x(t) + ay(t), \\ {}_0D_t^{q_3} z(t) &= b + z(t)\,(x(t) - c)\,, \end{aligned} \tag{5.75}$$

where conventional derivatives are replaced by the fractional ones.

Numerical solution of the fractional-order Rössler's system (5.75) is given as follows:

$$\begin{aligned} x(t_k) &= (-y(t_{k-1}) - z(t_{k-1}))\, h^{q_1} - \sum_{j=v}^{k} c_j^{(q_1)} x(t_{k-j}), \\ y(t_k) &= (x(t_k) + ay(t_{k-1}))\, h^{q_2} - \sum_{j=v}^{k} c_j^{(q_2)} y(t_{k-j}), \\ z(t_k) &= (b + z(t_{k-1})(x(t_k) - c))\, h^{q_3} - \sum_{j=v}^{k} c_j^{(q_3)} z(t_{k-j}), \end{aligned} \tag{5.76}$$

where T_{sim} is the simulation time, $k = 1, 2, 3, \ldots, N$, for $N = [T_{sim}/h]$, and $(x(0), y(0), z(0))$ is the start point (initial conditions). The binomial coefficients $c_j^{(q_i)}$, $\forall i$ are calculated according to the relation (2.54).

Let us consider the system (5.75) for the parameters $a = 0.5$, $b = 0.2$ and $c = 10$. The system has two equilibria: $E_1 = (9.98998; -19.97997; 19.97997)$ and $E_2 = (0.10010; -0.20020; 0.20020)$ and their corresponding eigenvalues are: $\lambda_1 \approx 0.47595$, $\lambda_{2,3} \approx 0.007017 \pm 4.57910\,j$ for the eqiulibrium E_1 and $\lambda_1 \approx -9.98800$, $\lambda_{2,3} \approx 0.249007 \pm 0.96808\,j$ for the equilibrium E_2. The equilibrium E_1 is unstable focus-node point and the equibrium E_2 is unstable saddle-focus point. The condition for chaotic behavior is satisfied. With the above eigenvalues and condition (4.42) we can determine that the minimal commensurate order of this system is $q > 0.839$.

When we assume the commensurate order $q_1 = q_2 = q_3 = 0.9$ and parameters $a = 0.5$, $b = 0.2$ and $c = 10$, we get the following characteristic equation of the linearized system for the equilibrium E_1:

$$\lambda^{27} - 0.489989\lambda^{18} + 20.974974\lambda^{9} - 9.979979 = 0,$$

with unstable root $\lambda_1 \approx 0.9208$. The characteristic equation for the equilibrium E_2 is

$$\lambda^{27} + 9.489989\lambda^{18} - 3.974974\lambda^{9} + 9.979979 = 0,$$

with unstable roots $\lambda_{1,2} \approx 0.9892 \pm 0.1460\,j$, because $|\arg(\lambda_{1,2})| = 0.1466 < \pi/2m$, where $m = 10$ (LCM of orders denominator).

In Fig. 5.44 is depicted phase trajectory of the fractional-order Rössler's system (5.75) for commensurate order $q = 0.9$ and parameters $a = 0.5$, $b = 0.2$, $c = 10$, with the initial conditions $(x(0), y(0), z(0)) = (0.5, 1.5, 0.1)$, for simulation time $120\,s$ and time step $h = 0.005$.

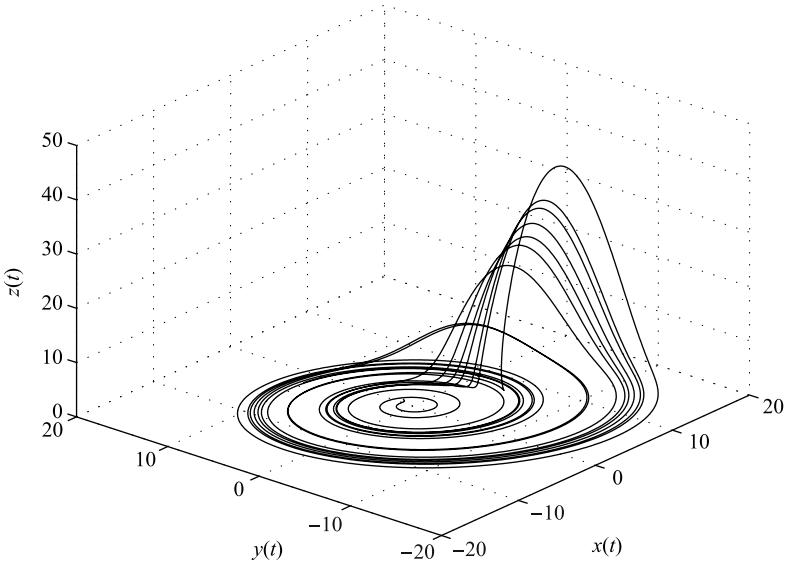

Fig. 5.44 Simulation result of the fractional-order Rössler's system (5.75) in state space for parameters $a = 0.5$, $b = 0.2$, $c = 10$ and orders $q_1 = q_2 = q_3 = 0.9$ for simulation time $120\,s$, with initial conditions $(x(0), y(0), z(0)) = (0.5, 1.5, 0.1)$.

When we assume the incommensurate order $q_1 = 0.90$, $q_2 = 0.85$, $q_3 = 0.95$ and parameters $a = 0.5$, $b = 0.2$ and $c = 10$, we get the following characteristic equation of the linearized system for the equilibrium E_1:

$$\lambda^{270} - 1/2\lambda^{185} + 0.010010\lambda^{175} + \lambda^{95} - 0.005005\lambda^{90} + 19.97997\lambda^{85} - 9.97997 = 0,$$

with unstable root $\lambda_1 \approx 0.9913$. The characteristic equation for the equilibrium E_2 is

$$\lambda^{270} - 1/2\lambda^{185} + 9.98998\lambda^{175} + \lambda^{95} - 4.994994\lambda^{90} + 9.97997 + 0.020020\lambda^{85} = 0,$$

with unstable roots $\lambda_{1,2} \approx 1.0000 \pm 0.0151\,j$, because $|\arg(\lambda_{1,2})| = 0.0151 < \pi/2m$, where $m = 100$ (LCM of orders denominator).

In Fig. 5.45 is depicted phase trajectory of the fractional-order Rössler's system (5.75) for incommensurate orders $q_1 = 0.90$, $q_2 = 0.85$, $q_3 = 0.95$ and parameters $a = 0.5$, $b = 0.2$, $c = 10$, with the initial conditions $(x(0), y(0), z(0)) = (0.5, 1.5, 0.1)$, for simulation time $120\,s$ and time step $h = 0.005$.

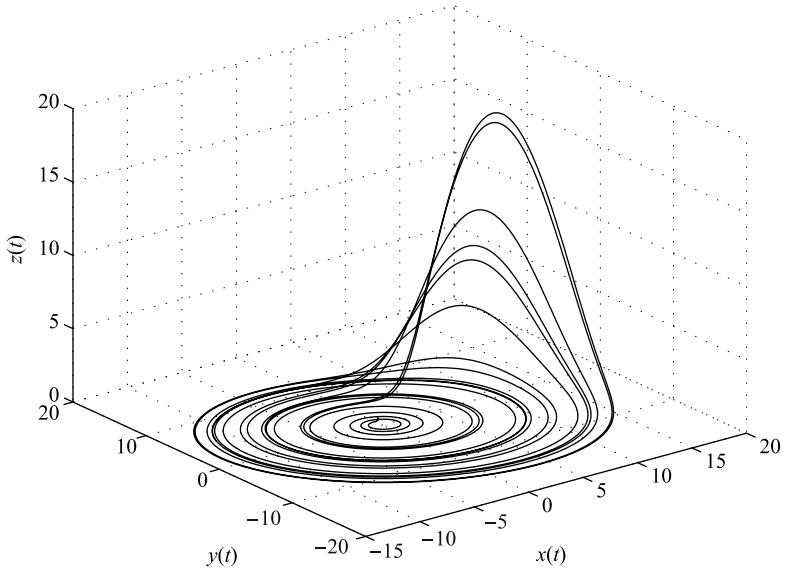

Fig. 5.45 Simulation result of the fractional-order Rössler's system (5.75) in state space for parameters $a = 0.5$, $b = 0.2$, $c = 10$ and orders $q_1 = 0.90$, $q_2 = 0.85$, $q_3 = 0.95$ for simulation time $120\,s$, with initial conditions $(x(0), y(0), z(0)) = (0.5, 1.5, 0.1)$.

The fractional-order Rössler hyperchaos equations were investigated in (Li and Chen, 2004), where chaotic behavior was cross-validated with the largest Lyapunov exponent.

5.12 Fractional-Order Newton-Leipnik's System

The Newton-Leipnik's system is described by the following nonlinear differential equations (Leipnik and Newton, 1981):

$$\begin{aligned} \frac{dx(t)}{dt} &= -ax(t) + y(t) + 10y(t)z(t), \\ \frac{dy(t)}{dt} &= -x(t) - 0.4y(t) + 5x(t)z(t), \\ \frac{dz(t)}{dt} &= bz(t) - 5x(t)y(t), \end{aligned} \tag{5.77}$$

where a and b are positive parameters.

In the paper (Leipnik and Newton, 1981), it has been noted that the Newton-Leipnik's system is a chaotic system with two strange attractors. When $a = 0.4$ and $b = 0.175$, with initial states $(0.349, 0, -0.16)$ and $(0.349, 0, -0.18)$, system (5.77) displays two strange attractors.

The system (5.77) with parameters $a = 0.4$ and $b = 0.175$ has five equilibrium points, where one of them is the origin. The other equilibria, approximately, are: $E_2 = (-0.23896; -0.03080; 0.21031)$, $E_3 = (-0.03154; 0.12237; -0.11031)$, $E_4 = (0.03154; -0.12237; -0.11031)$, and $E_5 = (0.23896; 0.03080; 0.21031)$.

The Jacobian matrix of the system (5.77) for equilibrium $E^* = (x^*, y^*, z^*)$ is

$$\mathbf{J} = \begin{bmatrix} -a & 1+10z^* & 10y^* \\ -1+5z^* & -0.4 & 5x^* \\ -5y^* & -5x^* & b \end{bmatrix}. \tag{5.78}$$

The eigenvalues of the Jacobian matrix (5.78) evaluated at all equilibrium points show that all equilibria are the saddle-focus points. For the equilibrium E_1 we obtain $\lambda_1 \approx 0.175$ and $\lambda_{2,3} \approx -0.4 \pm 1.0j$, for the equilibria E_2 and E_5 we get $\lambda_1 \approx -0.8$ and $\lambda_{2,3} \approx 0.0875 \pm 1.2113j$ and for the equilibria E_3 and E_4 we have $\lambda_1 \approx -0.8$ and $\lambda_{2,3} \approx 0.0875 \pm 0.8752j$. All these eigenvalues satisfy the condition for the system to be chaotic.

Here, the fractional-order Newton-Leipnik's system is considered, where integer-order derivative is replaced by a fractional one, as follows (Sheu et al., 2008):

$$\begin{aligned} {}_0D_t^{q_1} x(t) &= -ax(t) + y(t) + 10y(t)z(t), \\ {}_0D_t^{q_2} y(t) &= -x(t) - 0.4y(t) + 5x(t)z(t), \\ {}_0D_t^{q_3} z(t) &= bz(t) - 5x(t)y(t), \end{aligned} \tag{5.79}$$

where $0 < q_1, q_2, q_3 \leq 1$ are derivatives orders.

In the case of commensurate-order system, where $q_1 = q_2 = q_3 \equiv q$ we can determine a minimal order to satisfy a necessary condition (4.42) for chaotic behavior. For the equilibria E_2 and E_5 it is $q > 0.9540$ and for the equilibria E_3 and E_4 it is $q > 0.9365$.

Numerical solution of the fractional-order Newton-Leipnik's system (5.75) is given as follows:

$$\begin{aligned} x(t_k) &= \left(ax(t_{k-1}) + y(t_{k-1}) + 10y(t_{k-1})z(t_{k-1})\right) h^{q_1} - \sum_{j=v}^{k} c_j^{(q_1)} x(t_{k-j}), \\ y(t_k) &= \left(-x(t_k) - 0.4y(t_{k-1}) + 5x(t_k)z(t_{k-1})\right) h^{q_2} - \sum_{j=v}^{k} c_j^{(q_2)} y(t_{k-j}), \\ z(t_k) &= \left(bz(t_{k-1}) - 5x(t_k)y(t_k)\right) h^{q_3} - \sum_{j=v}^{k} c_j^{(q_3)} z(t_{k-j}), \end{aligned} \tag{5.80}$$

where T_{sim} is the simulation time, $k = 1,2,3,\ldots,N$, for $N = [T_{sim}/h]$, and $(x(0), y(0), z(0))$ is the start point (initial conditions). The binomial coefficients $c_j^{(q_i)}, \forall i$ are calculated according to the relation (2.54).

Let us consider the following parameters $a = 0.4$, $b = 0.175$, orders $q_1 = 0.95$, $q_2 = 0.95$, and $q_3 = 0.95$ of the system (5.79).

In Fig. 5.46 is depicted phase trajectory for derivative orders $q_1 = 0.95$, $q_2 = 0.95$, $q_3 = 0.95$, parameters $a = 0.4$, $b = 0.175$ for simulation time $200\,s$, time step $h = 0.005$ and with the initial conditions: $(x(0), y(0), z(0)) = (0.19, 0.0, -0.18)$. In the paper (Sheu et al., 2008). it has been noted that the system still approaches the same attractor for both initial states $(0.349, 0, -0.16)$ and $(0.349, 0, -0.18)$, and we can confirm it. Because of this we use a different set of initial conditions.

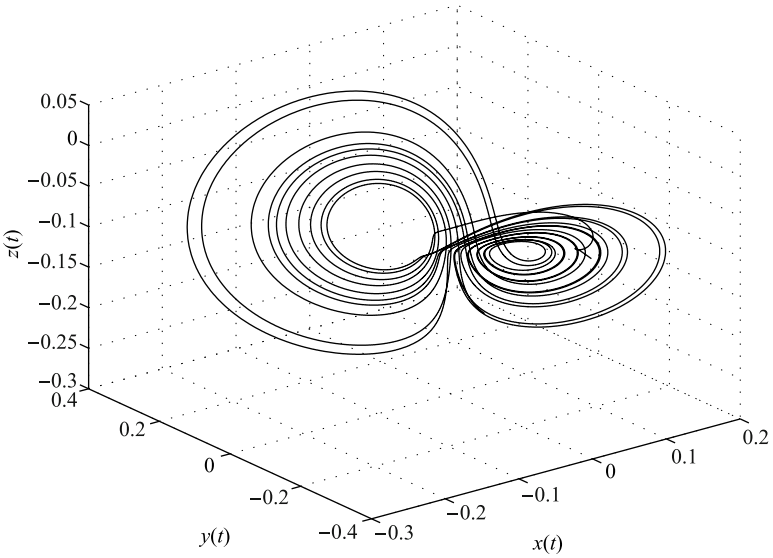

Fig. 5.46 Simulation result of the fractional-order Newton-Leipnik's system (5.79) in state space for parameters $a = 0.4$, $b = 0.175$ and orders $q_1 = q_2 = q_3 = 0.95$ for simulation time $200\,s$.

In Fig. 5.47 is depicted phase trajectory for derivative orders $q_1 = 0.95$, $q_2 = 0.95$, $q_3 = 0.95$, parameters $a = 0.4$, $b = 0.175$ for simulation time $200\,s$, time step $h = 0.005$ and with the initial conditions: $(x(0), y(0), z(0)) = (0.19, 0.0, -0.18)$ projected onto $x - y$ plane. We can observe that double scroll attractor surrounded the equilibria E_3 and E_4.

The characteristic equation of the linearized system evaluated at the equilibrium E_3 or E_4 is

$$\lambda^{285} + 5/8\lambda^{190} + 0.63369\lambda^{95} + 0.618953 = 0,$$

with unstable roots $\lambda_{1,2} \approx 0.9985 \pm 0.0155\,j$, because $|\arg(\lambda_{1,2})| = 0.0155 < \pi/2m$, where $m = 100$ (LCM of orders denominator).

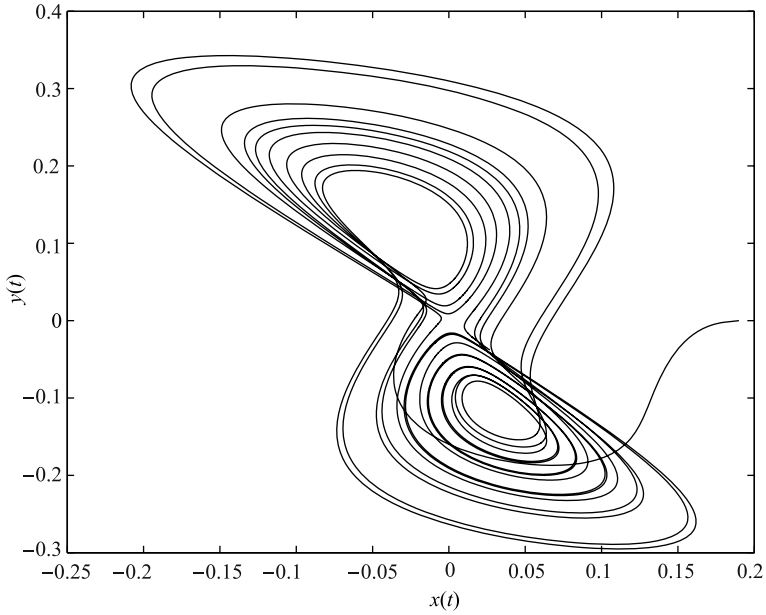

Fig. 5.47 Simulation result of the fractional-order Newton-Leipnik's system (5.79) projected onto $x-y$ plane for parameters $a=0.4$, $b=0.175$ and orders $q_1=q_2=q_3=0.95$.

The characteristic equation of the linearized system evaluated at the equilibrium E_1 is

$$\lambda^{285}+5/8\lambda^{190}+1.020\lambda^{95}-0.2030=0$$

with unstable root $\lambda\approx 0.9818$. The equilibria E_2 and E_5 are stable for the above parameters and orders of the system.

Let us consider the following parameters $a=0.4$, $b=0.175$, orders $q_1=1$, $q_2=0.97$, and $q_3=1$ of the system (5.79).

In Fig. 5.48 is depicted phase trajectory for derivative orders $q_1=q_3=1$, $q_2=0.97$, parameters $a=0.4$, $b=0.175$ for simulation time $200\,s$, time step $h=0.005$ and with the initial conditions: $(x(0),y(0),z(0))=(-0.8,0.0,0.18)$.

In Fig. 5.49 is depicted phase trajectory for derivative orders $q_1=q_3=1$, $q_2=0.97$, parameters $a=0.4$, $b=0.175$ for simulation time $200\,s$, time step $h=0.005$ and with the initial conditions: $(x(0),y(0),z(0))=(-0.8,0.0,0.18)$ projected onto $x-y$ plane. We can observe that double scroll attractor surrounded the equilibria E_2 and E_5.

The characteristic equation of the linearized system evaluated at the equilibrium E_2 or E_5 is

$$\lambda^{297}+2/5\lambda^{200}+9/40\lambda^{197}+1.35761\lambda^{100}-0.02255\lambda^{97}+1.18004=0,$$

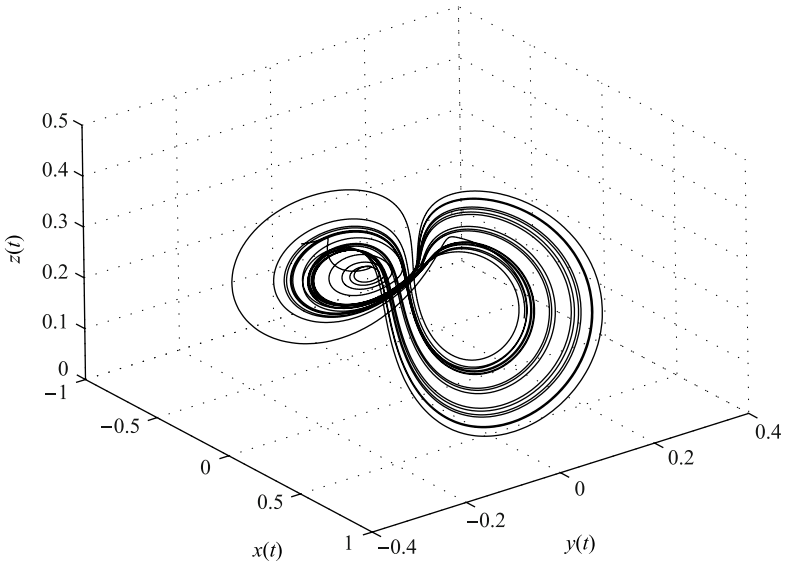

Fig. 5.48 Simulation result of the fractional-order Newton-Leipnik's system (5.79) in state space for parameters $a = 0.4$, $b = 0.175$ and orders $q_1 = q_3 = 1$, $q_2 = 0.97$ for simulation time $200\,s$.

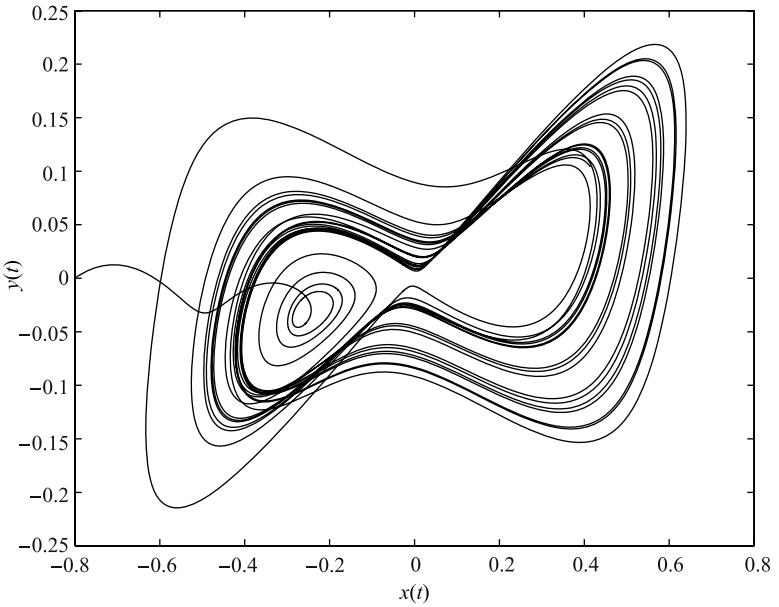

Fig. 5.49 Simulation result of the fractional-order Newton-Leipnik's system (5.79) projected onto $x - y$ plane for parameters $a = 0.4$, $b = 0.175$ and orders $q_1 = q_3 = 1$, $q_2 = 0.97$.

with unstable roots $\lambda_{1,2} \approx 1.0018 \pm 0.0152\,j$, because $|\arg(\lambda_{1,2})| = 0.0152 < \pi/2m$, where $m = 100$.

The characteristic equation of the linearized system evaluated at the equilibrium E_1 is

$$\lambda^{297} + 9/40\lambda^{197} + 2/5\lambda^{200} + 1.090\lambda^{100} - 7/100\lambda^{97} - 0.203 = 0,$$

with unstable root $\lambda \approx 0.9827$.

The characteristic equation of the linearized system evaluated at the equilibrium E_3 or E_4 is

$$\lambda^{297} + 2/5\lambda^{200} + 9/40\lambda^{197} - 0.04511\lambda^{100} + 0.67880\lambda^{97} + 0.61895 = 0,$$

with unstable roots $\lambda_{1,2} \approx 0.9986 \pm 0.0148\,j$, because $|\arg(\lambda_{1,2})| = 0.0148 < \pi/2m$, where $m = 100$.

It is interesting to observe that the system has two strange attractors to rotate by approximately 90° as depicted in Fig. 5.50. The dynamic of the fractional-order Newton-Leipnik's system was studied (Sheu et al., 2008), where the lowest total order of the system to yield chaos was found to be 2.82. This system displays better dynamic behavior.

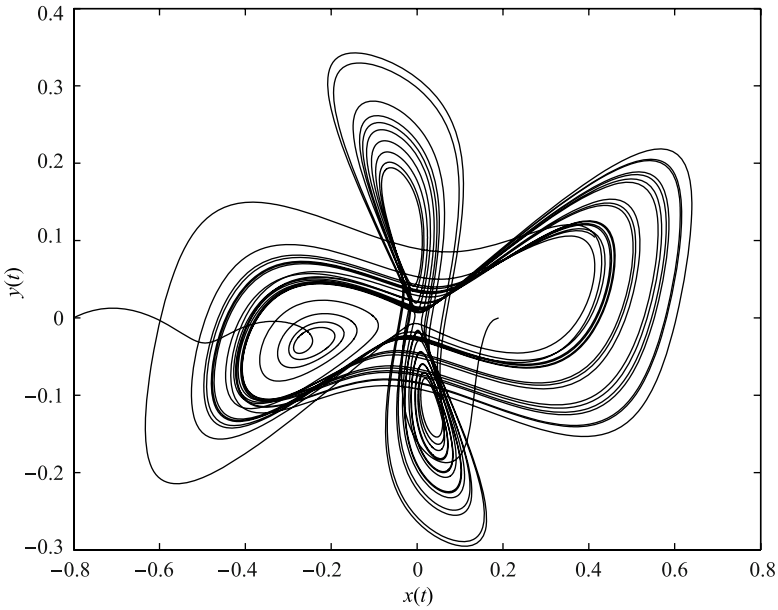

Fig. 5.50 Simulation results of the fractional-order Newton-Leipnik's system (5.79) projected onto $x-y$ plane for parameters $a = 0.4$, $b = 0.175$, orders $q_1 = q_2 = q_3 = 0.95$ and $q_1 = q_3 = 1$, $q_2 = 0.97$, respectively, for simulation time 200 s.

5.13 Fractional-Order Lotka-Volterra System

The Lotka-Volterra equations, also known as the predator-prey (or parasite-host) equations, are a pair of first order, non-linear, differential equations frequently used to describe the dynamics of biological systems in which two species interact on each other, one is a predator and the other is its prey. They were proposed independently by Alfred J. Lotka in 1925 and Vito Volterra in 1926.

Classical integer-order model of the Lotka-Volterra system is deffined as

$$\begin{aligned} \frac{dx(t)}{dt} &= x(t)(\alpha - \beta y(t)) \\ \frac{dy(t)}{dt} &= -y(t)(\gamma - \delta x(t)), \end{aligned} \tag{5.81}$$

where $y(t)$ is the number of some predators (for example, wolves); $x(t)$ is the number of its prey (for example, rabbits); $dy(t)/dt$ and $dx(t)/dt$ represent the growth of the two populations against time; t represents the time; and α, β, γ and δ are parameters representing the interaction of the two species.

The equations have periodic solutions which do not have a simple expression in terms of the usual trigonometric functions. However, an approximate linearized solution yields a simple harmonic motion with the population of predators following that of prey by 90°.

In the model system, the predators thrive when there are plentiful prey but, ultimately, outstrip their food supply and decline. As the predator population is low the prey population will increase again. These dynamics continue in a cycle of growth and decline. Hence the equation represents the change in the prey's numbers given by its own growth minus the rate at which it is preyed upon; the change in the predator population as the growth of the predator population, minus natural death. As the predator population is low the prey population will increase again. These dynamics continue in a cycle of growth and decline.

There are two equilibria when the system is solved for x and y. The above system of equations yields to $E_1 = (0;0)$ and $E_2 = (\lambda/\delta; \alpha/\beta)$.

The stability of the equlibrium point E_1 is of importance. If it were stable, non-zero populations might be attracted towards it. However, as the fixed point in origin is a saddle point, and hence unstable, we find that the extinction of both species is difficult in the model.

The second fixed point E_2 is not hyperbolic, so no conclusions can be drawn from the linear analysis. However, the system admits a constant of motion and the level curves are closed trajectories surrounding the fixed point. Consequently, the levels of the predator and prey populations cycle, and oscillate around this fixed point.

The fractional-order Lotka-Volterra (or fractional-order predator-prey model) system was proposed and described as (Ahmed et al., 2007):

$$\begin{aligned} {}_0D_t^q x(t) &= x(t)(\alpha - rx(t) - \beta y(t)) \\ {}_0D_t^q y(t) &= -y(t)(\gamma - \delta x(t)), \end{aligned} \tag{5.82}$$

where $0 < q \leqslant 1$, $x \geqslant 0$, $y \geqslant 0$ are prey and predator densities, respectively, and all constants r, α, β, γ and δ are positive. For $r = 0$ and $q = 1$ we obtain a well-known model (5.81). The stability analysis and numerical solutions of such kind of system have been studied (Ahmed et al., 2007).

In the paper (Samardzija and Greller, 1988) was proposed a two-predator and one-prey generalization of the Lotka-Volterra system. We assume its fractional-order modification as follows:

$$\begin{aligned} {}_0D_t^{q_1} x(t) &= ax(t) - bx(t)y(t) + ex^2(t) - sz(t)x^2(t), \\ {}_0D_t^{q_2} y(t) &= -cy(t) + dx(t)y(t), \\ {}_0D_t^{q_3} z(t) &= -pz(t) + sz(t)x^2(t), \end{aligned} \tag{5.83}$$

where a, b, c, d, e, p, s are model parameters and q_1, q_2, q_3 are fractional orders. When we consider $p = 0$, $s = 0$, $q_1 = q_2$ and $e = -r$ in the general model (5.83), we obtain the fractional-order (one predator and one prey) Lotka-Volterra model (5.82) upon the substitutions $\alpha \equiv a$, $\beta \equiv b$, $\gamma \equiv c$, and $\delta \equiv d$.

The proposed fractional-order Lotka-Volterra system (5.83) has five equilibrium points: $E_1 = (0;0;0)$, $E_2 = (-a/e;0;0)$, $E_3 = (\sqrt{sp}/s;0;(a + (e\sqrt{sp})/s)/\sqrt{sp})$, $E_4 = (-\sqrt{sp}/s;0;-(a - (e\sqrt{sp})/s)/\sqrt{sp})$, and $E_5 = (c/d;(da + ec)/db;0)$;

The Jacobian matrix of the system (5.83) for equilibrium $E^* = (x^*, y^*, z^*)$ is

$$\mathbf{J} = \begin{bmatrix} a - by^* + 2ex^* - 2sz^*x^* & -bx^* & -sx^{*2} \\ dy^* & -c + dx^* & 0 \\ 2sx^*z^* & 0 & -p + sx^{*2} \end{bmatrix}. \tag{5.84}$$

Numerical solution of the fractional-order Lotka-Volterra system (5.83) is given as follows:

$$\begin{aligned} x(t_k) &= (x(t_{k-1})(a - by(t_{k-1}) + ex(t_{k-1}) - sz(t_{k-1})x(t_{k-1})))\, h^{q_1} - \sum_{j=v}^{k} c_j^{(q_1)} x(t_{k-j}), \\ y(t_k) &= (-cy(t_{k-1}) + dx(t_k)y(t_{k-1}))\, h^{q_2} - \sum_{j=v}^{k} c_j^{(q_2)} y(t_{k-j}), \\ z(t_k) &= \left(-pz(t_{k-1}) + sz(t_{k-1})x^2(t_k)\right) h^{q_3} - \sum_{j=v}^{k} c_j^{(q_3)} z(t_{k-j}), \end{aligned} \tag{5.85}$$

where T_{sim} is the simulation time, $k = 1, 2, 3, \ldots, N$, for $N = [T_{sim}/h]$, and $(x(0), y(0), z(0))$ is the start point (initial conditions). The binomial coefficients $c_j^{(q_i)}$, $\forall i$ are calculated according to the relation (2.54).

Let us consider the following system parameters $a = 2, b = 1, c = 3, d = 1, e = 0, p = 0, s = 0$ and derivative orders $q_1 = q_2 = q_3 = 1$ and $q_1 = q_2 = q_3 = 0.9$, respectively. For these parameters the system (5.83) has two equilibria $E_1 = (0;0)$ and $E_2 = (3;2)$ and their corresponding eigenvalues are $\lambda_1 = 2$ and $\lambda_2 = -3$ for E_1

and $\lambda_{1,2} = \pm 2.4495j$ for E_2. Equilibrium E_1 is a saddle point and equilibrium E_2 is a center. The fixed point E_2 is not hyperbolic.

In Fig. 5.51 and Fig. 5.52 are depicted phase trajectories for various derivative orders $\bar{q} = 1.0$ and $\bar{q} = 0.9$, respectively, for simulation time $60\,s$, time step $h = 0.005$ and for the initial conditions: $(x(0), y(0), z(0)) = (1, 2, 0)$.

Let us consider the following system parameters $a = 1, b = 1, c = 1, d = 1, e = 2, p = 3, s = 2.7$ and orders $q_1 = q_2 = q_3 = 0.95$.

In Fig. 5.53 and Fig. 5.54 are depicted phase trajectories of the fractional-order Lotka-Volterra system (5.83) for orders $q_1 = q_2 = q_3 = 0.95$, and parameter $a = 1, b = 1, c = 1, d = 1, e = 2, p = 3, s = 2.7$, for simulation time $200\,s$, time step $h = 0.005$, and for the initial conditions: $(x(0), y(0), z(0)) = (1, 1.4, 1)$. We can observe the so-called "fractal torus" (Samardzija and Greller, 1988).

For the above parameters we obtain the following values of equilibrium points $E_1 = (0;0;0), E_2 = (-0.5;0;0), E_3 = (-1.0540;0;0.3893), E_4 = (1.0540;0;1.0921)$, and $E_5 = (1;3;0)$. The corresponding eigenvalues of the Jacobian matrix (5.84) evaluated at equilibrium points are: $\lambda_1 = -3$, $\lambda_2 = -1$, $\lambda_3 = 1$ for E_1, $\lambda_1 - -1$, $\lambda_2 = -1.5$, $\lambda_3 = -2.325$ for E_2, $\lambda_1 \approx -3.1266$, $\lambda_2 \approx 2.12661$, $\lambda_3 \approx -2.05409$ for E_3, $\lambda_1 = 0.5409$, $\lambda_{2,3} \approx -0.50 \pm 4.2894j$ for E_4, and $\lambda_1 = -0.3$, $\lambda_{2,3} \approx 1.0 \pm 1.4142j$ for E_5. The equlibrium E_1 is saddle point, the equilibrium E_2 is stable node, the equlibrium E_3 is saddle point, the equilibria E_4 and E_5 are saddle-focus points.

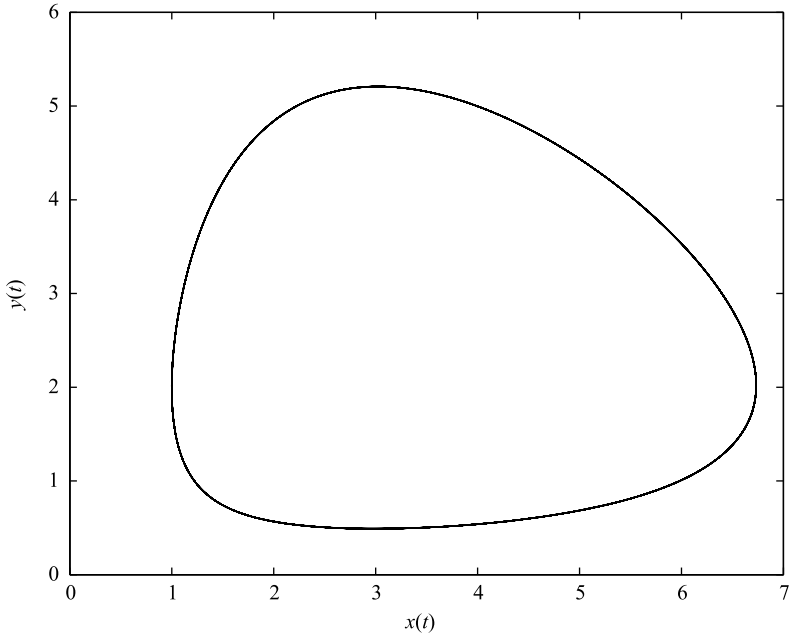

Fig. 5.51 Phase plane $x - y$ trajectory (limit cycle) for the Lotka-Volterra system with orders $q_1 = q_2 = 1.0$, $q_3 = 0$, and parameters $a = 2, b = 1, c = 3, d = 1, e = 0, p = 0, s = 0$.

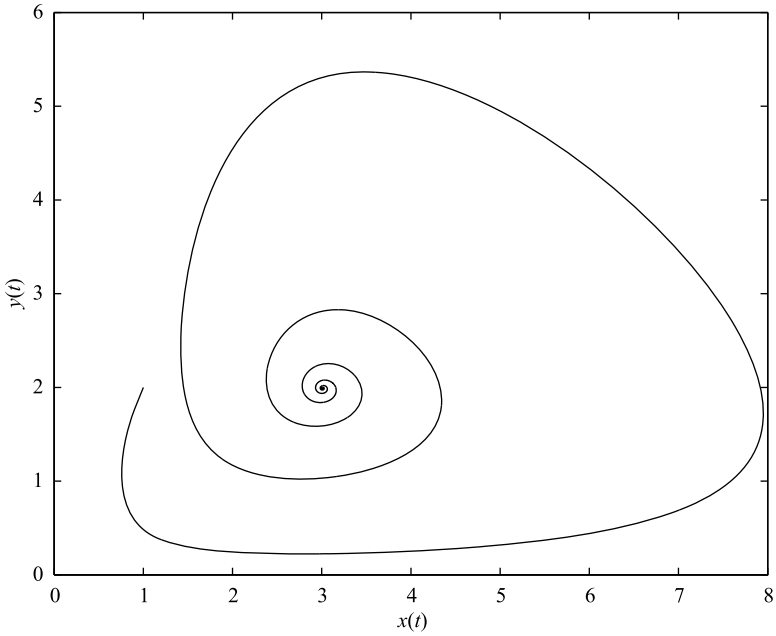

Fig. 5.52 Phase plane $x-y$ trajectory for the Lotka-Volterra with fractional-orders $q_1 = q_2 = q_3 = 0.9$, and parameters $a = 2, b = 1, c = 3, d = 1, e = 0, p = 0, s = 0$.

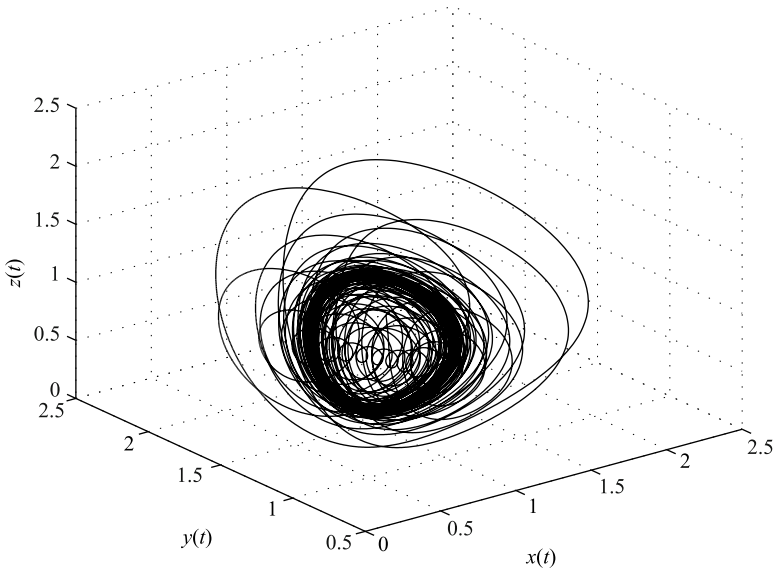

Fig. 5.53 Phase trajectory of the Lotka-Volterra system with orders $q_1 = q_2 = q_3 = 0.95$ and parameters $a = 1, b = 1, c = 1, d = 1, e = 2, p = 3, s = 2.7$ in state space.

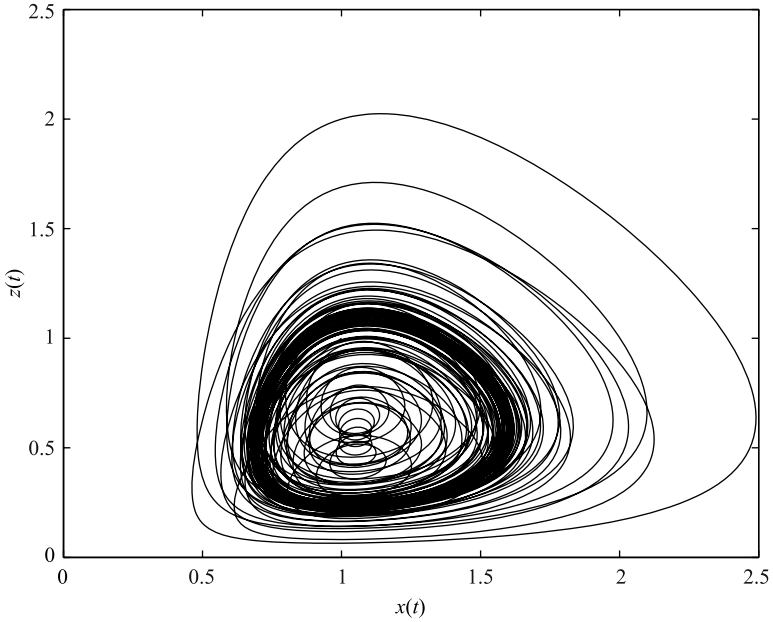

Fig. 5.54 Phase trajectory for the Lotka-Volterra with fractional-orders $q_1 = q_2 = q_3 = 0.95$, and parameters $a = 1, b = 1, c = 1, d = 1, e = 2, p = 3, s = 2.7$ in state plane $x - z$.

The characteristic equation of the linearized system (5.83) at the equlibrium point E_1 is

$$(\lambda^{95} - 1)(\lambda^{95} + 1)(\lambda^{95} + 3) = 0,$$

with unstable root $\lambda_1 = 1$. The characteristic equation at equilibrium E_2 is

$$(\lambda^{95} + 1.0)(\lambda^{95} + 1.5)(\lambda^{95} + 2.3250) = 0,$$

with stable roots. The characteristic equation of the linearized system (5.83) at equilibrium E_3 is

$$\lambda^{285} + 3.054092\lambda^{190} - 4.59501\lambda^{95} - 13.657888 = 0,$$

with unstable root $\lambda_1 \approx 1.0080$. The characteristic equation of the linearized system at equilibrium E_4 is

$$\lambda^{285} + 0.945907\lambda^{190} + 18.595018\lambda^{95} - 1.008778 = 0,$$

with unstable root $\lambda_1 \approx 0.9698$. Finally, the characteristic equation at equilibrium point E_5 is

$$\lambda^{285} - 1.7\lambda^{190} + 2.4\lambda^{95} + 0.9 = 0,$$

with unstable roots $\lambda_{1,2} \approx 1.0057 \pm 0.0101\,j$, because $|\arg(\lambda_{1,2})| = 0.0101 < \pi/2m$, where $m = 100$ (LCM of orders denominator). The condition for the chaotic system is satisfied.

The "fractal torus" attractor exhibited by the system (5.83) for certain values of the parameters and orders is interesting because it exhibits a structure entirely different from attractors such as, for instance, the Rössler or Lorenz attractors. Numerical simulations showed that different initial conditions often lead to different fast manifolds.

The system described in this section suggests that it is a reasonable biological or chemical model. It could be modified also to one-predator and two-prey scheme.

5.14 Fractional-Order Financial System

The chaotic phenomenon in macro economics was found in 1985. The continuos economical system was described and analyzed (Ma and Chen, 2001a,b). The simplified financial model is defined as:

$$\begin{aligned} \frac{dx(t)}{dt} &= z(t) + (y(t) - a)x(t), \\ \frac{dy(t)}{dt} &= 1 - by(t) - x(t)^2, \\ \frac{dz(t)}{dt} &= -x(t) - cz(t), \end{aligned} \tag{5.86}$$

where a is the saving amount, b is the cost per investment, and c is the elasticity of demand of commercial market. The state variables are: $x(t)$ is the interest rate, $y(t)$ is the investment demand, and $z(t)$ is the price index.

The system (5.86) has three equilibrium points: $E_1 = (0; 1/b; 0)$,

$$E_2 = (\sqrt{(c-b-abc)/c}; (1+ac)/c; -(1/c)\sqrt{(c-b-abc)/c},$$

$$E_3 = (-\sqrt{(c-b-abc)/c}; (1+ac)/c; (1/c)\sqrt{(c-b-abc)/c}.$$

The Jacobian matrix of the system (5.86), evaluated at the equilibrium $E^* = (x^*, y^*, z^*)$, is given by

$$\mathbf{J} = \begin{bmatrix} -a + y^* & x^* & 1 \\ -2^* & -b & 0 \\ -1 & 0 & -c \end{bmatrix}. \tag{5.87}$$

The fractional-order financial system is described as follows (Chen, 2008):

$$\begin{aligned} {}_0D_t^{q_1}x(t) &= z(t) + (y(t) - a)x(t), \\ {}_0D_t^{q_2}y(t) &= 1 - by(t) - x(t)^2, \\ {}_0D_t^{q_3}z(t) &= -x(t) - cz(t), \end{aligned} \tag{5.88}$$

where the total order of the system is denoted by $\bar{q} = (q_1, q_2, q_3)$.

The numerical solution of the fractional-order financial system has the following form:

$$\begin{aligned} x(t_k) &= (z(t_{k-1}) - (y(t_{k-1}) - a)x(t_{k-1}))\, h^{q_1} - \sum_{j=v}^{k} c_j^{(q_1)} x(t_{k-j}), \\ y(t_k) &= \left(1 - by(t_k) - x^2(t_k)\right) h^{q_2} - \sum_{j=v}^{k} c_j^{(q_2)} y(t_{k-j}), \\ z(t_k) &= (-x(t_k) - cz(t_{k-1}))\, h^{q_3} - \sum_{j=v}^{k} c_j^{(q_3)} z(t_{k-j}), \end{aligned} \tag{5.89}$$

where T_{sim} is the simulation time, $k = 1, 2, 3, \ldots, N$, for $N = [T_{sim}/h]$, and $(x(0), y(0), z(0))$ is the start point (initial conditions). The binomial coefficients $c_j^{(q_i)}$, $\forall i$ are calculated according to the relation (2.54).

Let us consider the following parameters of the system (5.88): $a = 1.0$, $b = 0.1$ and $c = 1.0$. The corresponsing eigenvalues for the system equilibrium $E_1 = (0; 10; 0)$ are: $\lambda_1 \approx 8.898979$, $\lambda_2 \approx -0.8989794$, and $\lambda_3 \approx -0.1$. It is a saddle point. For the equilibrium points $E_2 = (0.894427; 2; -0.894427)$ and $E_3 = (-0.894427; 2; 0.894427)$ they are: $\lambda_1 \approx -0.7608747$ and $\lambda_{2,3} \approx 0.3304373 \pm 1.411968j$. It is a saddle-focus point. Because it is an unstable equilibrium, the condition for chaos is satisfied and chaotic system (5.88) with the above parameters can exhibit chaotic behavior. The minimal commensurate order of the system is $q > 0.8536$.

Assume the commensurate order $q_1 = q_2 = q_3 = 0.9$ of the system (5.88) with the parameters $a = 1.0$, $b = 0.1$, and $c = 1.0$. The characteristic equation of the linearized system for equilibrium E_1 is

$$\lambda^{27} - 7.9\lambda^{18} - 8.8\lambda^9 - 0.8 = 0$$

and the unstable root for the equilibrium E_1 is $\lambda_1 \approx 1.2749$. The characteristic equation of the linearized system for equilibria E_2 and E_3 is

$$\lambda^{27} + 0.1\lambda^{18} + 1.6\lambda^9 + 1.6 = 0$$

and unstable eigenvalues for equilibria E_2 and E_3 are $\lambda_{1,2} \approx 1.0306 \pm 0.1547j$, because $|\arg(\lambda_{1,2})| = 0.1490 < \pi/2m$, where $m = 10$ (LCM of orders denominator).

In Fig. 5.55 is depicted the simulation result of the financial system (5.88) for the following parameters: $a = 1$, $b = 0.1$, and $c = 1.0$, orders $q_1 = 0.9$, $q_2 = 0.9$, $q_3 = 0.9$, and computational time $200\,s$, for time step $h = 0.005$.

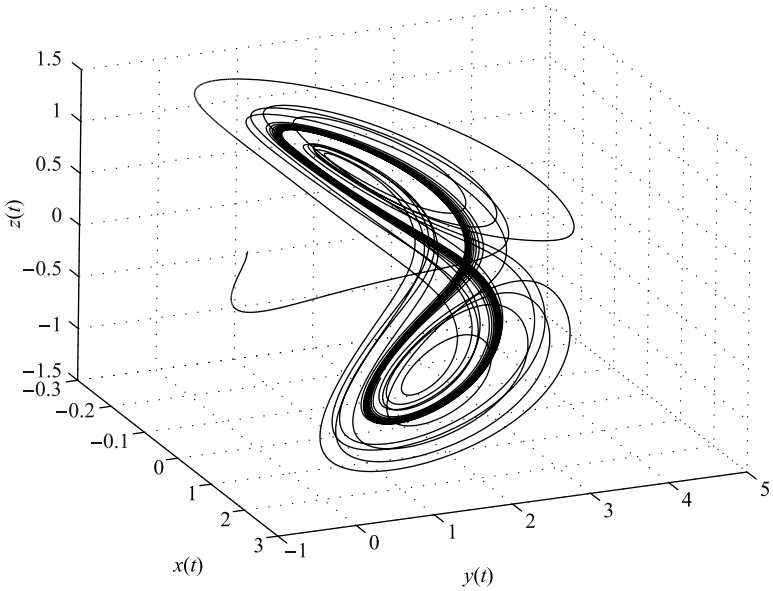

Fig. 5.55 Simulation result of the fractional-order financial system (5.88) in state space for the initial conditions $(x(0), y(0), z(0)) = (2, -1, 1)$.

Assume the incommensurate order $q_1 = 1.0$, $q_2 = 0.95$, $q_3 = 0.9$ of the system (5.88) with the parameters $a = 1.0$, $b = 0.1$, and $c = 1.0$. The characteristic equation of the linearized system for equilibrium E_1 is

$$\lambda^{285} + \lambda^{195} + 1/10\lambda^{190} - 9\lambda^{185} + 1/10\lambda^{100} - 8\lambda^{95} - 0.9\lambda^{90} - 0.8 = 0$$

and unstable root for the equilibrium E_1 is $\lambda_1 \approx 1.0221$. The characteristic equation of the linearized system for equilibria E_2 and E_3 is

$$\lambda^{285} + \lambda^{195} + 1/10\lambda^{190} - \lambda^{185} + 1/10\lambda^{100} + 1.5\lambda^{90} + 1.6 = 0$$

and unstable eigenvalues for equilibria E_2 and E_3 are $\lambda_{1,2} \approx 1.0035 \pm 0.0139j$, because $|\arg(\lambda_{1,2})| = 0.0138 < \pi/2m$, where $m = 100$ (LCM of orders denominator).

In Fig. 5.56 are depicted the simulation results of the financial system (5.88) for the following parameters: $a = 1.0$, $b = 0.1$, and $c = 1.0$, orders $q_1 = 1.0$, $q_2 = 0.95$, $q_3 = 0.9$, and computational time $200\,s$, for time step $h = 0.005$.

Investigation of chaos in various cases of the fractional-order financial system and its cross-validation with the largest Lyapunov exponent was done (Chen, 2008). The lowest order at which this system yielded chaos was 2.35.

In the next chapter we will use this system as a controlled system for the sliding mode control strategy.

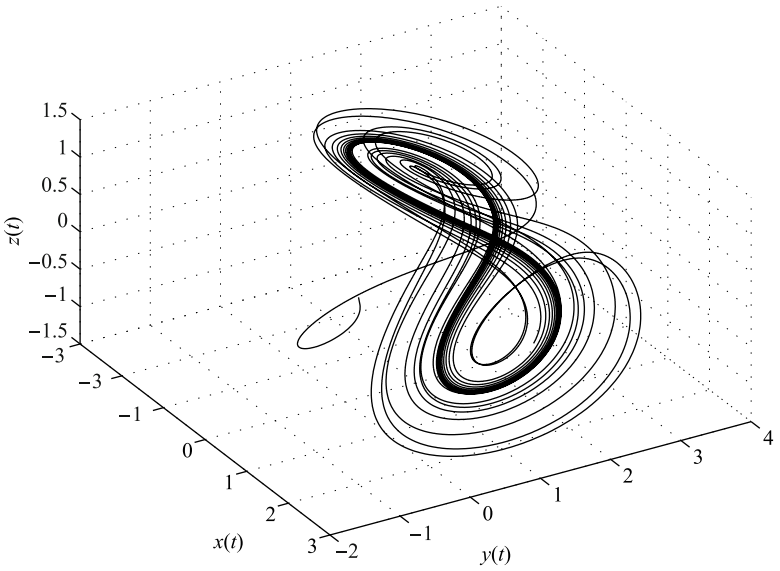

Fig. 5.56 Simulation result of the fractional-order financial system (5.88) in state space for the initial conditions $(x(0), y(0), z(0)) = (2, -1, 1)$.

5.15 Fractional-Order CNN

The basic circuit unit of the Cellular Neural Network (CNN) is a cell. The CNN was introduced by L. O. Chua in 1988. It contains linear and non-linear circuit elements, which typically are: linear capacitor, linear resistors, linear and non-linear controlled sources, and independent sources. Any cell in the CNN is connected only to its neighbor cells. Theoretically we can define the CNN of any dimension, e.g. two-dimensional array of $M \times N$, having M rows and N columns. We call the cell on the i-th row and the j-th column the cell $C(i, j)$. Observe from Fig. 5.57 that each cell $C(i, j)$ contains one independent voltage source $E_{i,j}$, one independent current source I, one linear capacitor C, two linear resistors R_x and R_y, controlling input voltage u_{ij}, state voltage of the cell x_{ij}, feedback from the output voltage y_{ij} of each neighbor cell $C(k,l)$. In fact each cell $C(i, j)$ mutually interacts with all the cells belonging to its neighbors $N_r(i, j)$ by means of the voltage-controlled current source $I_{xy}(i, j; k, l) = A(i, j; k, l)y_{kl}$, $I_{xu}(i, j; k, l) = B(i, j; k, l)u_{kl}$ and $I_{xx}(i, j; k, l) = C(i, j; k, l)x_{kl}$. The constant coefficients $A(i, j; k, l)$, $B(i, j; k, l)$ and $C(i, j; k, l)$ are known as the cloning templates. If they are equal for each cell, they are called space-invariant. The CNN is described by the following state equation of all its cells (Chua and Roska, 1993):

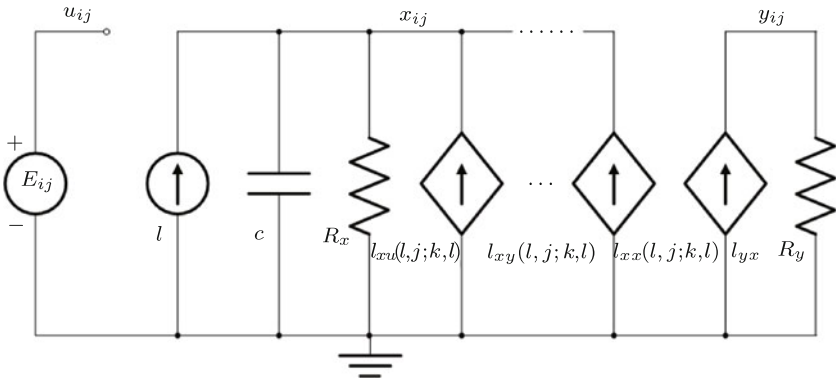

Fig. 5.57 The CNN cell

$$C\frac{dx_{ij}(t)}{dt} = -\frac{1}{R_x}x_{ij}(t) + \sum_{C(k,l)\in N_r(i,j)} A(i,j;k,l)y_{kl}(t) + \sum_{C(k,l)\in N_r(i,j)} B(i,j;k,l)u_{kl}(t) + C(i,j;k,l)x_{kl}(t) + I, \quad (5.90)$$

with $x_{ij}(0) = x_{ij0}$, $C > 0$, $R_x > 0$, $1 \le i \le M$, and $1 \le j \le N$, where

$$N_r(i,j) = \{C(k,l) : \max(|k-i| - |l-j|) \le r\}$$

is the r-neighborhood. Input equation is: $u_{ij}(t) = E_{ij}$. Output equation is:

$$f(x_{ij}) = y_{ij}(t) = \frac{1}{2}(|x_{ij}(t)+1| - |x_{ij}(t)-1|). \quad (5.91)$$

This model with direct dependence of state variable on the state of the neighboring cells is known as a state-controlled CNN. Such kind of CNNs is also able to show chaotic behavior (Chua and Roska, 1993; Biey et al., 2003; Zou and Nossek, 1993).

The only non-linear element in each cell is a piecewise-linear voltage-controlled current source: $I_{yx} = (1/R_y)f(x_{ij})$.

In addition, in this section we derive the fractional-order model of the CNN described by (5.90). For this purpose we will consider the general model of a capacitor described by Equation (2.75). Westerlund and Ekstam provided in their work (Westerlund and Ekstam, 1994) the table of various capacitor dielectric with appropriate constant m (derivative order), which has been obtained experimentally by measurements. Carlson also studied, in 1963, the fractional capacitor and appropriate approximation technique for its model (Carlson and Halijak, 1963).

Applying the Kirchhoff law and the relation (2.75) to standard model of the CNN which is described by Equation (5.90), we obtain a fractional-order model of the CNN in the following form (Petráš, 2006):

$$C\frac{d^m x_{ij}(t)}{dt^m} = -\frac{1}{R_x}x_{ij}(t) + \sum_{C(k,l)\in N_r(i,j)} A(i,j;k,l)y_{kl}(t) + \sum_{C(k,l)\in N_r(i,j)} B(i,j;k,l)u_{kl}(t) + C(i,j;k,l)x_{kl}(t) + I, \quad (5.92)$$

with $x_{ij}(0) = x_{ij0}$, $C > 0$, $0 < m < 1$, $R_x > 0$, $1 \le i \le M$, and $1 \le j \le N$.

In the works (Arena at al., 1998; Arena et al., 2000), the parameter m is $1 < m < 1.5$ and two-cell CNN was studied. Considering that $0 < m < 1$ and the fact that we would like to study the behavior of system with the total order less than three, we have to consider three-cell fractional-order CNN. Referring to the general definition of CNN given by (5.92) and choosing the opposite-sign template we obtain the following three-cell CNN ($M = 3$, $N = 1$, $C = 1$, $R = 1$, and $u_{kl} = 0$):

$$\begin{aligned} {}_0D_t^{q_1}x_1(t) &= -x_1(t) + p_1 f(x_1(t)) - sf(x_2(t)) - sf(x_3(t)),\\ {}_0D_t^{q_2}x_2(t) &= -x_2(t) - sf(x_1(t)) + p_2 f(x_2(t)) - rf(x_3(t)),\\ {}_0D_t^{q_3}x_3(t) &= -x_3(t) - sf(x_1(t)) + rf(x_2(t)) + p_3 f(x_3(t)), \end{aligned} \quad (5.93)$$

where $p_1 > 1$, $p_2 > 1$, $p_3 \ge 1$, $r > 0$, and $s > 0$ are the CNN parameters, q_1, q_2, and q_3 are the derivative orders for each cell (related to the capacitor order m).

Let us assume that we have the three-identical-cell CNN described by Eqs. (5.93), with fractional commensurate order $q_1 = q_2 = q_3 = 0.99$ (orders of real analog capacitors). We can use the relations (2.53) and (2.54) to derive a numerical solution of the fractional-order CNN described by (5.93) as follows:

$$\begin{aligned} x_1(t_k) &= (-x_1(t_{k-1}) + p_1 f(x_1(t_{k-1})) - sf(x_2(t_{k-1})) - sf(x_3(t_{k-1})))\,h^{q_1} - \sum_{j=v}^{k} c_j^{(q_1)} x_1(t_{k-j}),\\ x_2(t_k) &= (-x_2(t_{k-1}) - sf(x_1(t_k)) + p_2 f(x_2(t_{k-1})) - rf(x_3(t_{k-1})))\,h^{q_2} - \sum_{j=v}^{k} c_j^{(q_2)} x_2(t_{k-j}),\\ x_3(t_k) &= (-x_3(t_{k-1}) - sf(x_1(t_k)) + rf(x_2(t_k)) + p_3 f(x_3(t_{k-1})))\,h^{q_3} - \sum_{j=v}^{k} c_j^{(q_3)} x_3(t_{k-j}), \end{aligned} \quad (5.94)$$

where a nonlinear function $f(.)$ is defined by (5.91), T_{sim} is the simulation time, $k = 1, 2, 3, \ldots, N$, for $N = [T_{sim}/h]$, and $(x_1(0), x_2(0), x_3(0))$ is the start point (initial conditions).

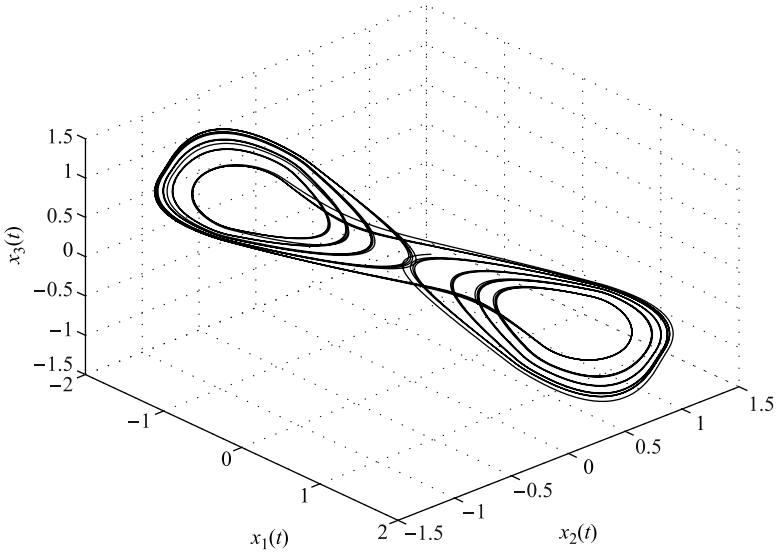

Fig. 5.58 State space trajectory of the CNN (5.93) for the parameters: $p_1 = 1.24$, $p_2 = 1.1$, $p_3 = 1$, $s = 3.21$, $r = 4.4$, orders $q_1 = q_2 = q_3 = 0.99$, with initial conditions: $(x_1(0), x_2(0), x_3(0)) = (0.1, 0.1, 0.1)$.

The simulation result for time step $h = 0.005$ and simulation time $T_{sim} = 100\,s$ is depicted in Fig. 5.58. The result shows the chaotic double scroll attractor of the three-cell fractional-order CNNs (5.93) for the parameters $p_1 = 1.24$, $p_2 = 1.1$, $p_3 = 1$, $s = 3.21$, $r = 4.4$, and system orders $q_1 = 0.99$, $q_2 = 0.99$, and $q_3 = 0.99$ with the initial conditions: $(x_1(0), x_2(0), x_3(0)) = (0.1, 0.1, 0.1)$.

5.16 Fractional-Order Volta's System

The system was discovered by Volta – a student at the Department of Physics, Genova University, in 1984, when writing his thesis with Prof. Antonio Borsellino and Dr. Francisco Fu Arcardi.

Volta's system is described by the system of state differential equations (Hao, 1989):

$$\begin{aligned} \dot{x}(t) &= -x(t) - 5y(t) - z(t)y(t), \\ \dot{y}(t) &= -y(t) - 85x(t) - x(t)z(t), \\ \dot{z}(t) &= 0.5z(t) + x(t)y(t) + 1. \end{aligned} \tag{5.95}$$

The Lyapunov exponents (LE) of the system (5.95) computed according to the method described in the work (Wolf et al., 1985) are: $LE_1 = 0.064979$, $LE_2 = -1.0708$, and $LE_3 = -1.4936$ for initial values (8, 2, 1).

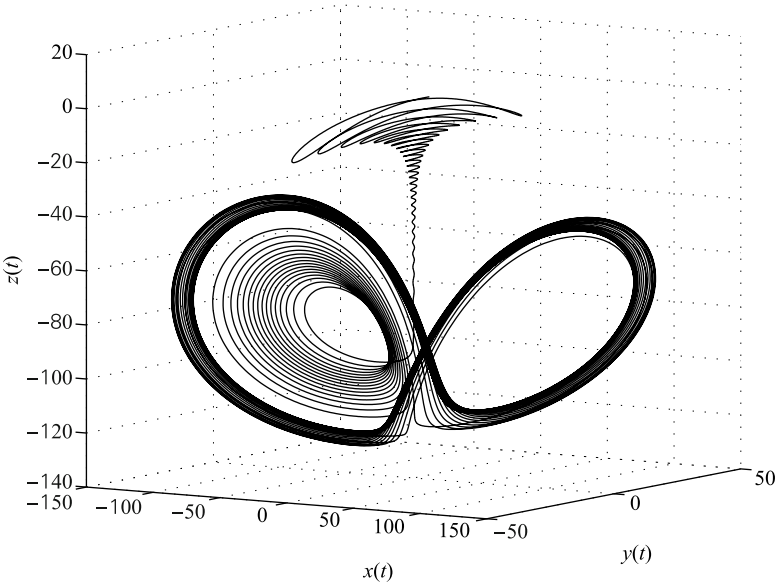

Fig. 5.59 Chaotic attractor of Volta's system (5.95) projected into 3D state space for initial conditions $(x(0), y(0), z(0)) = (8, 2, 1)$ and $T_{sim} = 20\,s$.

Fig. 5.60 shows the time histories of variables $x(t)$, $y(t)$, and $z(t)$ of the system (5.95), for $T_{sim} = 10\ s$. In Fig. 5.59 is depicted a phase trajectory in 3D state-space of Volta's system (5.95) for $T_{sim} = 20\,s$ starting from $(x(0), y(0), z(0)) = (8, 2, 1)$.

In Fig. 5.61 are shown the phase trajectories, starting from $(x(0), y(0), z(0)) = (8, 2, 1)$, and projected into 2D phase planes, respectively.

Obviously, if the Laypunov exponent LE_1 is positive and if we observe strange attractors in Fig. 5.59 and Fig. 5.61, the system (5.95) has chaotic behavior toward initial values $(x(0), y(0), z(0)) = (8, 2, 1)$.

We can generalize Volta's system (5.95) to the following form:

$$\begin{aligned} \frac{dx(t)}{dt} &= -x(t) - ay(t) - z(t)y(t), \\ \frac{dy(t)}{dt} &= -y(t) - bx(t) - x(t)z(t), \\ \frac{dz(t)}{dt} &= cz(t) + x(t)y(t) + 1. \end{aligned} \tag{5.96}$$

The Jacobian matrix of the system (5.96), evaluated at the equilibrium $E^* = (x^*, y^*, z^*)$, is given by

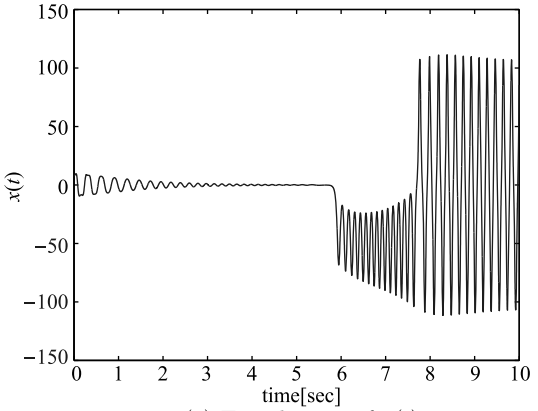

(a) Time history of $x(t)$

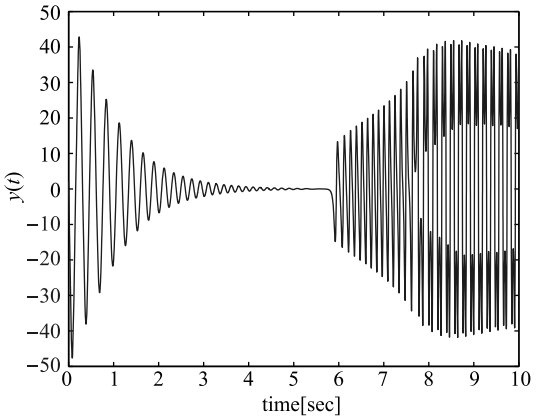

(b) Time history of $y(t)$

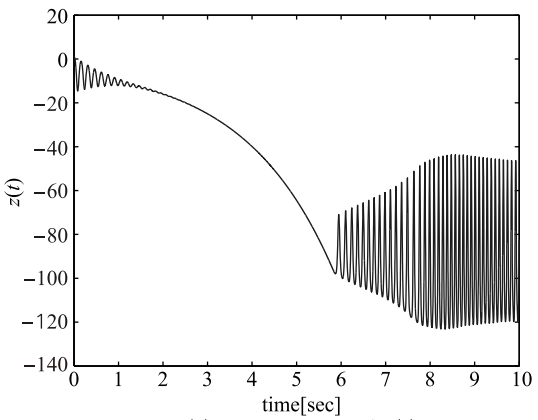

(c) Time history of $z(t)$

Fig. 5.60 Time responses of Volta's system (5.95) to $T_{sim} = 10\,s$ and $(x(0), y(0), z(0)) = (8, 2, 1)$.

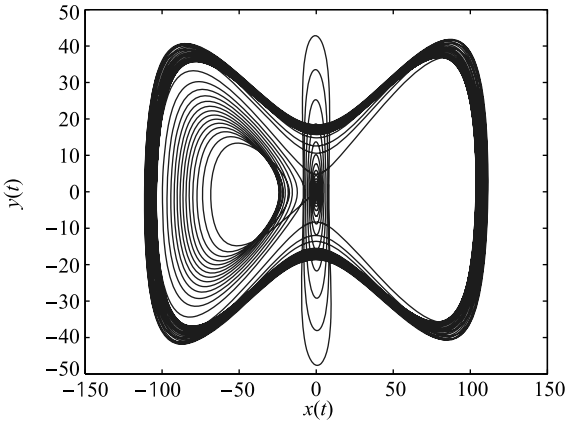

(a) Phase plane $x(t)$ vs. $y(t)$

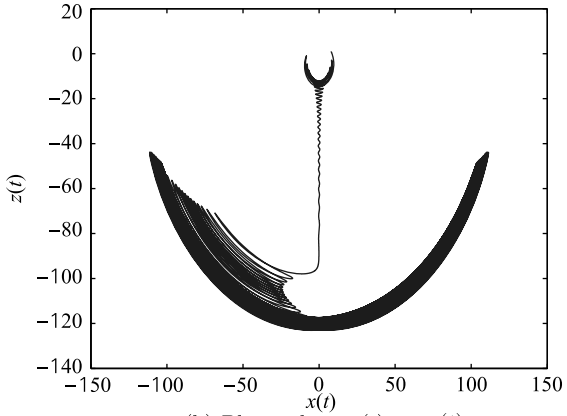

(b) Phase plane $x(t)$ vs $z(t)$

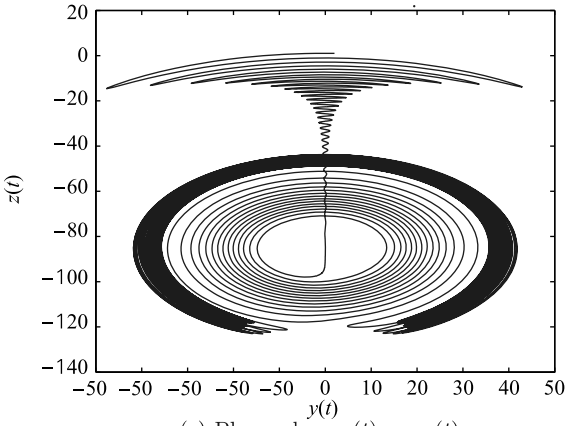

(c) Phase plane $y(t)$ vs. $z(t)$

Fig. 5.61 Phase plane projections of Volta's system (5.95) for $T_{sim} = 20\,s$.

$$\mathbf{J} = \begin{bmatrix} -1 & -a-z^* & -y^* \\ -b-z^* & -1 & -x^* \\ y^* & x^* & c \end{bmatrix}. \tag{5.97}$$

When $(a,b,c) = (5,85,0.5)$, Volta's system shows chaotic behavior (Fig. 5.59 and Fig. 5.61). For these system parameters, Volta's system has three quilibria $E_1 = (0;0;-2)$, $E_2 = (-57.6282;-0.7202;-85.0124)$, $E_3 = (57.6282;0.7202;-85.0124)$ and their corresponding eigenvalues are: $\lambda_1 \approx 14.7797$, $\lambda_2 \approx -16.7797$, $\lambda_3 = 0.5$ for E_1, $\lambda_1 = -2$, $\lambda_{2,3} \approx 0.25 \pm 57.6322j$ for E_2, and $\lambda_1 \approx -10.6861$, $\lambda_2 \approx 11.18617$, $\lambda_3 - 2$ for E_3.

Hence, the equilibria E_1 and E_3 are unstable saddle points. The equilibrium E_2 is a saddle-focus point. According to the stability conditions (4.40), where $q = 1$, we have eigenvalues for equilibria E_1, E_2 and E_3 in the unstable region and therefore we can confirm the chaotic behavior of Volta's systems (5.95) for the initial conditions $(x(0),y(0),z(0)) = (8,2,1)$.

Now, we consider the fractional-order Volta's system, where integer-order derivatives are replaced by fractional-order ones. The mathematical description of the fractional-order chaotic system is expressed as (Petráš, 2009a):

$$\begin{aligned} {}_0D_t^{q_1} x(t) &= -x(t) - ay(t) - z(t)y(t), \\ {}_0D_t^{q_2} y(t) &= -y(t) - bx(t) - x(t)z(t), \\ {}_0D_t^{q_3} z(t) &= cz(t) + x(t)y(t) + 1, \end{aligned} \tag{5.98}$$

where q_1, q_2, and q_3 are the derivative orders. The total order of the system is $\bar{q}$=(q_1, q_2, q_3).

For numerical solution of the chaotic system (5.98) we use the relationship (2.53), which leads to approximation in FIR form. By setting $N = [T_{sim}/h]$, we have

$$\begin{aligned} x(t_k) &= \left(-x(t_{k-1}) - ay(t_{k-1}) - z(t_{k-1})y(t_{k-1})\right) h^{q_1} - \sum_{j=v}^{k} c_j^{(q_1)} x(t_{k-j}), \\ y(t_k) &= \left(-y(t_{k-1}) - bx(t_k) - x(t_k)z(t_{k-1})\right) h^{q_2} - \sum_{j=v}^{k} c_j^{(q_2)} y(t_{k-j}), \\ z(t_k) &= \left(cz(t_{k-1}) + x(t_k)y(t_k) + 1\right) h^{q_3} - \sum_{j=v}^{k} c_j^{(q_3)} z(t_{k-j}), \end{aligned} \tag{5.99}$$

where T_{sim} is the simulation time, $k = 1,2,3,\ldots,N$ and $(x(0),y(0),z(0))$ is the start point (initial conditions). The binomial coefficients $c_j^{(q_i)}$, $\forall i$ are calculated according to the relation (2.54).

When we assume the same orders of derivatives in state equations (5.98), i.e. $q_1 = q_2 = q_3 \equiv q$, we get a commensurate-order system. According to condition (4.42) it is determined that the commensurate order q of derivatives has to be

$q > 0.99$. It means that for system parameters $(a,b,c) = (5,85,0.5)$, only for integer order $q = 1$, chaos can be observed. If we would like to go to the fractional (commensurate) order, we have to change the system parameters, e.g. for system parameters $(a,b,c) = (19,11,0.73)$, chaos can be observed if $q > 0.977$. For these parameter sets, Volta's system has three equilibria $E_1 = (0;0;-1.3698)$, $E_2 = (-1.26310;-10.26032;-19.12310)$, $E_3 = (1.26310;10.26032;-19.12310)$ and their corresponding eigenvalues are $\lambda_1 \approx 12.0299$, $\lambda_2 \approx -14.0299$, $\lambda_3 - 0.73$ for E_1, $\lambda_1 = -2$, $\lambda_{2,3} \approx 0.3650 \pm 10.3313\,j$ for E_2, and $\lambda_1 \approx -7.2088$, $\lambda_2 \approx 7.93883$, $\lambda_3 = -2$ for E_3.

Hence, the equilibria E_1 and E_3 are saddle points and the equilibrium E_2 is saddle-focus point. The characteristic equation evaluated at equilibrium E_1 is

$$\lambda^{294} + 127/100\lambda^{196} - 170.2406\lambda^{98} + 123.2098 = 0,$$

with unstable roots $\lambda_1 \approx 0.9968$ and $\lambda_2 \approx 1.0257$.

The characteristic equation evaluated at equilibrium E_2 is

$$\lambda^{294} + 127/100\lambda^{196} + 105.40980\lambda^{98} + 213.7396 = 0,$$

with unstable roots $\lambda_{1,2} \approx 1.0240 \pm 0.0160\,j$, becasue $|\arg(\lambda_{1,2})| = 0.0157 < \pi/2m$, where $m = 100$ (LCM of orders denominator).

The characteristic equation evaluated at equilibrium E_3 is

$$\lambda^{294} + 127/100\lambda^{196} - 58.6898\lambda^{98} - 114.45960 = 0,$$

with unstable root $\lambda_1 \approx 1.0214$.

According to the stability conditions (4.40), where $q = 0.98$, we have eigenvalues of the equilibrium points E_1, E_2 and E_3 in the unstable region and therefore we can confirm the chaotic behavior of Volta's systems (5.98) for the initial conditions $(8,2,1)$. Instability measure is 0.0157. It means that commensurate fractional-order Volta's system is chaotic.

In Fig. 5.62 is shown the chaotic behavior toward fractional-order system (5.98), where system parameters are $(a,b,c) = (19,11,0.73)$, commensurate order of the derivatives is $q = 0.98$, the initial conditions are $(x(0),y(0),z(0)) = (8,2,1)$ for simulation time $T_{sim} = 20\,s$ and time step $h = 0.0005$.

When we assume the different orders of derivatives in state equations (5.98), i.e. $q_1 \neq q_2 \neq q_3$, we get a general incommensurate-order system. There is no exact condition for determining the orders to obtain chaotic behavior of the system. We experimentally found the following orders (Petráš, 2010): $q_1 = 0.89$, $q_2 = 1.10$, and $q_3 = 0.91$ for system parameters $(a,b,c) = (5,85,0.5)$.

The stability can be investigated according to characteristic equation (4.41). For the above derivative orders and the system parameters, and for the Jacobian matrix (5.97) evaluated at the equilibrium points E^*, Equation (4.41) becomes

$$\det(\mathrm{diag}([\lambda^{89}\ \lambda^{110}\ \lambda^{91}]) - \mathbf{J}) = 0, \tag{5.100}$$

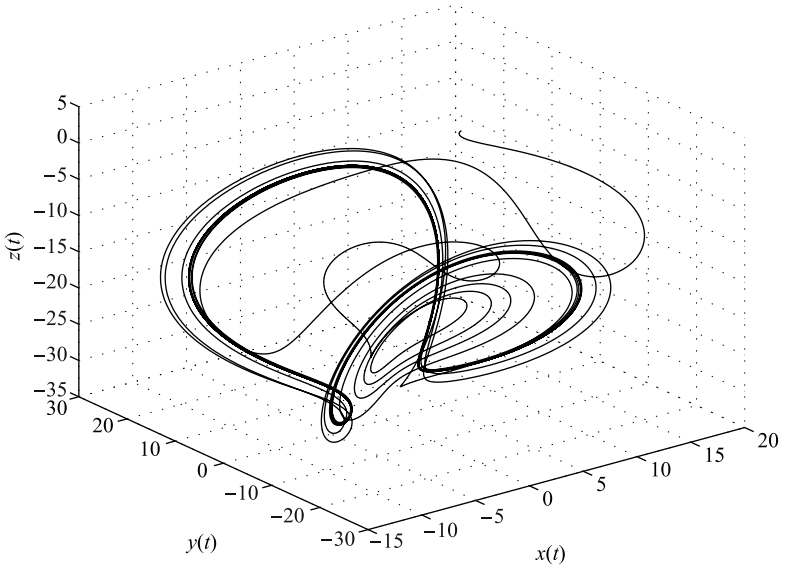

Fig. 5.62 Chaotic attractor of Volta's system (5.98) projected into 3D state space for initial conditions $(x(0), y(0), z(0)) = (8, 2, 1)$, parameters $(a, b, c) = (19, 11, 0.73)$, orders $(q_1, q_2, q_3) \equiv (q = 0.98)$ and $T_{sim} = 20\,s$.

where the LCM is $m = 100$. The characteristic equation (5.100) evaluated at equilibrium E_1 is

$$\lambda^{290} + \lambda^{201} - 1/2\lambda^{199} + \lambda^{180} - 1/2\lambda^{110} - 248\lambda^{91} - 1/2\lambda^{89} + 124 = 0,$$

with unstable roots $\lambda_1 \approx 1.0274$ and $\lambda_2 \approx 0.9924$.

The characteristic equation evaluated at equilibrium E_2 is

$$\lambda^{290} - 1/2\lambda^{199} + \lambda^{180} + 3320.5186\lambda^{89} + \lambda^{201} + 0.01874\lambda^{110} - 0.127x10^{-28}\lambda^{91} + 6643.0748 = 0,$$

with unstable roots $\lambda_{1,2} \approx 1.0411 \pm 0.0161\,j$, becasue $|\arg(\lambda_{1,2})| = 0.0155 < \pi/2m$, where $m = 100$ (LCM of orders denominator).

The characteristic equation evaluated at equilibrium E_3 is

$$\lambda^{290} - 1/2\lambda^{199} + \lambda^{180} - 0.5186\lambda^{89} + \lambda^{201} - 120.0187\lambda^{110} + 0.333 \times 10^{-29}\lambda^{91} - 239.0748 = 0,$$

which has unstable root $\lambda_1 = 1.0270$.

Because the system has unstable roots, the system satisfies the necessary condition for exhibiting chaotic attractor. Instability measure is 2.137×10^{-4}.

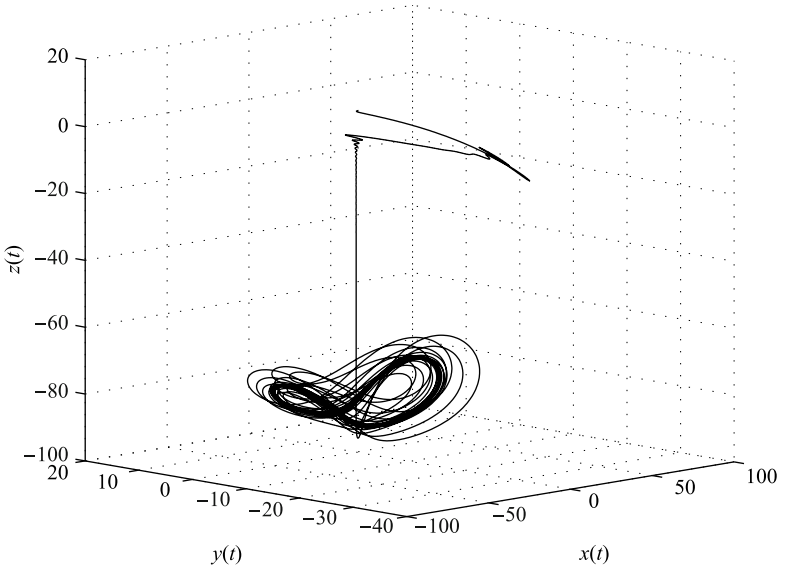

Fig. 5.63 Chaotic attractor of Volta's system (5.98) projected into 3D state space for initial conditions $(x(0), y(0), z(0)) = (8, 2, 1)$, parameters $(a, b, c) = (5, 85, 0.5)$, orders $(q_1, q_2, q_3) \equiv \bar{q} \in (0.89, 1.10, 0.91)$ and $T_{sim} = 20\,s$.

In Fig. 5.63 is shown the chaotic behavior for fractional-order chaotic system (5.98), where system parameters are $(a, b, c) = (5, 85, 0.5)$, incommensurate orders of the derivatives are: $q_1 = 0.89,\ q_2 = 1.10,$ and $q_3 = 0.91$, and the initial conditions are $(x(0), y(0), z(0)) = (8, 2, 1)$ for the simulation time $T_{sim} = 20\,s$ and time step $h = 0.0005$. As we can see, behavior of the fractional-order Volta's system is still chaotic because we have observed double-scroll attractor (Tavazoei and Haeri, 2007b) and total order of the system is $\bar{q} = 2.9$.

The state equations of the fractional-order Volta's chaotic system (5.98) with parameters $(a, b, c) = (5, 85, 0.5)$ are given by using the integration operation and the properties (2.50), and (2.51) and have form:

$$\begin{aligned} x(t) &= {}_0D_t^{1-q_1}\left(\int_0^t [-x(t) - 5y(t) - z(t)y(t)]dt\right), \\ y(t) &= {}_0D_t^{1-q_2}\left(\int_0^t [-y(t) - 85x(t) - x(t)z(t)]dt\right), \\ z(t) &= {}_0D_t^{1-q_3}\left(\int_0^t [0.5z(t) + x(t)y(t) + 1]dt\right). \end{aligned} \tag{5.101}$$

The system model developed from the state equations (5.101) for system parameters $(a,b,c) = (5,85,0.5)$ by using the Matlab/Simulink environment is depicted in Fig. 5.64.

The simulation results for simulation time $T_{sim} = 20\ s$ obtained from model (5.101) for real order $q_1 = 0.93,\ q_2 = 0.99,$ and $q_3 = 0.98$ are dipicted in Fig. 5.65. As we can see, behavior of the fractional-order Volta's system is chaotic because we have observed double scroll attractor in $x-y$ plane (Tavazoei and Haeri, 2007b) and the total order of the system is $\bar{q} = 2.9$.

In Fig. 5.65 are shown the phase trajectories of the Simulink system model, starting from (x(0), y(0), z(0))=(8, 2, 1), and projected into 2D phase planes, respectively.

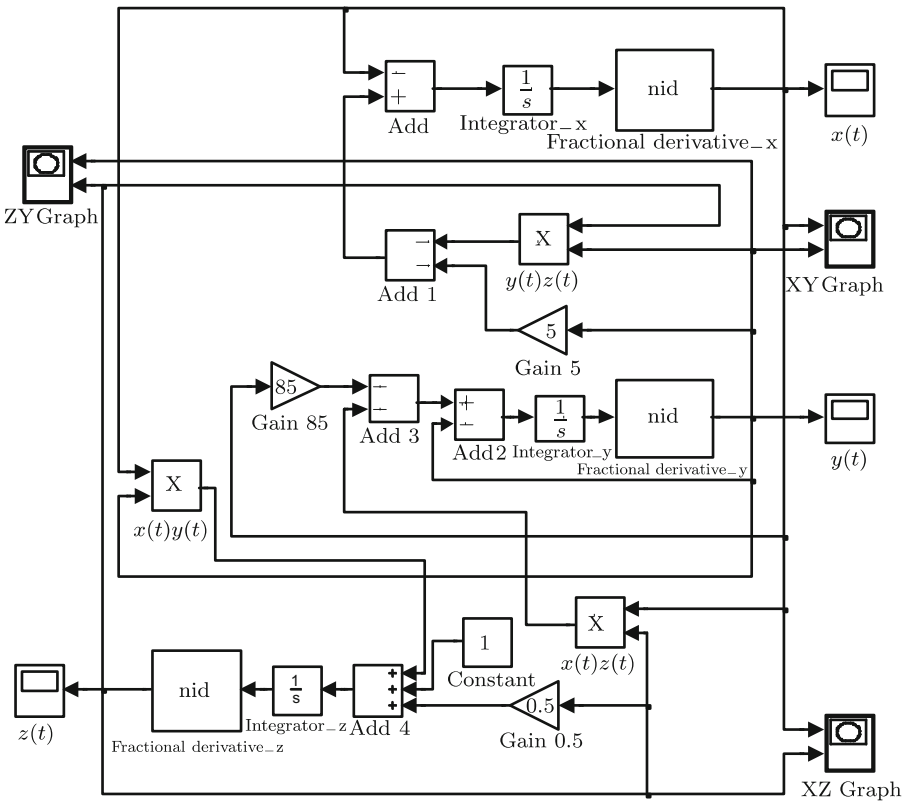

Fig. 5.64 Matlab/Simulink block diagram (model) for fractional order Volta's system (5.101).

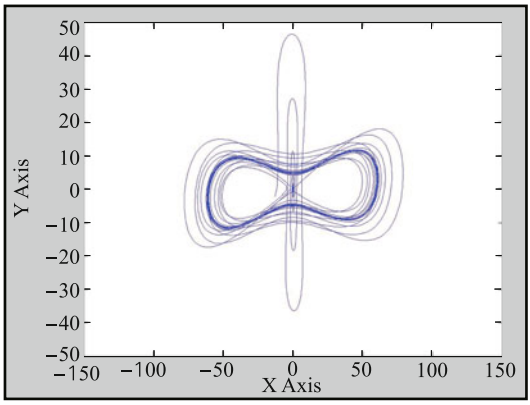

(a) Phase plane $x(t)$ vs. $y(t)$

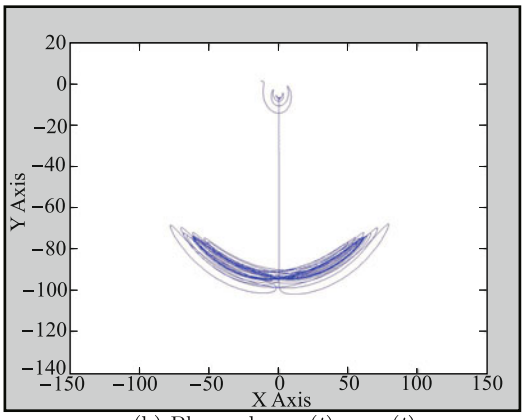

(b) Phase plane $x(t)$ vs. $z(t)$

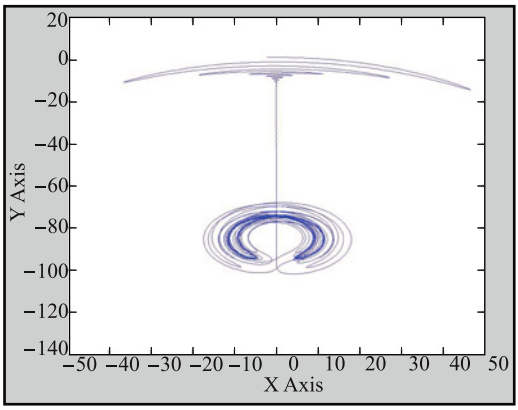

(c) Phase plane $y(t)$ vs. $z(t)$

Fig. 5.65 Phase plane projections of fractional-order Volta's system (5.101) for $T_{sim} = 20\,s$.

References

Ahmed E., El-Sayed A. M. A. and El-Saka H. A. A., 2007, Equilibrium points, stability and numerical solutions of fractional-order predator-prey and rabies models, *J. Math. Anal. Appl.*, **325**, 542–553.

Arena P., Caponetto R., Fortuna L. and Porto D., 1998, Bifurcation and chaos in noninteger order cellular neural networks, *International Journal of Bifurcation and Chaos*, **8**, 1527–1539.

Arena P., Caponetto R., Fortuna L. and Porto D., 2000, *Nonlinear Noninteger Order Circuits and Systems – An Introduction*, World Scientific, Singapore.

Barbosa R. S., Machado J. A. T, Vinagre B. M. and Calderón A. J., 2007, Analysis of the Van der Pol oscillator containing derivatives of fractional order, *Journal of Vibration and Control*, **13**, 1291–1301.

Bartissol P. and Chua L. O., 1988, The double hook, *IEEE Transactions on Circuits and Systems*, **35**, 1512–1522.

Biey M., Checco P. and Gilli M., 2003, Bifurcation and chaos in cellular neural networks, *Journal of Circuits, Systems, and Computers*, **12**, 417–433.

Caponetto R., Dongola G., Fortuna L. and Petráš I., 2010, *Fractional Order Systems: Modeling and Control Applications*, World Scientific, Singapore.

Carlson G. E. and Halijak C. A., 1963, Approximation of fractional capacitors $(1/s)^{1/n}$ by a regular Newton process, *Proc. of the Sixth Midwest Symposium on Circuit Theory*, May 6–7, Madison, Wisconsin.

Cruz J. M., 1993, An IC chip of Chua's circuit, *IEEE Transactions on Circuits and Systems –II: Analog and Digital Signal Processing*, **40**, 614–625.

Chen J. H. and Chen W. Ch., 2008, Chaotic dynamics of the fractionally damped van der Pol equation, *Chaos, Solitons and Fractals*, **35**, 188–198.

Chen W. Ch., 2008, Nonlinear dynamic and chaos in a fractional-order financial system, *Chaos, Solitons and Fractals*, **36**, 1305–1314.

Chua L. O., 1971, Memristor – the missing circuit element, *IEEE Transaction on Circuit Theory*, **CT-18**, 507–519.

Chua L. O., Komuro M. and Matsumoto T., 1986, The double scroll family, *IEEE Trans. on Circuit and Systems*, **CAS-33**, 1073–1118.

Chua L. O. and Roska T., 1993, The CNN paradigm, *IEEE Transactions on Circuits and Systems–I: Fundamental Theory and Applications*, **40**, 147–157.

Chua L. O., Wu Ch. W., Huang A. and Zhong G. Q., 1993, A universal circuit for studying and generating chaos – part I: Routes to chaos, *IEEE Transactions on Circuits and Systems –I: Fundamental Theory and Applications*, **40**, 732–744.

Deng W. H. and Li C. P., 2005, Chaos synchronization of the fractional Lü system, *Physica A*, **353**, 61–72.

Deregel P., 1993, Chua's oscillator: A zoo of attractors, *Journal of Circuits, Systems, and Computers*, **3**, 309–359.

Gao X. and Yu J., 2005, Chaos in the fractional order periodically forced complex Duffing's oscillators, *Chaos, Solitons and Fractals*, **24**, 1097–1104.

Ge Z. M. and Hsu M. Y., 2007, Chaos in a generalized van der Pol system and in its fractional order system, *Chaos, Solitons and Fractals*, **33**, 1711–1745.

Ge Z. M. and Ou Ch. Y., 2007, Chaos in a fractional order modified Duffing system, *Chaos, Solitons and Fractals*, **34**, 262–291.

Gejji V. D. and Bhalekar S., 2010, Chaos in fractional ordered Liu system, *Computers & Mathematics with Applications*, **59**, 1117–1127.

Genesio R. and Tesi A., 1992, Harmonic balance methods for the analysis of chaotic dynamics in nonlinear systems, *Automatica*, **28**, 531–548.

Guo L. J., 2005, Chaotic dynamics and synchronization of fractional-order Genesio-Tesi systems, *Chinese Physics*, **14**, 1517–1521.

Hao B., 1989, *Elementary Symbolic Dynamics and Chaos in Dissipative Systems*, World Scientific, Singapore.

Hartley T. T., Lorenzo C. F. and Qammer H. K., 1995, Chaos on a fractional Chua's system, *IEEE Trans. Circ. Syst. Fund. Theor. Appl.*, **42**, 485–490.

Itoh M. and Chua L. O., 2008, Memristor oscillation, *International Journal of Bifurcation and Chaos*, **18**, 3183–3206.

Itoh M. and Chua L. O., 2009, Memristor cellular automata and memristor discrete-time cellular neural networks, *International Journal of Bifurcation and Chaos*, **19**, 3605–3656.

Kennedy M. P., 1992, Robust OP AMP realization of Chua's circuit, *Frequenz*, **46**, 66–80.

Kennedy M. P., 1993a, Three steps to chaos – part I: Evolution, *IEEE Transactions on Circuits and Systems –I: Fundamental Theory and Applications*, **40**, 640–656.

Kennedy M. P., 1993b, Three steps to chaos – part II: A Chua's circuit primer, *IEEE Transactions on Circuits and Systems –I: Fundamental Theory and Applications*, **40**, 657–674.

Leipnik R. B. and Newton T. A., 1981, Double strange attractors in rigid body motion with linear feedback control, *Physics Letters A*, **86**, 63–67.

Li C. and Chen G., 2004, Chaos and hyperchaos in the fractional-order Rössler equations, *Physica A*, **341**, 55–61.

Li C. and Yan J., 2007, The synchronization of three fractional differential systems, *Chaos, Solitons and Fractals*, **32**, 751–757.

Liu C., Liu L. and Liu T., 2009, A novel three-dimensional autonomous chaos system, *Chaos, Solitons and Fractals*, **39**, 1950–1958.

Lu J. G., 2005, Chaotic dynamics and synchronization of fractional-order Arneodo's systems, *Chaos, Solitons and Fractals*, **26**, 1125–1133.

Lu J. and Chen G., 2002, A new chaotic attractor coined, *International Journal of Bifurcation and Chaos*, **12**, 659–661.

Lu J. G. and Chen G., 2006, A note on the fractional-order Chen system, *Chaos, Solitons and Fractals*, **27**, 685–688.

Ma J. H. and Chen Y. S., 2001a, Study for the bifurcation topological structure and the global complicated character of a kind of nonlinear finance system (I), *Applied Mathematics and Mechanics*, **22**, 1240–1251.

Ma J. H. and Chen Y. S., 2001b, Study for the bifurcation topological structure and the global complicated character of a kind of nonlinear finance system (II), *Applied Mathematics and Mechanics*, **22**, 1375–1382.

Matsumoto T., 1984, A chaotic attractor from Chua's circuit, *IEEE Transactions on Circuit and Systems*, **CAS-31**, 1055–1058.

Oustaloup A., Levron F., Mathieu B. and Nanot F. M., 2000, Frequency-band complex noninteger differentiator: characterization and synthesis, *IEEE Trans. on Circuits and Systems I: Fundamental Theory and Applications I*, **47**, 25–39.

Petráš I., 2006, A Note on the fractional-order cellular neural networks, *Proc. of the International Joint Conference on Neural Networks*, July 16-21, Vancouver, Canada, 1021–1024.

Petráš I., 2008, A note on the fractional-order Chua's system, *Chaos, Solitons and Fractals*, **38**, 140–147.

Petráš I., 2009a, Chaos in the fractional-order Volta's system: modeling and simulation, *Nonlinear Dynamics*, **57**, 157–170.

Petráš I., 2009b, *Fractional-Order Chaotic Systems*, Reprocentrum, Faculty of BERG, Technical University of Kosice.

Petráš I. and Bednárová D., 2009, Fractional – order chaotic systems, *Proc. of the IEEE Conference on Emerging Technologies & Factory Automation, ETFA 2009*, September 22–25, Palma de Mallorca, Spain.

Petráš I., 2010, A note on the fractional-order Volta's system, *Commun. Nonlinear. Sci. Numer. Simulat.*, **15**, 384–393.

Pivka L., Wu C. W. and Huang A., 1994, Chua's Oscillator: A Compendium of Chaotic Phenomena, *Journal of the Franklin Institute*, **33/B**, 705–741.

Podlubny I., 1999, *Fractional Differential Equations*, Academic Press, San Diego.

Samardzija N. and Greller L. D., 1988, Explosive route to chaos through a fractal torus in a generalized Lotka-Volterra model, *Bulletin of Mathematical Biology*, **50**, 465–491.

Schafer I. and Kruger K., 2008, Modelling of lossy coils using fractional derivatives, *J. Phys. D: Appl. Phys.*, **41**, 1–8.

Sheu L. J., Chen H. K., Chen J. H., Tam L. M., Chen W. C., Lin K. T. and Kang Y., 2008, Chaos in the Newton–Leipnik system with fractional order, *Chaos, Solitons and Fractals*, **36**, 98–103.

Tavazoei M. S. and Haeri M., 2007a, Unreliability of frequency-domain approximation in recognising chaos in fractional-order systems, *IET Signal Proc.*, **1**, 171–181.

Tavazoei M. S. and Haeri M., 2007b, A necessary condition for double scroll attractor existence in fractional – order systems, *Physics Letters A*, **367**, 102–113.

Valerio D., 2005, Toolbox `ninteger` for Matlab, v. 2.3 (September 2005), http://web.ist.utl.pt/duarte.valerio/ninteger/ninteger.htm.

Westerlund S. and Ekstam L., 1994, Capacitor theory, *IEEE Trans. on Dielectrics and Electrical Insulation*, **1**, 826–839.

Westerlund S., 2002, *Dead Matter Has Memory*! Causal Consulting, Kalmar, Sweden.

Wolf A., Swift J. B., Swinney H. L. and Vastano J. A., 1985, Determining Lyapunov exponents from a time series, *Physica D*, **16**, 285–317.

Zaslavsky G. M., 2005, *Hamiltonian Chaos and Fractional Dynamics*, Oxford University Press, Oxford.

Zhong G. Q., 1994, Implementation of Chua's circuit with a cubic nonlinearity, *IEEE Transactions on Circuits and Systems –I: Fundamental Theory and Applications*, **41**, 934–941.

Zou F. and Nossek J. A., 1993, Bifurcation and chaos in cellular neural networks, *IEEE Transactions on Circuits and Systems-I: Fundamental Theory and Applications*, **40**, 166–173.

Zhou T., Tang Y. and Chen G., 2004, Chen's attractor exists, *International Journal of Bifurcation and Chaos*, **14**, 3167–3177.

Zhu H., Zhou S. and Zhang J., 2009, Chaos and synchronization of the fractional-order Chua's system, *Chaos, Solitons and Fractals*, **39**, 1595–1603.